Role of appetite-regulating peptides in adipose tissue physiology in broiler chicks

Steven L. Shipp

Thesis submitted to the faculty of the Virginia Polytechnic Institute and State University in partial fulfillment of the requirements for the degree of

Master of Science
In
Animal and Poultry Sciences

Elizabeth R. Gilbert, Chair
Mark A. Cline
Paul B Siegel
D. Michael Denbow

December 2016
Blacksburg, VA

Keywords: chick, adipose, adipogenesis, lipolysis, NPY, α-MSH

Role of appetite-regulating peptides in adipose tissue physiology in broiler chicks

Steven L. Shipp

ABSTRACT (Academic)

Peptides that regulate feeding behavior via the brain may also regulate energy storage and expenditure in the adipose tissue, a system collectively known as the "brain-fat axis". Neuropeptide Y (NPY) is orexigenic and promotes adipogenesis in both birds and mammals, although mechanisms in adipose tissue are unclear. The first objective was thus to evaluate effects of NPY on chick preadipocyte proliferation and differentiation. Preadipocytes were treated with NPY and gene expression and cellular proliferation were evaluated. Cells were also treated with NPY during differentiation and harvested during the later stages. With increased gene expression of proliferation markers in preadipocytes, and during differentiation increased expression of adipogenesis-associated factors, increased lipid accumulation, and increased activity of an adipogenic enzyme, glycerol-3-phosphate dehydrogenase, results suggest that NPY may enhance preadipocyte activity and adipogenesis and promotes lipid accumulation throughout chicken adipocyte differentiation. Another appetite-regulatory peptide, alpha-melanocyte stimulating hormone (α-MSH), is anorexigenic and mediates lipolysis in adipose tissue, but effects on fat in avians are unreported. The second objective was thus to determine the effects of exogenous α-MSH on adipose tissue physiology in broiler chicks. Chicks were intraperitoneally injected with α-MSH and adipose tissue and plasma collected. Cells isolated from abdominal fat of a different set of chicks were treated with α-MSH. Results suggest that α-MSH increases lipolysis and reduces adipogenesis in chick adipose tissue. Collectively, results of this research provide insights on how appetite-regulatory peptides like NPY and α-MSH affect

adipose tissue physiology, thereby playing important roles in regulating whole-body energy balance.

Public

Peptides that contribute to feeding behavior via the brain may also affect the way energy is stored and released in the adipose tissue. Neuropeptide Y (NPY) is a neurotransmitter that induces hunger, and promotes the growth of adipose tissue in both birds and mammals, although mechanisms in adipose tissue are unclear. The first objective was thus to evaluate effects of NPY on chick preadipocyte activity and the process by which preadipocyte cells differentiate into fully matures adipocytes, a process termed adipogenesis. Preadipocytes were treated with NPY and gene expression and cellular division were evaluated. Cells were also treated with NPY during differentiation and harvested during the later stages. With increased activity in preadipocytes, and during differentiation greater activity leading to increased fat accumulation, results suggest that NPY may enhance preadipocyte activity and adipogenesis and promotes fat accumulation throughout chicken adipocyte differentiation. Another appetite-regulatory peptide, alpha-melanocyte stimulating hormone (α-MSH), inhibits hunger and breaks down adipose tissue, but effects on fat in avians are unreported. The second objective was thus to determine the effects of α-MSH on adipose tissue physiology in chicks. Chicks were injected with α-MSH and cells isolated from abdominal fat of a different set of chicks were treated with α-MSH. Results suggest that α-MSH breaks down fat and reduces adipogenesis in chick adipose tissue. Collectively, results of this research provide insights on how NPY and α-MSH affect adipose tissue physiology, thereby playing important roles in regulating whole-body energy balance.

Table of Contents

List of Tables

List of Figures

Chapter 1: Introduction

The adipose tissue is a dynamic and highly vascularized and innervated organ comprised of numerous cell types and is involved in many aspects of physiology. Overgrowth of the adipose tissue can lead to many adverse health effects, including cardiovascular disease [1], hypertension [2], type II diabetes [3], and some types of cancer [4]. Increased adipose tissue mass is also a concern in the poultry industry, as excess fat represents waste during broiler processing and is associated with metabolic disorders and impaired reproduction in broiler breeders [5]. From a fundamental biology perspective, adipose tissue represents an evolutionary adaptation to provide energy during times of food shortage, physical cushioning from injury, and insulation to maintain body temperature. In migrating birds and hibernating mammals, for example, adipose tissue mass fluctuates seasonally in response to photoperiod-modulated hyperphagia. A greater understanding of adipose tissue physiology is necessary for implementing strategies to prevent or treat metabolic diseases and for improving management strategies to maximize animal health and productivity, while also providing information that may be used in breeding or wildlife/zoo management programs. Thus, understanding the physiological mechanisms associated with formation of adipocytes and lipid remodeling in adipose tissue may have far-reaching implications across multiple scientific disciplines.

There are numerous methods and animal models to study adipose tissue physiology, both *in vitro* and *in vivo*. While *in vitro* techniques can shed light on how specific cell types respond in isolation to a particular stimulus, *in vivo* studies are also important in order to demonstrate physiological relevance in a whole-body context. Adipose tissue deposition is a complicated process that is not fully understood. The events associated with developing a mesenchymal stem

cell into a fully mature adipocyte are termed adipogenesis. Adipocyte differentiation can be impacted by hormones and neurotransmitters, as well as nutrients and factors released by other cell types in the adipose tissue. Lipid metabolism in the mature adipocyte is also highly dynamic; there is still an incomplete understanding of the mechanisms that regulate lipid deposition and liberation. The molecular regulation of adipocyte differentiation and lipid metabolism in adipose tissue will be described in greater detail in Chapter 2.

There are many factors that regulate food intake (via the central nervous system), some of which also affect adipose tissue physiology, but the impact of these factors on adipocyte differentiation is still poorly understood, especially so in avian species. As will be discussed in Chapter 2, neuropeptide Y (NPY; hunger-stimulating) and α-melanocyte stimulating hormone (α-MSH; promotes satiety) are two such factors that are the focus of this thesis research. The objectives of the research were to elucidate cellular mechanisms underlying the effects of these appetite-regulatory peptides on adipose tissue physiology. Receptors for these peptides are expressed in adipose tissue and there are multiple paths through which effects on adipose tissue might be mediated including the endocrine, neurocrine, autocrine and paracrine routes. Many pharmacological drugs used to treat diseases target receptors, thus identifying the intracellular signaling pathways through which factors such as NPY and α-MSH affect physiological processes may shed light on potential pharmacological targets to modulate body composition and fat mass. Following the literature review in Chapter 2, the remainder of the thesis will focus on two studies, the objectives of which were to evaluate the effects of NPY (Chapter 3) and α-MSH (Chapter 4) on chick adipogenesis and adipocyte lipid metabolism. Finally, the implications for future research and integrative perspectives are discussed in the epilogue (Chapter 5).

Chapter 2: Literature Review

Recent advances in the understanding of how neuropeptide Y and α-melanocyte stimulating hormone function in adipose tissue physiology

[6]

Steven L Shipp, Mark A Cline, and Elizabeth R Gilbert

Virginia Tech, Animal and Poultry Sciences, Blacksburg, Virginia 24061

Abstract

Communication between the brain and the adipose tissue has been the focus of many studies in recent years, with the "brain-fat axis" identified as a system that orchestrates the assimilation and usage of energy to maintain body mass and adequate fat stores. It is now well-known that appetite-regulating peptides that were studied as neurotransmitters in the central nervous system can act both on the hypothalamus to regulate feeding behavior and also on the adipose tissue to modulate the storage of energy. Energy balance is thus partly controlled by factors that can alter both energy intake and storage/expenditure. Two such factors involved in these processes are neuropeptide Y (NPY) and alpha melanocyte stimulating hormone (α-MSH). NPY, an orexigenic factor, is associated with promoting adipogenesis in both mammals and chickens, while α-MSH, an anorexigenic factor, stimulates lipolysis in rodents. There is also evidence of interaction between the two peptides. This review aims to summarize recent advances in the study of NPY and α-MSH regarding their role in adipose tissue physiology, with an emphasis on the cellular and molecular mechanisms. A greater understanding of the brain-fat axis and regulation of adiposity by bioactive peptides may provide insights on strategies to prevent or treat obesity and also enhance nutrient utilization efficiency in agriculturally-important species.

Introduction

Many different factors are involved in regulating adipose tissue physiology. Because white adipose tissue is comprised of many different cell types, including preadipocytes, adipocytes, blood cells, immune cells, and mesenchymal stem cells among others, and is innervated by the sympathetic nervous system and is highly vascularized, there are multiple routes through which factors can act on cells in the adipose tissue (neural, endocrine, paracrine, autocrine, etc.) and numerous cells that play a role in the acquisition and storage of energy, including the adipocyte that stores triacylglycerols and cholesterol esters in lipid droplets that occupy most of the volume of the cell. The majority of studies in adipose tissue physiology focus on mammalian models, with fewer studies in birds, however, with the ease of availability of chickens and the bulk of avian research being conducted in the domestic chicken, it has emerged as an attractive model for understanding the relationship between appetite regulation and adipocyte lipid metabolism.

Two peptides that play a major role in regulating food intake are neuropeptide Y (NPY) and alpha – melanocyte stimulating hormone (α-MSH). These peptides are regarded as neurotransmitters, however because most studies do not distinguish between actions in vivo that originate centrally or peripherally (both factors and their receptors are produced in adipose tissue and both are found in the circulation), they will be referred to as "peptides" for the remainder of this review. NPY is highly orexigenic in many species, and its receptor sub-types are well characterized in mammals [7], while α-MSH is anorexigenic and is part of the melanocortin system. The two peptides are also associated with each other, with the NPY system acting to regulate the activity of α-MSH in the hypothalamus by decreasing its phosphorylation capacity

and amount present in the paraventricular nucleus (PVN) [8]. Both peptides also affect adipose tissue physiology; NPY mainly affects adipogenesis, while α-MSH primarily affects lipolysis.

Neuropeptide Y, a 36 amino acid peptide, was first isolated from the pig brain [9], and its orexigenic properties have been studied in a multitude of species, including rodents [10], rabbits [11], teleost fish [12], white-crowned sparrows [13] and chickens [14, 15]. It is involved in promoting adipogenesis in mouse 3T3-L1 cells [16], and chicken preadipocytes [17]. Adrenocorticotropic hormone (ACTH) is a peptide derived from pro-opiomelanocortin (POMC), and α-MSH is then further derived from ACTH, as the first 13 amino acids of ACTH are what make up α-MSH [18]. It is involved in energy balance and is an agonist to 4 out of 5 melanocortin receptors (MCR) [19]. It is also anorexigenic in multiple species, including rats [20], goldfish [21], and chicks [22]. A lipolytic effect mediated through MC5R was reported in mouse 3T3-L1 cells [23], but is yet to be determined in chicken or any other avian species.

Although our group recently published a review on hypothalamus-adipose tissue crosstalk with a focus on NPY [24], many developments have since been reported on the study of appetite-regulating factors and their role in adipose tissue metabolism. The purpose of this review is to incorporate recent information about the actions of NPY and α-MSH in adipose tissue, with an emphasis on the molecular mechanisms. Additionally, because the information reviewed is in the subject of adipose tissue physiology; adipogenesis, adipose tissue expansion, and models used for studying adipogenesis are also discussed.

Adipogenesis and Adipose Tissue Expansion

Adipose cells originate from mesenchymal stem cells, which are found in the adipose tissue [25]. Although accepted as being of mesenchymal origin, adipose cells are also derived from areas outside of the mesoderm such as the neural crest (NC) [26, 27]. Mesenchymal stem cells can differentiate into a multitude of different cell types, including adipocytes, chondrocytes, osteoblasts, and myoblasts [28-34], as well as neuron-like cells [35-37], with considerable transcriptional regulation by a diverse array of factors to determine the route of differentiation. Adipogenesis encompasses the many steps of differentiation; from a stem cell being determined to become a preadipocyte to the preadipocyte during the early (clonal expansion) and late (terminal) stages of differentiating into the fully mature adipocyte [38]. For the remainder of this review, differentiation will refer to terminal differentiation of the adipocyte, unless stated otherwise.

Transcription factors and adipocyte differentiation

There are several major transcription factors that have been widely studied for their role in adipogenesis, with mechanisms underlying their actions well-understood in mammals. The transcription factors discussed herein and the times during differentiation that they are expressed are described in Table 1.

Peroxisome proliferator activated receptor gamma (PPARγ) is part of the nuclear receptor superfamily, and is known as the "master regulator" of preadipocyte differentiation [39], and is necessary for development of adipose tissue [40]. Expression is induced early in differentiation [41], and induced expression in fibroblasts can cause differentiation into adipocytes [42], as well as trans-differentiation of myoblasts into adipocytes [43]. Expression after adipocyte maturity is

also important, as 3T3-L1 cells containing a dominant-negative PPARγ, a mutant form that is able to bind DNA but not ligands, are induced to de-differentiate [44]. Knockout (KO) of PPARγ in adipocytes *in vivo* leads to adipocyte death due to necrosis, which then stimulates the generation of new adipocytes [45], cells that the authors hypothesized were derived from fibroblast-like cells; adipose progenitor cells are widely distributed in connective tissue and possess the ability to proliferate and differentiate into adipocytes [45, 46].

Another transcription factor, sterol regulatory element binding protein (SREBP), plays a role in adipogenesis. Its main function is to control expression of enzymes involved in cholesterol, fatty acid, triacylglycerol, and lipid synthesis, as reviewed [47]. SREBP 1 and 2 activate transcription of more than 30 genes that are related to lipid synthesis and transport, particularly in the liver [48, 49]. Diet-derived polyunsaturated fatty acids suppress hepatic expression of genes contributing to fatty acid synthesis, with SREBP 1 and 2 purported to be involved [49]. SREBP increases the activity of PPARγ by producing endogenous ligands that bind to the ligand-binding domain of PPARγ, as conditioned media from NIH 3T3 cells expressing SREBP activated PPARγ [50]; although it was not specified which specific endogenous ligands were produced, authors noted that secreted lipid(s) in the fatty acid family serve as endogenous ligands of PPARγ [50-53]. SREBP is also involved in insulin-mediated signaling to induce lipid accumulation by increasing expression of the lipogenic genes fatty acid synthase (FAS) and lipoprotein lipase (LPL) [54].

The CCAAT enhancer binding protein (C/EBP) family of transcription factors is also important during adipocyte differentiation, with early expression of C/EBPβ and C/EBPδ during the first two days of differentiation leading to induction of C/EBPα [38, 55, 56]. C/EBPα KO mice die shortly after birth, but when expression is limited to the liver they survive with greatly reduced

amounts of white adipose tissue [57]. When C/EBPα null mice have the C/EBPα gene replaced with C/EBPβ, leading to expression of C/EBPβ from the C/EBPα gene locus in addition to its own endogenous expression, mice are able to survive, but amounts of white adipose tissue are still reduced [58], demonstrating that C/EBPβ is not sufficient to fully replace the function of C/EBPα in regulating adipose tissue mass, although it is sufficient for survival.

While the C/EBP transcription factors are important for differentiation, they cannot induce differentiation without PPARγ. While C/EBPα deficient mice produce less adipose tissue, they also do not induce endogenous PPARγ gene transcription, as fibroblast cell lines isolated from C/EBPα KO mice lack expression of PPARγ that is rescued by partially restoring expression of C/EBPα with a retroviral vector expressing C/EBPα [59]; thus showing the importance of communication between these two transcription factors. Additionally, treating mouse embryo fibroblasts (MEF) lacking a functional PPARγ gene with C/EBPβ does not induce expression of C/EBPα [60], further supporting the role of communication between the C/EBP's and PPARγ in orchestrating adipocyte differentiation.

Adipose Tissue Depots

Adipose tissue is divided into two major types, white adipose tissue (WAT) and brown adipose tissue (BAT), with WAT being an energy storage and endocrine tissue [61], and BAT being involved in the production of heat, present in greater amounts in neonates and hibernators [62, 63]. Existence of BAT is still questionable in avian species [64-67], and is not reviewed here. The two main classifications of WAT depots in humans are subcutaneous adipose tissue and

visceral adipose tissue, the visceral adipose tissue being the adipose tissue surrounding the inner organs [68].

The different depots have many distinctions including differences in cellularity, adipokine production, and gene expression, as recently reviewed [69]. In the developing chicken embryo, fat is first deposited subcutaneously [70], and develops through a combination of hyperplasia and hypertrophy [71]. Subcutaneous and clavicular fat depots are heavier than abdominal fat at four days post-hatch [72], but as a percentage of body weight, the amount of abdominal fat increases with age [72]. It is unclear if birds are similar to humans in regards to metabolic differences between adipose tissue depots, although we have reported that there are differences in gene expression between adipose tissue depots in chickens [72-74].

In addition to the differences we have reported in meat-type broiler chickens, we have also found adipose tissue depot differences lines of chickens selected for high and low body weight, the Virginia lines of chickens, which have undergone divergent selection for either low (LWS) or high (HWS) juvenile body weight at 56 days of age for 58 generations. This selection has resulted in more than a ten-fold difference in body weight at age of selection, with associated physiological and behavioral differences in feeding, adiposity, development, and body composition, with the LWS being lean and hypophagic, while the HWS are obese and hyperphagic as juveniles [75-78]. The LWS has greater PPARγ mRNA than HWS in the subcutaneous and clavicular adipose tissue, and pyruvate dehydrogenase kinase 4 (PDK4), and forkhead box 01A (FOX01), two enzymes important in metabolic flexibility [79-83], also differ in expression between the lines, with greater expression of PDK4 in the clavicular adipose tissue of the LWS and subcutaneous adipose tissue of the HWS, and greater expression of FOX01 in

the subcutaneous adipose tissue of the HWS [74]. These differences in adipose tissue depot expression of metabolic factors may contribute to the differences in adiposity of these chicken lines.

Models for Studying Adipogenesis

With the adipose tissue being so diverse with numerous cell types present, and cross-talk with other systems in the body, many different models have emerged for studying the adipose tissue. A popular practice for *in vitro* studies is the use of cell lines. A common preadipocyte model, the mouse preadipocyte 3T3-L1 cell line, is very widely used to study adipogenesis. Their ability to differentiate into adipocytes and the ease through which different experiments can be conducted make them an attractive model. However, information on how these cells communicate with other cell types normally found in close proximity *in vivo* is impossible to determine through studies with single cell types. Cell lines are not available for every species, thus many studies in alternative animal models make use of a primary cell culture model to study adipogenesis.

Using 3T3-L1 cells allows for the study of a single cell type free of contamination by other cells that are present in the tissue. On the other hand, when generating a primary cell culture model, isolating one cell type proves more difficult especially in the absence of cell sorting technology, and thus there are usually multiple cell types present. There are numerous cell lines available, or types of cells and cell groups that can be isolated from a primary cell model, as noted in a review on cell models used to study differentiation [84]. Additionally, while some protocols enrich for a specific cell type through isolation, other primary cell models enrich for a certain cell type through the media containing known factors that either push cells towards a certain goal, like

differentiation, or enrich for a particular cell type. For example, a study by Billon et al., 2007, used a primary and secondary culture method of developing quail neural crest (NC) cells. Although these cells are not preadipocytes, they found that by including specific factors in the media cocktail, these cells were able to differentiate into adipocytes [26]. Another example would be isolating cells from the stromal vascular fraction (SVF), the cells isolated after completion of enzymatic digestion, centrifugation, cellular filtration, and red blood cell lysis of the adipose tissue [85], a mixture of cells that include mesenchymal stem cells, preadipocytes, endothelial cells, and immune cells [86-88]. This technique has been applied in mice [89], humans [90], and chickens [17].

In addition to generating single cell suspensions for culture, whole tissue can also be cultured as explants. By isolating the tissue, but preserving the cross-talk between cells in the tissue, explants offer the benefit of more closely mimicking the *in vivo* environment of the cells [91, 92]. As *in vitro* studies provide further understanding in fields of physiology, culturing whole tissue explants will become increasingly important to study conditions *in vivo*.

While there are numerous cell lines available for mammalian species, for avian species *in vitro* studies on adipogenesis often use a primary cell culture model. Some differences in methodology are adapted when studying differentiation, including using chicken serum (CS) in the differentiation cocktail, and using a combination of insulin, dexamethasone, and heparin [93]. The concentration of insulin is also greater than what is included in mammalian studies, because birds are naturally insulin resistant [94, 95]. These studies are also conducted with tissue collected from the abdominal fat of young chicks, usually 2-4 weeks old, because there is

sufficient fat accumulation to yield ample cells for culture from a single chicken, and cell viability and proliferative capacity of adipose-derived mesenchymal stem cells decreases with age [96]. We also recently showed that cells isolated from chicks at this age had robust proliferative capacity and ability to differentiate [17].

Factors that regulate both energy intake and storage in the animal

Identifying factors that regulate how adipose tissue is remodeled, as well as how energy is stored in different animals becomes increasingly important as more advances are made in understanding diseases related to the adipose tissue. The adipose tissue is indeed an endocrine organ associated with the release of multiple hormones [97]. While these hormones are important in energy balance and function, crosstalk between the brain and hypothalamus, as well as the sympathetic nervous system is also important in providing reciprocal signals that serve as feedback loops in times of energy restriction or excess. Multiple studies from the Bartness group used the pseudorabies virus (PRV) to elucidate the brain network controlling the sympathetic innervation of WAT [98] and BAT [99]. The PRV is a neurotropic virus that is able to infect neurons trans-synaptically, thus providing the ability to trace a neural network in a retrograde fashion when injected into a specific tissue [100, 101]. In Siberian hamsters (a species that displays seasonal changes in appetite and adipose tissue mass in response to alterations in photoperiod) and rats, they found that areas of the brain stem, midbrain, and hypothalamus were connected to the WAT and BAT, with the paraventricular nucleus (PVN) and medial preoptic area (MPA) in the hypothalamus showing greatest concentration of the virus in connection to the WAT and BAT [98, 99]. They also showed that the WAT is not innervated by any parasympathetic pathways in Siberian hamsters, rats, or mice, which has been contested [102].

Many neurotransmitters are expressed in areas other than neurons, and have effects on the fat. Serotonin is involved in regulating energy homeostasis, as KO and inhibition of tryptophan hydroxylase 1, one of the enzymes responsible for conversion of tryptophan into serotonin, causes a reduction in body weight gain, improved glucose tolerance, increased thermogenic activity in BAT and decreased lipogenesis in WAT [103]. Other amino acid neurotransmitters are also found in the adipose tissue; with immunohistochemical labeling used to detect gamma amino butyric acid (GABA), glutamate, the GABA producing enzyme glutamate decarboxylase, and transporters and receptors for glutamate and GABA [104]. There is also regulation by POMC peptides in adipose tissue to promote browning of WAT and lipolysis [105, 106], and sympathetic innervation of the adipose tissue [107]. The neurotransmitter NPY has received much attention in recent years, highlighted in our recent previous review [24], but is still an active area of research, which is reviewed herein. The POMC-derived peptide α-MSH has also been identified as a regulator of fat mass, and while developments in relation to adipose tissue are relatively new, they are also reviewed herein.

Adipose Tissue Physiology: NPY

While well regarded as an orexigenic peptide in the brain, NPY functions in many other aspects of physiology, such as learning and memory [108], tumor growth and progression [109], and other processes related to adipose tissue.

NPY co-exists with norepinephrine (NE) in sympathetic nerve terminals [110]. The specific action of co-release of NPY and NE is often studied in the cardiovascular system [111, 112], but

is not well annotated in the adipose tissue. Obese (fa/fa) Zucker rats reduce food intake and display enhanced metabolic rates when infused with both NPY and NE, suggestive of a synergistic effect [113]. In 3T3-L1 cells, NPY is able to potentiate lipolysis that is stimulated by isoproterenol, a β-adrenergic agonist [114], further showing synergy between NPY and NE. In another study, mice overexpressing NPY in noradrenergic neurons show increased body, WAT, and BAT weight [115]. The effect is possibly determined by how much of each is present, distribution and abundance of receptor sub-types, with increases in adipose tissue development observed when NPY is more abundant, but the synergetic lipolytic effect being observed when amounts are similar.

Stem Cells to Preadipocytes to Adipocytes

Prenatal stress can increase the chances of progeny developing obesity [116], and most adipocytes originate from adipose progenitor cells that were committed prenatally or early postnatally [117]. To understand the effect of prenatal stress on development of adipose tissue, epinephrine (EPI) was included in the adipocyte differentiation cocktail of murine embryonic stem cells to stimulate stress, after which NPY and NPY1R and NPY2R mRNAs were up-regulated [118]. Treatment with EPI was also associated with increased adipogenesis, through increased proliferation, mRNA expression of FABP4 and PPARγ, and enhanced neutral lipid accumulation. This effect was blocked by combined antagonism of NPYR's 1, 2, and 5 [118], indicating that the NPY system is important in the generation of more adipose cells from mesenchymal stem cells in response to stress.

Preadipocytes of the 3T3-L1 cell line were more viable and proliferated more when treated with a low dose of NPY (10^{-15}M and 10^{-13}M), but less viable and proliferative when treated with a much higher dose (10^{-7}M) [119]. It was speculated that high concentrations of NPY may be contributing to differentiation of the preadipocyte rather than proliferation, explaining why the effect on proliferation is not observed at a higher concentration of NPY [119]. When included in the differentiation cocktail, NPY up-regulates PPARγ and C/EBPα protein expression, and increases lipid accumulation in cells [119]. These data indicate that NPY stimulates preadipocytes to multiply and then undergo hypertrophy during differentiation.

NPY also has effects on brown fat during cellular differentiation and after isolation of cells from the SVF of brown fat. Results from a study that used a mesenchymal stem cell line, C3H10T1/2, that is able to be induced to behave in a brown-like manner, demonstrated that including NPY in the differentiation cocktail at either 0, 1, 10, or 100 nM concentration had no effect on brown fat cell adipogenesis (it did not cause browning of the cells induced to differentiate), but was associated with inhibition of brown fat cell-associated marker uncoupling protein-1 (UCP-1) [120], providing more evidence for NPY's role in suppressing brown fat activation, as reviewed earlier [24].

Bone-Adipose Crosstalk

The bone and adipose tissue have considerable cross-talk, and both contribute to energy balance, with NPY and its receptors also being involved in the regulation of these two systems to control energy balance. A 40% reduction of plasma NPY was observed in mice that have an osteoblast-specific deletion of p38α mitogen activated protein kinase (p38 MAPK). A 20% increase in

energy expenditure, measured by locomotor activity, O_2 consumption, CO_2 expenditure and energy expenditure monitored through an indirect calorimetric analysis, and up-regulation of UCP-1 without a change in energy intake was also observed in WAT and BAT, as well as a decrease in body weight and total adiposity. The mRNA distribution of NPY was evaluated in bone, primary osteoblasts, whole brain, hypothalamus, sympathetic superior cervical ganglia, adrenal gland, muscle, adipose tissue, and jejunum, and was reduced in bone and primary osteoblasts, and increased in the hypothalamus and adipose tissue of p38 MAPK-osteoblast-null mice. Although NPY was increased in the hypothalamus, the distribution of brain NPY immunoreactivity did not differ between the wild and KO mice. An increase in feeding during the first few hours was observed, but the effect normalized over time. Intraperitoneal injection of NPY partially restored adipose tissue mass in the mice lacking p38 MAPK in their osteoblasts [121].

A review by Shi and Baldock, 2012, highlighted the relationship between NPY, bone, and adipose tissue [122]. In bone, NPY represses bone formation, mainly through NPYR 1 and 2, and a lack of NPY expression increases osteoblast activity (bone formation), and bone mass. The two systems may be coordinately regulated, although effects of NPY on bone and adipose tissue homeostasis are complicated by how the brain perceives the negative energy balance state. Bone formation is similarly affected by elevated NPY in various energy states, whereas the adipose tissue reacts differently. When there is elevated NPY, for instance during a negative energy balance state, bone metabolism is optimized for energy conservation and inhibition of bone formation, while in the adipose tissue, elevated NPY leads to increases in body weight and WAT mass [123, 124].

Although the interaction between the adipose tissue and bone remains to be further elucidated, they seem to be an attractive target for pharmacological intervention. NPY KO mice show increased bone formation [125], thus while targeting NPY to reduce obesity, an intervention currently underway [126], bone formation could possibly be positively affected.

NPY Knockout, Knockdown, and NPYR Antagonism

There are reports of NPY KO mice, knockdown in specific tissues, as well as pharmacological inhibition of receptor sub-types; all models to better understand the role of NPY in adipose tissue physiology and to identify the specific receptor(s) through which it mediates various functions in adipose tissue.

As reviewed earlier [24], NPY and NPYR 1, 2, and 5 are expressed in the adipose tissue. The NPY1R has the widest body distribution, with expression being greatest in the paraventricular nucleus (PVN) of the hypothalamus [127]. It is regarded as the NPYR most involved in regulating food intake, although NPY2R is also expressed in the arcuate nucleus (ARC) of the hypothalamus and contributes to appetite regulation [128]. The NPY5R is most similar to NPY1R in amino acid sequence identity [129], and is co-localized with NPY1R in many areas of the nervous system where NPY5R is expressed [130]. Adipose-specific production of NPY5R remains debated, as it has been detected in the adipose tissue of rodents [131, 132] and chickens [73], but at other times is undetectable [133, 134]. Additionally, NPY2R was expressed in human [16], mouse [16] and chicken preadipocytes [17], while in another study NPY2R was not detected in mouse preadipocytes [134]. While *in vivo* studies may show the importance of each

receptor in whole body adipose tissue biology, *in vitro* studies allow more specific quantification and study of regulation in a particular cell type.

Sirtuin 1 (SIRT1) has been reported to play a role in fat metabolism and may mediate some NPY-induced changes in adipose tissue physiology. It is a deacetylase involved in lipid mobilization from fat [135] that also promotes brown fat cellular remodeling [136], thereby contributing to an increase in energy release [137]. A transcription factor, cAMP response element binding protein (CREB), is also important in this role as it induces expression of UCP-1 [138], which as described earlier is a factor important for the thermogenic function of BAT [139].

In NPY-KO mice, adipogenesis-associated factor mRNAs are down-regulated, while expression of genes involved in lipolysis increase in gonadal white adipose tissue (gWAT) [140]. Age related decreases in gWAT lipogenesis, and thermogenesis in inguinal WAT are also reduced in NPY KO mice [140]. SIRT1 has been reported to promote fat mobilization due to repressed PPARγ activity [135], and the changes due to NPY KO are thought to be associated with activation of SIRT1, and subsequent inactivation of PPARγ- mediated pathways. This is supported by the finding that NPY treatment inhibits lipolysis in 3T3-L1 cells via NPY1R-mediated signaling and reduced CREB and SIRT1 protein expression [140]. Deletion of NPY in mice clearly affects pathways involving SIRT1, as well as regulation of transcription factors PPARγ and CREB. Because the NPY system is widely distributed, targeting factors that are affected by NPY, such as SIRT1, may thereby target the fat, especially since this factor is associated with the loss of fat, a major goal of modulating the NPY system to treat obesity [126].

Dorsomedial hypothalamic NPY has effects independent of ARC NPY, and is a major source of NPY that has been well studied in relation to energy balance [141]. Additionally, this nucleus was shown to be connected to the innervation of the adipose tissue through the afore-mentioned PRV studies [98, 99]. Knockdown of NPY expression in the dorsomedial hypothalamus (DMH) via adeno-associated virus-mediated RNA interference reduced fat depot weights in rats and ameliorated high-fat diet-induced hyperphagia and obesity. Knockdown also promoted BAT development and increased UCP-1 expression [142].

Daily IP injection of the NPY antagonist S.A.0204 for 30 days caused a decrease in body weight, and an increase in WAT lipolysis and apoptosis in diet-induced obese rats [143]. Intraperitoneal injection of the NPY2R antagonist BIIE 0246 into male mice for 14 days decreased adipocyte cell number but did not change cell size, indicating that NPY2R is important in producing new cells, but may not necessarily be involved in hypertrophy of adipocytes [144]. Although this study did not measure gene expression, future studies could evaluate whether the genes involved in adipogenesis/lipolysis are affected by NPYR antagonism. Serum deprivation of 3T3-L1 cells can induce lipolysis, an effect that is inhibited by NPY treatment, with NPY's effects in turn blocked by the NPY1R antagonist BIBO3304, demonstrating that the ability of NPY to rescue cells from the lipolytic effect of serum starvation is specific to NPY-mediated signaling [140].

Insulin Resistance and Sensitivity

Obesity is associated with insulin resistance, a pathology where cells are unable to normally respond to insulin [145], thus it is worth noting the relationship of NPY function to insulin resistance in the adipose tissue. In biopsies from human subjects, mRNA abundance of adipose-

derived hormones involved in insulin sensitivity, including adiponectin, visfatin, and omentin, was correlated with mRNA expression of NPY and its receptors. In subcutaneous fat all three were positively correlated with expression of NPY, and adiponectin, visfatin, and omentin were positively correlated with expression of NPYR 1 and 5, NPYR 1, 2, and 5, and NPY5R, respectively. The three were also positively correlated with NPY expression in the visceral fat, and visfatin was positively correlated with NPYR 1, 2, and 5 in visceral fat. There was no correlation of expression between depots, implying that the depots function differently [146]. Long-term over-expression of NPY in the PVN leads to increased adipose tissue weight and insulin resistance in mice, as determined by a euglycemic-hyperinsulinemic clamp test and intravenous glucose tolerance test. Glucose uptake was decreased in adipose tissue but was not affected in skeletal muscle, suggesting that effects of NPY over-expression on insulin resistance were tissue specific [147]. In the same study, 3T3-L1 cells were differentiated and treated with NPY, which decreased basal glucose consumption and decreased glucose uptake. This effect was not blocked by antagonism of NPY1R, but was blunted by antagonism of NPY5R [147]. It is difficult to directly attribute the increased PVN NPY to the insulin resistance in the adipose tissue, but that the *in vitro* effect of NPY can be blocked by antagonism of NPY5R suggests that this may be the case; nonetheless, more studies are needed to confirm this hypothesis. Such studies may provide evidence that NPY5R may be the key NPYR through which NPY signaling leads to insulin resistance, as overexpression of NPY is associated with insulin resistance that can be blunted when NPYR5 signaling is blocked. That adiponectin [148, 149], visfatin [150], and omentin [151] are involved in insulin sensitivity and are all correlated with NPY and NPY5R expression in subcutaneous adipose tissue [146] also implies that NPY and NPY5R play a role in insulin sensitivity.

Although NPY is already a target for drug development to combat obesity [126], these correlations must be considered when targeting the NPY system pharmacologically. Antagonizing the NPY system could decrease fat accretion while increasing bone formation, a potentially positive side effect of treating obesity; but because of their correlated expression, decreased expression of adiponectin, visfatin, or omentin could exacerbate insulin resistance. Additionally, in addition to obesity and bone physiology, NPY also effects many other systems and diseases, including anxiety, depression, epilepsy, alcoholism, pain, cancer, cardiovascular regulation, gastrointestinal tract, and circadian regulation, as reviewed [7]. Drug development has proved difficult when targeting NPY, as targeting central NPY is not very specific and concerns the blood brain barrier, thus targeting the periphery warrants further exploration [152].

NPY and Adipose Tissue Development in Chickens

Adipose tissue develops as a consequence of both hyperplasia and hypertrophy, with hyperplasia leading to hypertrophy. We reported changes in the adipose tissue of broiler chicks during the first two weeks post-hatch [72]. Specifically, for the subcutaneous, abdominal, and clavicular fat depots at days 4 and 14 of age, there were depot-specific differences with larger adipocytes and the greatest glycerol–3–phosphate dehydrogenase (G3PDH) activity in the subcutaneous fat at day 4. The abdominal fat grew more rapidly than the other two depots from day 4 to 14, and clavicular fat was intermediate for most traits that were measured. These changes were most likely due to a combination of hypertrophy and hyperplasia [72]. Neuropeptide Y and its receptors were also measured and from day 4 to 14 there was an increase in mRNA abundance of NPY and NPY receptor 5 (NPY5R) and a decrease in NPY2R in the clavicular adipose tissue.

The orexigenic properties of NPY are mostly associated with NPY1R [128], mRNA of which was not affected by age in clavicular adipose tissue, but did increase in the hypothalamus of broiler chicks from day 4 to 14 [72]. NPY receptors 1, 2, and 5 were all increased in the liver at 14 days post-hatch, implying that the NPY system may function in the liver during development [72]. Thus, NPY and several of its receptors are transcribed in chick adipose tissue and liver and appear to be differentially regulated during early post-hatch development, although functional implications are still unclear.

Our group also conducted an *in vitro* study showing that 4 hours of NPY treatment increased mRNA abundance of NPY and NPY2R in abdominal fat preadipocytes isolated from day 14 of age broilers [17]. With NPY being included in the differentiation cocktail, abundance of NPY was also increased on days 2 and 6 post induction of differentiation, whereas NPYR2 expression was not affected during this time [17]. That NPY2R mRNA expression was upregulated in preadipocytes in response to NPY may imply that NPY2R is more important to NPY function in the preadipocyte than in the differentiating adipocyte. On days 5 and 6 post-induction of differentiation, there was increased cell proliferation and G3PDH activity, respectively. This indicates that NPY treatment was associated with increased hyperplasia, as well as fat synthesis, as G3PDH activity is an indirect marker of triacylglycerol synthesis [153, 154]. Thus in chicken adipose cells, NPY may contribute to both hyperplasia and hypertrophy. While NPYR 1 and 5 seem to play a role based on data from *in vivo* studies, expression of NPYR 1 and 5 could not be detected in adipose cells in our *in vitro* studies [17]. This may be due to the difference in cell types included in each study. The *in vivo* studies included the whole adipose tissue, whereas in

the *in vitro* studies isolated the stromal vascular fraction of cells from adipose tissue and then enriched for mesenchymal stem cells and preadipocytes.

Interestingly, we reported heterosis for NPYR 1 and 5 mRNA in the adipose tissue of chickens from the Virginia body weight lines, suggesting that the NPY system is important for energy balance in chickens [73]. HWS chickens expressed more NPY and NPYR 1 and 5 mRNA in the abdominal fat [73], while LWS chicks expressed more NPY and NPYR 2 and 5 in the hypothalamus [155]. Additionally, expression of NPY5R in the hypothalamus is regulated differently between the fed vs fasted state, where in the fed state, NPY5R was more highly expressed in the LWS, and the magnitude of difference between the LWS and HWS was lessened by fasting [156].

Adipose Tissue Physiology: α-MSH

The peptide α-MSH is a part of the melanocortin system, which is made up of α, β, and γ – MSH, ACTH, melanocortin receptors (MCR) 1-5, and two endogenous MCR antagonists, agouti and agouti-related peptide (AgRP), as reviewed [157, 158]. All of the melanocortin peptides are derived from POMC [18], and have some function in regulating food intake. Our group recently showed that ACTH, and the C-terminal fragment of ACTH, beta-cell-tropin (βCT) have effects on food intake in chicks, with ACTH being anorexigenic [159], and βCT being orexigenic [160]; the same effects on food intake were reported in rats [20]. All of the MSH peptides decrease food intake in mice, with α-MSH being the most potent [161], but in chicks β and γ-MSH had no effect on food intake [22].

MC1R is mainly associated with pigmentation [162], but is also involved in the control of inflammation [163, 164], and has the highest affinity for α-MSH [165]. MC2R is the ACTH receptor, and is mainly associated with the action of ACTH on the periphery [166], namely the release of glucocorticoids [167]. It is also expressed in the adipocyte, and may function in regulating lipolysis [168]. MCR 3 and 4 are highly expressed in the brain [169, 170], and are involved in food intake and energy balance [171], and MC3R-deficient mice have increased fat mass [172]. MC4R is the receptor for both ACTH and α-MSH in the brain of rats [20], and α-MSH in the brain of chicks [22]. MC5R is expressed in many sebaceous and exocrine glands [173], regulates fatty acid oxidation in skeletal muscle [174], and is associated with lipolytic effects in the adipose tissue [23, 168].

In addition to its anorexigenic function, α-MSH is associated with decreasing body weight [19, 20]. α-MSH promoted lipolysis *in vitro*[23] and in mice reduced their fat mass [175, 176]. Signaling via MC5R increased lipolysis and impaired fatty acid re-esterification in 3T3-L1 adipocytes [23], providing a plausible route of action of α-MSH in adipose tissue. Because POMC is a precursor to multiple peptides, KO of POMC does not correlate with determining the function of a specific POMC cleavage product, which has led to other techniques to overexpress the specific peptides in order to ascertain their function. In two month-old male C57BL/6N mice, overexpression of α-MSH by a lentiviral vector (LVi-α-MSH-EGFP) in the nucleus tractus solitarius decreased fat mass, food intake, and body weight [175]. The phosphatidylinositol 3-kinase (PI3K) pathway is important in the regulation of food intake and energy homeostasis in the hypothalamus [177, 178], and inhibition of two PI3K's, PI3Kβ and PI3Kγ, led to increased NE concentrations in the adipose tissue, which then led to decreased fat mass and was associated

with increased lipolysis and browning of white adipose tissue in adult mice [176]. It was suggested that the increase in NE was due to increased α-MSH-dependent sympathetic drive as cAMP production was also increased in the intermediolateral nucleus, an area where energy expenditure is regulated by α-MSH [179]. Moreover, intracerebroventricular injection of α-MSH into wild-type mice caused increased phosphorylation of hormone sensitive lipase (HSL), a lipase known to be activated by NE [180, 181], to the same extent as in PI3Kβ- and PI3Kγ-inhibited mice [176]. In humans, α-MSH stimulated lipolysis in intact white adipose tissue but not in isolated preadipocytes that were differentiated into adipocytes, suggesting that the effect may be dependent on neuronal innervation [182]. Clearly, α-MSH has effects on the adipose tissue, some of which may relate to its role in the sympathetic nervous system.

The nuclear hormone receptor (NR) 4A subgroup is involved in adipose tissue metabolism, with effects on differentiation and proliferation [183, 184]. Treatment of differentiated 3T3-L1 cells with an α-MSH agonist (NDP-MSH) for 2 hours was associated with increased mRNA expression of members of the NR4A subgroup, but not other subgroups in the NR superfamily [185]. Furthermore, siRNA-mediated knockdown of nuclear hormone receptor subfamily 4 group A member 1 (NR4A1) attenuated the effects of NDP-MSH treatment on gene expression in 3T3-L1 adipocytes. Intraperitoneal (IP) injection of NDP-MSH into seven-week-old C57 BL/6J male mice was associated with increased expression of NR4A1, suggesting that expression of NR4A1 is necessary for the action of α-MSH.

These studies collectively indicate that α-MSH has effects on the adipose tissue that are lipolytic, and signaling initiated from the brain and sympathetic nervous system can act to decrease fat mass. Involvement of the NR superfamily has also been implicated in the action of α-MSH, and

MC5R may be an important receptor for mediating effects of the melanocortin system in the adipose tissue. More *in vivo* studies are needed to confirm that MC5R is important for adipose tissue function, and whether or not there are different effects through the various receptors. To date, effects of the melanocortin system in adipose tissue has not been reported in non-mammalian species.

Communication between α-MSH and NPY

Both NPY and α-MSH have strong, opposing effects on food intake, with effects conserved across a range of vertebrate species. In chicks, combined intracerebroventricular (ICV) injection of both α-MSH and NPY results in a decrease in food intake [186], the orexigenic effect of NPY likely overpowered by the anorexigenic effect of α-MSH. Because α-MSH is a peptide derived from POMC, post-translational processing becomes very important in regulating the quantity of the active peptide, and serves as a point of entry for intervention, either through pharmaceutical means, feedback loops, or action of other neurotransmitters. NPY has been implicated in inhibiting post-translational processing of POMC to yield α-MSH by decreasing prohormone convertase 2 (PC2) protein; this effect is associated with downregulation of early growth response protein 1 (EGR-1) and is likely occurring via NPY1R, as blocking NPY1R is able to restore PC2 activity and α-MSH release [8]. After ICV injection, NPY decreased the phosphorylation of CREB, an effect normally caused by α-MSH, and NPY also decreased the amount of α-MSH in the PVN [8]. When co-injected, α-MSH overpowers the orexigenic effect of NPY [186], but when promoting positive energy balance NPY signals to decrease the amount of α-MSH in the hypothalamus [8]. This may imply that the effect of combined injection is more of a pharmacological response than physiological.

Potential Physiological Routes through which NPY and α-MSH Affect Adipose Tissue

Although most studies concerning the interaction of NPY and α-MSH are in relation to the brain and control of food intake, there may also be interactions between them in adipose tissue. Melanotan-II is a non-selective MCR agonist, and a 7 day-long central infusion into rats reduced feeding and adiposity, and when infused simultaneously with NPY reduced feeding and attenuated NPY-mediated increases in fat pad weight [187]. Although combined injection is thus able to inhibit some of the effects of NPY, it does not block NPY-mediated inhibition of the gonadotropic and somatotropic axes [187], suggesting that crosstalk between MSH and NPY is tissue and/or axis specific rather than global.

Circulating plasma levels of NPY are increased in obese and overweight humans, but circulating α-MSH levels are similar between normal, overweight and obese individuals [188]. This indicates that increased weight from adipose tissue has impacts on circulating NPY, but may not impact plasma α-MSH. Moreover, in obese subjects after weight loss, cerebrospinal fluid (CSF) concentrations of NPY decrease whereas α-MSH levels remained unchanged [189].
The interaction of NPY and α-MSH is complex, and much is still unknown as there is little reported on the role of α-MSH and its interaction with NPY and other factors in the adipose tissue. The fat-loss effect of α-MSH may not be a direct effect on the adipose tissue, but rather an indirect effect of decreasing the amount of energy available from reduced energy intake, thus forcing the animal to tap into its energy reserves in the adipose tissue to maintain energy balance. Likewise, the fat-synthesizing effect of NPY in the adipose tissue is likely a response to increased energy intake (and thus availability) mediated via the hypothalamus.

Conclusions

Factors involved in regulating energy balance and adipose tissue physiology are crucial to understand in light of the current obesity epidemic and increasing importance of enhancing nutrient utilization efficiency and meat production in agricultural species to meet the demand for dietary protein as the global population continues to increase. The adipose tissue is a diverse endocrine organ, with many cell types and models used to study its function. Because of its complicated physiology, there are multiple cellular pathways to explore for pharmacological targeting, but also many functions that may not directly relate to whole-body energy balance. NPY exerts multiple functions in the adipose tissue mediated by distinct receptor sub-types, but also regulates metabolism in other tissues such as bone. Knockout and antagonism of NPY are associated with reduced adiposity and body weight, but because of its diverse physiological functions, affecting solely the lipid metabolism in adipose tissue is a challenge in targeting this system to treat obesity. Regulation of α-MSH could also be a potential route of intervention, as it is associated with not only a decrease in feeding, but also decreased body weight and increased lipolysis. The interaction of these two peptides is also important and multi-faceted; the two have opposing effects on appetite and adipocyte metabolism and at times one may inhibit the expression and activity of the other. Further study of NPY and α-MSH functions in the brain-fat axis, as well as identification of other appetite-regulatory factors that affect adipose tissue physiology will provide useful information in the development of pharmacological strategies to treat obesity and also approaches to modulate energy utilization in animals raised for food consumption.

Table 2.1. Transcription factors involved in adipocyte differentiation

Transcription Factor[1]	**Time when expression is induced during differentiation**	**Citation**
PPARγ	Early and throughout	[40-42]
C/EBPβ	Early	[55, 56, 58]
C/EBPδ	Early	[55, 56]
C/EBPα	Following expression of C/EBPβ and C/EBPδ	[55-57]
SREBP	Early	[50, 54]

[1]PPARγ: Peroxisome proliferator-activated receptor γ; C/EBPβ, C/EBPδ, and C/EBPα: CCAAT/Enhancer Binding Protein β, δ, and α, respectively; SREBP: sterol regulatory element-binding protein

Table 2.2. Physiological actions of Neuropeptide Y (NPY) related to energy balance and the receptors (NPYR) involved

Action[1]	**Impact (+/-)**	**Receptor**	**Citation**
Lipid Accumulation	+	NPYR 2 & 5	[17, 118, 132, 190]
Lipolysis	-	NPY1R	[140, 191]
Cellular Proliferation	+	NPY2R	[16, 17, 119, 144]
Food Intake	+	NPYR 1 & 2	[127, 128, 192]
Body Weight Gain	+	NPYR 1, 2 & 5	[115, 193, 194]
WAT Formation	+	NPYR 1 & 2	[115, 143, 195]
BAT Formation	-	NPYR 1 & 5	[120, 142, 196]
Insulin Resistance	+	NPY5R	[147]
Glucose Consumption	-	NPY5R	[147]
Bone Formation	-	NPYR 1 & 2	[121-125]

[1]WAT: white adipose tissue; BAT: brown adipose tissue

Table 2.3. Effects of NPY receptor (NPYR) antagonism in preadipocytes and adipocytes

Receptor Antagonized	**Effect of Antagonism**	**Citation**
NPY1R	Blocks NPY-induced inhibition of lipolysis	[140]
NPY2R	Decreased cell number	[144]
NPY5R	Blocks decrease in glucose uptake	[147]
NPYR 1, 2, & 5	Blocks increase in adipogenesis by epinephrine	[118]

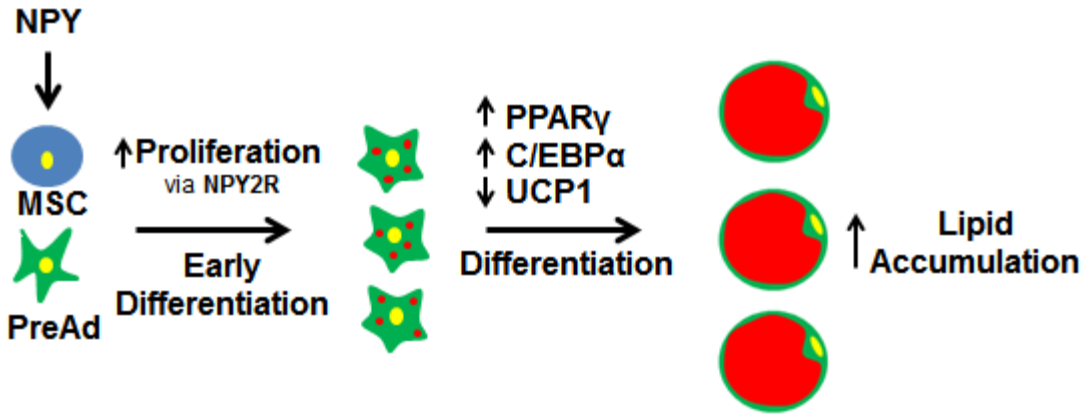

Figure 2.1. Adipogenic effect of NPY during adipocyte differentiation.
When neuropeptide Y (NPY) is included in the differentiation cocktail of isolated cells from the stromal vascular fraction (mesenchymal stem cells (MSC) and preadipocytes (PreAd)) there is increased cellular proliferation of not-yet fully differentiated cells via NPY receptor 2 (NPY2R) early on in differentiation. Throughout differentiation, there is increased expression of peroxisome proliferator activated receptor (PPARγ) and CCAAT/enhancer-binding protein alpha (C/EBPα), and decreased expression of uncoupling protein 1 (UCP1), thereby leading to increased lipid accumulation in the terminally differentiated adipocyte. Yellow represents the cell nucleus and red represents the lipid droplet.

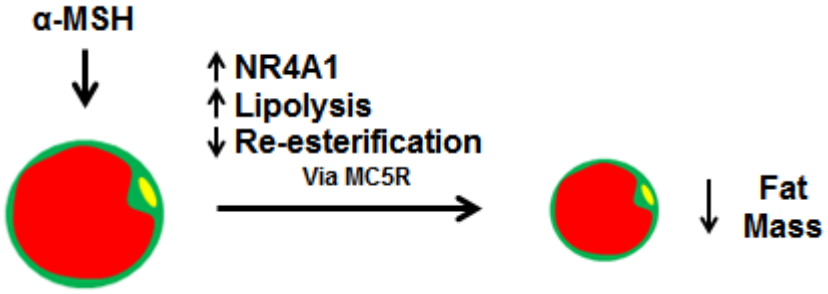

Figure 2.2. Action of α-MSH on the adipocyte.
When α-melanocyte stimulating hormone (α-MSH) reaches the adipocyte, it binds to melanocortin receptor 5 (MC5R) and increases expression of nuclear hormone receptor subfamily 4 group A member 1 (NR4A1), and increases lipolysis while also inhibiting re-esterification, leading to a decrease in fat mass and body weight. Yellow represents the cell nucleus and red represents the lipid droplet.

Chapter 3: Promotion of adipogenesis by neuropeptide Y during the later stages of chicken preadipocyte differentiation

[197]

Steven L Shipp, Mark A Cline, Elizabeth R Gilbert

Department of Animal and Poultry Sciences, Virginia Tech, Blacksburg, VA 24061

Abstract

Neuropeptide Y (NPY) promotes adipogenesis in both mammals and chickens. The objective of this study was to evaluate effects of NPY on male chick preadipocyte proliferation and differentiation. Preadipocytes were treated with 0, 1, 10, or 100 nM NPY for 12, 24, or 48 hours and gene expression and proliferation measured. Cells were also treated with NPY during differentiation and cells harvested at 8, 10, and 12 days post-induction of differentiation. At 12 hours, expression of topoisomerase II alpha (TOP2A), and thioredoxin-dependent peroxidase 2 was up-regulated and NPY was down-regulated in response to NPY (0 vs. 100 nM) in preadipocytes. At day 8 post-induction of differentiation, there was increased lipid accumulation (0 vs. 10 and 100 nM), expression of CCAAT/enhancer binding protein β and fatty acid binding protein 4 (FABP4) (0 vs. 100 nM), and sterol regulatory element-binding protein (0 vs. 10 and 100 nM) mRNA in NPY-treated cells. At day 10, FABP4 and Kruppel-like factor 7 mRNAs were downregulated (0 vs. 10 and 100 nM, and 100 nM, respectively), and at day 12, TOP2A mRNA was down-regulated in response to NPY treatment (0 vs. 100 nM). Proliferating cells decreased on day 8 in response to NPY (0 vs. 10 nM). Activity of glycerol-3-phosphate (G3PDH) was increased on days 10 and 12 in NPY-treated cells (0 vs. 100 nM). Increased expression of proliferation markers in preadipocytes, and during differentiation increased expression of transcription factors and a fatty acid transporter, increased lipid accumulation, and increased activity of G3PDH suggest that NPY may enhance preadipocyte activity, adipogenesis and promotes lipid accumulation throughout chicken adipocyte differentiation.

Keywords: chick, NPY, adipogenesis, proliferation, differentiation

Introduction

Neuropeptide Y (NPY) plays an important role in regulating whole-body energy balance. Its orexigenic properties have been documented in numerous vertebrates, including mammalian [10, 11], teleost [12], and avian species [13-15]. NPY also promotes adipose tissue expansion in mice and humans [16], with the adipogenic action of NPY mostly likely mediated via NPY receptor 2 (NPY2R) [16]. NPY also inhibits lipolysis in 3T3-L1 cells, mediated by NPY1R [140], and brown adipose tissue thermogenesis [195].

Our group was the first to report effects of NPY on adipose-derived cells in an avian model. We found that the stromal vascular fraction (SVF) of cells from the abdominal fat of young broiler chickens respond to NPY with increased NPY and NPY2R mRNA expression at 4 hours post-treatment [17], suggesting that NPY promotes positive feedback of its own expression through NPY2R. There was also decreased expression [17] of proliferation markers thioredoxin-dependent peroxidase 2 (TPX2) [198] and topoisomerase II alpha (TOP2A) [199]. In that same study, we evaluated effects of daily NPY treatment on differentiation into adipocytes. After induction of differentiation, in response to NPY there was increased mRNA abundance of preadipocyte and proliferation markers until day 6 and decreased mRNA expression of transcription factors on days 4-6 post-induction of differentiation [17]. There was increased cellular proliferation on day 5 post-induction of differentiation in NPY-treated cells, suggesting that NPY promotes mitotic expansion of chick preadipocytes during the initial stages of differentiation [17]. On day 6 post-induction however, there was increased mRNA expression of lipoprotein lipase (LPL) and fatty acid binding protein 4 (FABP4) [17], two factors important for cellular release and transport of fatty acids during adipogenesis [200-202], and increased activity of glycerol-3-phosphate dehydrogenase (G3PDH) [17], an indirect marker of triacylglycerol

synthesis [153, 154]. These data suggest that NPY enhances chick preadipocyte activity during the early stages of differentiation and promotes lipid deposition during the terminal stages of adipocyte maturation, although effects have not been reported after 12 hours post-treatment in preadipocytes and after day 6 post-induction of differentiation.

Hence, to better understand NPY's effects on preadipocytes and during the later stages of adipocyte differentiation in chicken adipose cells, we evaluated gene expression and proliferation at 12, 24, and 48 hours post-treatment with NPY, and cellular proliferation, G3PDH specific activity, neutral lipid accumulation, and gene expression on days 8, 10, and 12 post-induction of differentiation in cells treated with NPY during differentiation.

Materials and Methods

Animals

All animal protocols were approved by the Institutional Animal Care and Use Committee at Virginia Tech and animals were cared for in accordance with the Guide for the Care and Use of Laboratory Animals. Day of hatch Cobb-500 broiler chicks were obtained from a local hatchery. Chicks were group caged at 30 ± 1 °C and 50 ± 5% relative humidity with free access to water and a mash diet (22% crude protein and 3,000 kcal metabolizable energy/kg), the composition of which has been reported elsewhere [203]. The ambient temperature was gradually decreased from 30 °C on day 1 to 25 °C by 0.5 °C per day, and then 25 °C until 14 days post-hatch.

Primary adipose cell culture

Reagents were purchased from Sigma Aldrich (MO, USA) unless otherwise stated. Approximately two grams of abdominal fat was collected from 14 day-old male chicks by sterile

dissection and submerged in DMEM/F12 Glutamax (Gibco, NY, USA) media containing 1% penicillin/streptomycin (HyClone, MA, USA) warmed to 37 °C. Under the biological safety cabinet, adipose tissue was minced into fine sections with scalpel blades and incubated in 10 mL of 4-(2-hydroxyethyl) piperazine-1-ethanesulfonic acid (HEPES) solution (0.1 M HEPES, 5 mM d-glucose, 1.5 % bovine serum albumin; BSA) containing 500 units/mL Collagenase, Type I (Worthington Biochemical Corporation, NJ, USA) for 1 hour at 37 °C in a shaking water bath. After the incubation, the contents were filtered through 250 μm filters (Pierce, IL, USA). The filtrate was then centrifuged at 200 ×g for 10 min to separate floating adipocytes from the other cell types. The supernatant was discarded, and cell pellets were resuspended in 10 mL of red blood cell lysis buffer (155 mM NH_4Cl, 10 mM $KHCO_3$, 0.1 mM EDTA) to remove the red blood cells. The contents were then filtered through a 20 μm mesh (Celltrics, NJ, USA) to filter out the endothelial clumps. The filtrate was then centrifuged at 200 ×g for 5 min to obtain the stromal vascular fraction (SVF) of cells. The SVF was resuspended in plating media (DMEM/F12 containing 10% defined fetal bovine serum (FBS); HyClone, and 1% penicillin/streptomycin) and seeded directly into a petri dish. After 72 hours, cells were passaged one time, and then seeded 48 hours later at a density of 3×10^4 cells per mL into 12-well plates (Falcon, MA, USA) and incubated at 37 °C in a 5 % CO_2 humidified atmosphere for at least 48 h (to minimize pro-inflammatory cytokine secretion) before beginning experiments. For all experiments, there were at least three biological replicates, where the experimental unit represented cells from an individual chick (n = 3 chicks), with triplicate wells of each treatment within an experiment for cells collected from a single chick. The triplicate values were averaged before statistical analysis.

NPY treatment and cellular proliferation

Cells were seeded in 12-well plates and cultured in plating media until 50% confluence. Cells were then cultured in serum-free media for 24 h for cell cycle synchronization. In order to minimize the confounding effects of serum-derived NPY, cells were cultured in basic media (DMEM/F12 with 1% penicillin/streptomycin) containing 1.5% FBS and 0, 1, 10, or 100 nM chicken NPY (custom synthesized by AnaSpec; > 98 % purity).

The effect of NPY on cellular proliferation was evaluated using the Click-iT® EdU Alexa Fluor® 488 Imaging Kit (Invitrogen, CA, USA). The EdU contains a nucleoside analog of thymidine and alkyne, which allows the thymidine analog to be incorporated into DNA during active DNA synthesis and be detected by the Alexa Fluor dye that contains the azide. Briefly, 1 μL of EdU was added into each well 2 hours before the assay was conducted, a time recommended by the company to allow for adequate incorporation of Edu. Culture media was removed, and cells were fixed with 3.7% methanol-free formaldehyde in phosphate-buffered saline (PBS) for 15 min. Buffer containing 0.5% Triton X-100 in PBS was then added to each well and cells were incubated for 20 min, followed by addition of 0.5 mL of Click-iT reaction cocktail and incubation for 30 min. Cells were then stained with Hoechst 33342 solution for determining total cell number. Using a Nikon Eclipse Ti inverted microscope representative images were captured and digitized with a charge-coupled camera (SPOT, Diagnostic Imaging, Sterling Heights, MI, USA), and analyzed using image overlay functions of NIS-Elements Advanced Research Software (Nikon, NY, USA). Briefly, five images were captured from different fields in each well for both of the fluorophores and image overlays performed. The new proliferating cells and total cell number were counted for statistical analysis.

NPY treatment was given at 8:00 am for the 24 and 48 hour treatments and at 8:00 pm for the 12 hour treatment in order to conduct each individual collection at the same time of day. At 12, 24, and 48 hours post-NPY treatment, as well as days 8, 10, and 12 post-induction of differentiation, cells were evaluated for cellular proliferation and harvested for total RNA isolation and gene expression analysis of proliferation markers as described in the methods below.

NPY treatment and cellular differentiation

The adipocyte differentiation protocol was similar to a method that has been described [93]. Briefly, cells were cultured in plating media and allowed to reach complete confluence. Plating media (DMEM/F12 basic media with 10% FBS) was replaced with induction media (DMEM/F12 basic media containing 200 nM insulin, 1 μM dexamethasone, 10 U/mL heparin, and 2.5% chicken serum; CS) containing 0, 1, 10, or 100 nM chicken NPY. At 48 h post-induction, media was replaced with insulin-containing media (DMEM/F12 basic media containing 2.5% CS and 200 nM insulin). After another 48 h, and for the remainder of the study, cells were cultured in maintenance media (DMEM/F12 basic media with 2.5% CS). Daily NPY treatment, the changing of media and time each experiment was conducted were always between the hours of 8:00 and 10:00 am.

Oil Red O staining and lipid quantification

Cells were fixed with 10% neutral-buffered formalin for 30 min at room temperature and Oil Red O staining was performed according to the manufacturer's instructions (Oil Red O Stain Kit; American Master Tech). Propylene glycol was added to each well and incubated for 5 minutes,

replaced with pre-heated Oil Red O working solution and incubated for another 5 minutes at room temperature, and rinsed with distilled water. Cells were then counterstained with Modified Mayer's Hematoxylin (supplied in kit) for 1 minute and rinsed with distilled water, then digital images captured to estimate the lipid content. To quantify neutral lipids, water was removed from each well, and 250 µl of 100% isopropanol was added to each well and incubated for 5 minutes to solubilize Oil Red O, and absorbance measured at 510 nm with a multi-mode plate reader (Tecan Infinite M200 Pro) [204].

Glycerol-3-phosphate dehydrogenase (G3PDH) specific activity

The method for assaying G3PDH specific activity was adapted from two other studies [205, 206]. Briefly, cells were cultured in 12-well plates and treated as described above. On days 10 and 12 post-induction of differentiation, cells were washed with PBS, 200 µL of lysis buffer (50 mM Tris–Cl, 1 mM EDTA, and 1 mM β-mercaptoethanol, pH 7.5) was added to each well, and cells were detached from the plate using cell scrapers. Lysates were transferred to microcentrifuge tubes and further lysed with a 21-gauge needle, then sonicated at 4 °C using a Bioruptor 300 (Diagenode) with 4 cycles of 30 sec on and 30 sec off at high frequency. Lysates were then centrifuged at 12,000 ×g at 4 °C for 30 min, and the supernatant used for measuring G3PDH activity and for determining total protein concentration. The G3PDH activity was measured for each sample in duplicate in assay buffer (100 mM triethanolamine–HCl, 2.5 mM EDTA, 0.12 mM NADH, 0.2 mM dihydroxyacetone phosphate (DHAP), 0.1 mM β-mercaptoethanol, pH 7.5) in a total reaction volume of 200 µL in UV transparent plates (Corning, MA, USA) using a µQuant plate reader and KC Junior software (Bio-Tek, VT, USA). Absorbance was measured at 340 nm for 20 cycles at 25 °C and the maximum slope calculated

from the absorbance data. Protein concentration was quantified with Bradford BCA reagent (Sigma-Aldrich, MO, USA) using an Infinite M200 Pro multi-mode plate reader and Magellan software (Tecan, CA, USA). The maximum slope was normalized to the protein concentration to calculate specific activity, which is reported as μmol/min · mg.

Total RNA isolation and real time PCR

Cells in 12-well plates were washed with PBS and lysed with a 21-gauge needle in 350 μL RLT buffer (Qiagen, CA, USA). The total RNA was extracted with the RNeasy Mini kit (Qiagen, CA, USA) according to the manufacturer's instructions. The eluted total RNA samples were quantified and assessed for purity by spectrophotometry at 260/280/230 nm using a Nanophotometer™ Pearl (IMPLEN, CA, USA), and their integrity evaluated by agarose gel electrophoresis. The first strand cDNA was synthesized from 200 ng total RNA using the High Capacity cDNA Reverse Transcription kit (Applied Biosystems, NY, USA). Primers were designed in Primer Express 3.0 (Applied Biosystems, NY, USA; sequences given in [17]). All primers were evaluated for amplification efficiency before use. Efficiency of target genes was within 5% of the reference gene (actin). A total volume of 10 μL in each reaction contained 5 μL fast SYBR Green Master Mix (Applied Biosystems, NY, USA), 0.25 μL each of 5 μM forward and reverse primers, and 3 μL of 10-fold diluted cDNA. Real-time PCR reactions were performed in duplicate for all samples on an Applied Biosystems 7500 FAST system, under the following conditions: enzyme activation for 20 sec at 95 °C and 40 cycles of 1) melting step for 3 seconds at 95 °C and 2) annealing/extension step for 30 seconds at 60 °C. A melting curve analysis was performed after all reactions to ensure amplification specificity.

Statistical analysis

The real time PCR data were analyzed using the ΔΔCT method, where ΔCT = CT target gene − CT Actin, and ΔΔCT = ΔCT target sample − ΔCT calibrator [207]. The average of the control group within a time point was used as the calibrator sample. The relative quantity ($2^{-\Delta\Delta CT}$) values were subjected to ANOVA using the Fit Model Platform of JMP (SAS Ins., Cary, NC). The statistical model included the main effect of treatment. Tukey's test was used post-hoc in all experiments, except for the proliferation study in which Dunnett's test was used to compare control and NPY-treated groups for mRNA abundance of the preadipocyte and proliferation markers. A similar model was used for the cell count/percentage data, Oil Red O absorbance, and for G3PDH specific activity data. For the proliferation experiment, an arcsine transformation was applied to the percentage of proliferating cells before analysis. Results were considered significant at $P < 0.05$.

Results

Cellular proliferation

After reaching 50% confluence, the cells were cultured in serum-free media for cell cycle synchronization for 24 hours and then cells were cultured in basic media containing 1.5% FBS and 0, 1, 10, or 100 nM chicken NPY. There was no effect of NPY treatment on proliferating cell number or proliferating cells as a percentage of total cells at 12, 24, or 48 hours post-treatment of NPY (Figure 3.1). There is no difference between treatment groups, and when all groups from each time point were compared, there was a decrease in the percentage of proliferating cells from 12 hours to 24 and 48 hours post-treatment, but no difference between 24 and 48 hours post-treatment ($P = 0.0002$).

Gene expression of preadipocyte and proliferation markers

After reaching 50% confluence, the cells were cultured in serum-free media for cell cycle synchronization for 24 hours and then cells were cultured in basic media containing 1.5% FBS and 0, 1, 10, or 100 nM chicken NPY. At 12 hours post-treatment of NPY, there was increased TPX2 mRNA in response to 100 nM NPY, increased TOP2A mRNA in response to both 10 and 100 nM NPY, and decreased NPY mRNA in response to 100 nM NPY (Figure 3.2). There was no effect of NPY treatment on mRNA abundance of any of the genes measured at 24 or 48 hours post-treatment of NPY (data not shown).

Cellular proliferation during differentiation

On day 8, 10, and 12 post-induction of differentiation, cells were treated with Edu 2 hours before collection, and there was a decrease in proliferation in response to 10 nM NPY on day 8 (Figure 3.3). NPY had no effect on proliferation on either day 10 or 12 for any dose. When the controls from each day are compared based on time there was a decrease in the percentage of proliferating cells from day 8 to day 10 and 12, but no difference between day 10 and 12 (P = 0.006).

G3PDH specific activity and lipid accumulation during differentiation

There was increased G3PDH activity in response to 100 nM NPY on both day 10 and 12 post-induction of differentiation (Figure 3.4).

Oil Red O staining and lipid accumulation during differentiation

There was increased lipid accumulation (absorbance of Oil Red O at 510 nm) at day 8 post-induction of differentiation ($P = 0.006$) in response to 10 and 100 nM NPY (Figure 3.5A). There was no effect of treatment on absorbance at day 10 ($P = 0.09$) or 12 ($P = 0.43$) post-induction of differentiation (Figure 3.5A). Representative micrographs are shown in Figures 3.5 B and C.

Gene expression during differentiation.

On day 8 post-induction of differentiation, there was increased mRNA abundance of C/EBPβ and FABP4 in response to 100 nM NPY, and up-regulation of SREBP mRNA in response to 10 and 100 nM NPY (Figure 3.6A). On day 10, there was decreased mRNA abundance of FABP4 in response to 10 and 100 nM NPY (Figure 3.7A), and decreased mRNA abundance of KLF7 in response to 100 nM NPY (Figure 3.7B). On day 12 post-induction of differentiation there was decreased TOP2A mRNA in response to 100 nM NPY, and decreased expression of Ki67 in response to 100 as compared to 10 nM NPY (Figure 3.8B).

Discussion

Effects of NPY on adipose cell proliferation

To understand NPY's effects on growth of the precursor cells isolated from the SVF of chick adipose tissue, we measured cellular proliferation and gene expression at several time points post-treatment in precursor cells grown under conditions to promote proliferation. In our earlier study, effects on gene expression were measured at 4 hours and cellular replication at 12 hours post-treatment with NPY [17]. The number of proliferating cells was not affected by NPY at 12 hours post-treatment in the previous study [17]. To evaluate whether this was sufficient time for effects of NPY to be observed as transcriptional or cell number changes, the present study was extended to include 12, 24, and 48 hours as the end points. In our previous study, at 4 hours post-

treatment with NPY, there was decreased TPX2 and TOP2A mRNA [17], the opposite of what we observed in the current study at 12 hours post-treatment. Because expression of these genes decreased at 4 hours, but increased at 12 hours, the increase at 12 hours may not be a direct response to NPY, but rather recovering from the decrease in expression observed at 4 hours to reestablish normal growth. Also, at 4 hours, expression of NPY and NPY2R increased [17], whereas at 12 hours NPY mRNA decreased in response to the same dose. This could be due to a similar mechanism as for TPX2 and TOP2A; that the decrease in NPY at 12 hours may not be a direct response to NPY, but rather a recovery to normal homeostatic levels of expression. This is further evidenced by the absence of changes in expression at 24 and 48 hours. The direct effects of NPY on the SVF of cells may occur earlier than twelve hours. Because of the lack of an effect on cell proliferation at any of the time points measured in either study (12, 24, or 48) it is likely that NPY does not act to enhance cell proliferation in adipose precursor cells in chickens. However, that some transcriptional effects were observed early on during treatment suggests that NPY is affecting metabolic activity of the cells.

When the percentage of proliferating cells is compared by effect of time, there is a decrease in proliferation from 12 to 24 hours post-treatment of NPY, and no difference between 24 and 48 hours post-treatment of NPY. This is most likely due to the design of the experiment. Prior to NPY treatment, the cells are cultured in serum-free media for cell cycle synchronization. They are then cultured in basic media containing 1.5% FBS and the respective NPY treatments, thus they have adequate nutrients available to proliferate. After the first 12 hours, there are fewer cells available that have not undergone cell division, and this is most likely why the decrease in the percentage of proliferating cells is seen from 12 to 24 hours. Because there is also no difference

in proliferation between 24 and 48 hours, the cells have most likely come to a homeostatic level of proliferation within 24 hours.

In 3T3-L1 preadipocytes, low doses of NPY (10^{-15} M and 10^{-13} M) enhance proliferation after 24 hours, but higher doses had no such effect [119]. The current study did not evaluate an NPY dose lower than 1 nM (10^{-9}), thus it is possible that a lower dose would produce an effect on proliferation. An effect with a dose that low would be unexpected, as the lowest dose used in our studies had no effect on expression of any of the genes measured at any time point (4, 12, 24, and 48 hours) in our previous [17] and current study.

Effects of NPY on adipose cell differentiation

During differentiation, PPARγ, C/EBP α and β, and SREBP are important transcription factors that are sequentially induced and function to regulate expression of factors that are involved in lipid accumulation and expansion of the adipocyte, as reviewed [38, 39]. In our previous study, PPARγ, C/EBPα, and SREBP mRNAs decreased in response to NPY on day 4 post-induction of differentiation [17]. Expression of preadipocyte and proliferation markers TOP2A, TPX2, GATA2, and Ki67 increased in response to NPY throughout the first 6 days post-differentiation [17]. Taken together, this may suggest that NPY is delaying differentiation by inhibiting expression of these transcription factors important for development of the adipocyte in order to increase preadipocyte proliferation and activity during the early stages of adipogenesis [17]. That there was increased expression of two transcription factors on day 8, C/EBPβ and SREB, in the present study, further supports that the effect of NPY during differentiation may be to increase preadipocyte activity early on and delay differentiation until the later stages, where transcription

factors were observed to increase in the current study. SREBP has also been reported to cause chicken embryo fibroblasts to transdifferentiate into adipocyte-like cells when expressed by retrovirus-mediated gene transfer [208], showing its importance during adipocyte differentiation and suggesting that in the current study increased expression on day 8 contributes to adipocyte differentiation. There was also decreased expression of KLF7 on day 10 and TOP2A on day 12 in response to NPY, possibly due to the increased adipogenic activity and fewer preadipocyte cells at this stage of differentiation. Another explanation for the decreased expression of TOP2A on day 12 could be due to apoptosis from cells that were unable to fully differentiate.

On day 5 post-induction of differentiation there was increased proliferation in NPY-treated cells [17], an effect that may have been due to the presence of preadipocytes still undergoing differentiation that were either induced to proliferate again or to undergo the mitotic expansion that is characteristic of mammalian 3T3L-1 preadipocytes [209]. To better understand this unexpected effect, we measured cellular proliferation on days 8, 10, and 12 post-induction, times at which a greater proportion of the cells should be terminally differentiated. That there was no increase of proliferation during the later time points suggests that the effect on proliferation at day 5 is from cells that have not yet terminally differentiated into adipocytes. This is further evidenced by the decrease in proliferation on day 8, and combined with gene expression data suggests that transcriptional regulation has switched from increasing preadipocyte activity to increasing adipogenic activity. Further, when the control groups from days 8, 10, and 12 post-induction are compared, there is a decrease in the percentage of proliferating cells from day 8 to day 10, and no significant difference in proliferation from day 10 to 12. This suggests that there are fewer cells available to proliferate in the later stages of differentiation, and mature adipocytes

are thought to be incapable of division [210]. These data support that our experimental design is representative of preadipocyte differentiation, and that by day 10 most cells have terminally differentiated.

At day 6 post-induction of differentiation, G3PDH activity was greater in NPY-treated cells [17], suggesting that NPY affects triacylglycerol synthesis either directly or indirectly as an important component of terminal differentiation [153, 154]. In the present study this effect persisted through days 10 and 12, suggesting that NPY continued to have an effect on terminal differentiation through the later stages of adipocyte maturation. That there was no change in G3PDH activity during the first 4 days post-induction of differentiation in our earlier study [17], but a clear effect on days 6-12 suggests that NPY is increasing fat synthesis during the later stages of differentiation. This is further supported by the increase in neutral lipid accumulation at day 8, an effect also observed in 3T3-L1 cells at day 8 of differentiation [119]. Decreased expression of FABP4 on day 10 may suggest that elevated levels of this specific binding protein are no longer needed past day 10 in the lipid-droplet-containing adipocyte, but that expression of FABP4 increased on days 2, 6, and 8 suggests that NPY signaling is associated with increasing the amount of fatty acids available in the cell to be transported to build the triacylglycerols in adipocytes.

In conclusion, results suggest that NPY increases chick preadipocyte activity within the first 12 hours post-treatment, but has no effect on proliferation. During chick preadipocyte differentiation, NPY treatment may be associated with enhanced preadipocyte activity during the early phase, thereby delaying differentiation until the terminal stages, where increased

expression of SREBP, C/EBPβ, and FABP4, increased lipid accumulation, increased G3PDH activity, and decreased expression of KLF7 and TOP2A all support that there was greater adipogenic activity. Understanding the mechanisms underlying effects of appetite-regulating peptides on physiological pathways associated with energy metabolism in the periphery in an avian model may have implications for understanding metabolic disorders in humans and also agricultural relevance.

Grants

This research was supported by a National Science Foundation EAGER grant (IOS 1420285) and in part, by the Virginia Agricultural Experiment Station and the Hatch Program of the National Institute of Food and Agriculture, U.S. Department of Agriculture.

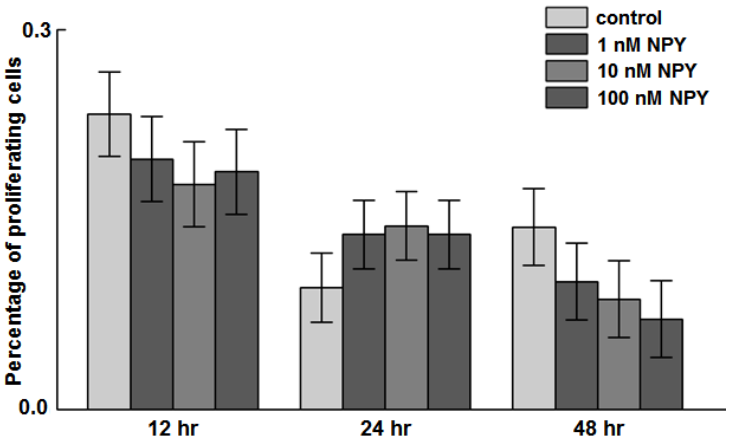

Figure 3.1. Effects of neuropeptide Y (NPY) treatment on proliferating cell number at 12, 24, and 48 hours. The stromal–vascular fraction of cells isolated from 14 day-old chicken abdominal adipose tissue was treated with 0, 1, 10 or 100 nM chicken NPY. Total cell number and number of proliferating cells were counted and the percentage of proliferating cells arcsine transformed before analysis. Values represent least squares means ± SEM of the percentage of proliferating cells (n = 3).

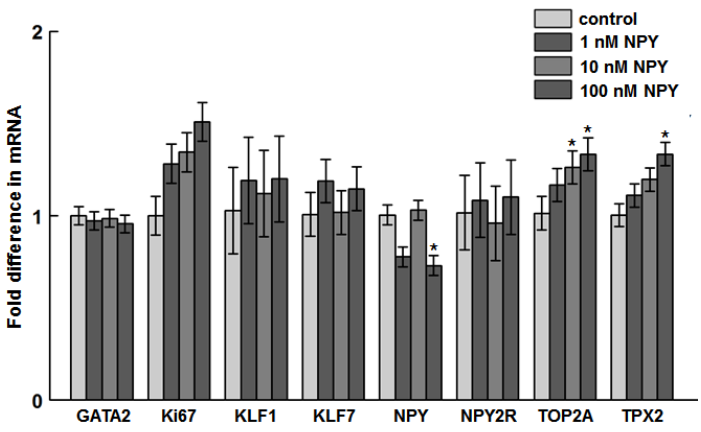

Figure 3.2. Effects of NPY treatment on gene expression of preadipocyte and proliferation markers at 12 hours post-treatment in the stromal–vascular fraction of cells isolated from abdominal fat of 14 day-old broilers. GATA2: GATA-binding protein 2 ($P = 0.98$); Ki67: Ki67 ($P = 0.09$); KLF1: Krüppel-like factor 1 ($P = 0.79$); KLF7: Krüppel-like factor 7 ($P = 0.67$); NPY: neuropeptide Y ($P = 0.02$); NPY2R: NPY receptor sub-type 2 ($P = 0.88$); TOP2A: topoisomerase II alpha ($P = 0.04$); TPX2: thioredoxin-dependent peroxidase 2 ($P = 0.03$). Values represent least squares means ± pooled SEM (n = 3). Asterisk denotes a significant difference from the control ($P < 0.05$; Dunnett's test).

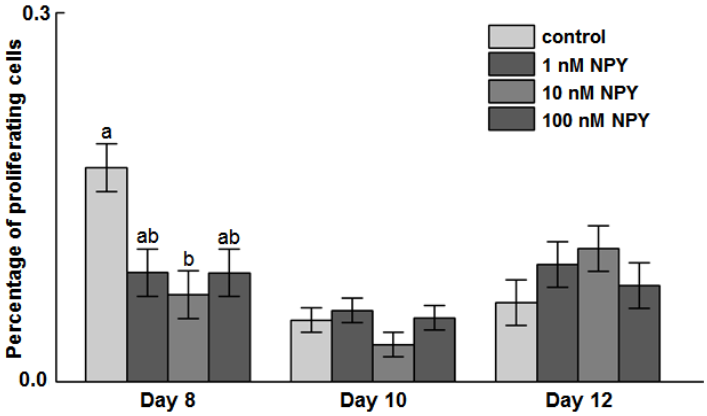

Figure 3.3. Effects of neuropeptide Y (NPY) treatment on cellular proliferation in chicken adipose cells at days 8, 10, and 12 post-induction of differentiation. The stromal–vascular fraction of cells was isolated from abdominal fat of 14 day-old broilers and upon confluence induced to differentiate in the presence of 0, 1, 10 or 100 nM chicken NPY. At days A) 8, B) 10, and C) 12 post-differentiation, cells were incubated in media containing 5-ethynyl-2′-deoxyuridine (EdU) and stained at 2 hours post-treatment with EdU. Cells were counted and the percentage of EdU-positive cells was arcsine transformed and analyzed by ANOVA. Values represent least squares means ± SEM (n = 3). Different letters indicate a significant difference within day ($P < 0.05$; Tukey's test).

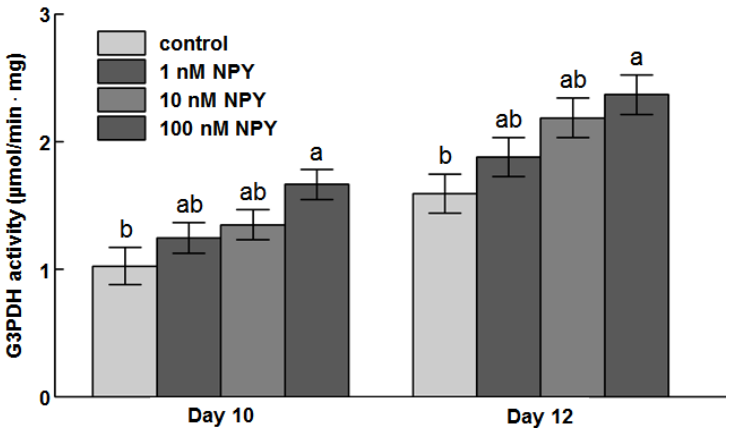

Figure 3.4. Specific activity of glycerol-3-phosphate dehydrogenase (G3PDH) at days 10 and 12 post-induction of differentiation in chicken abdominal adipose cells induced to differentiate in the presence of 0, 1, 10, or 100 nM NPY. Values represent least squares means ± SEM (n = 3). Different letters indicate a significant difference within day ($P < 0.05$; Tukey's test).

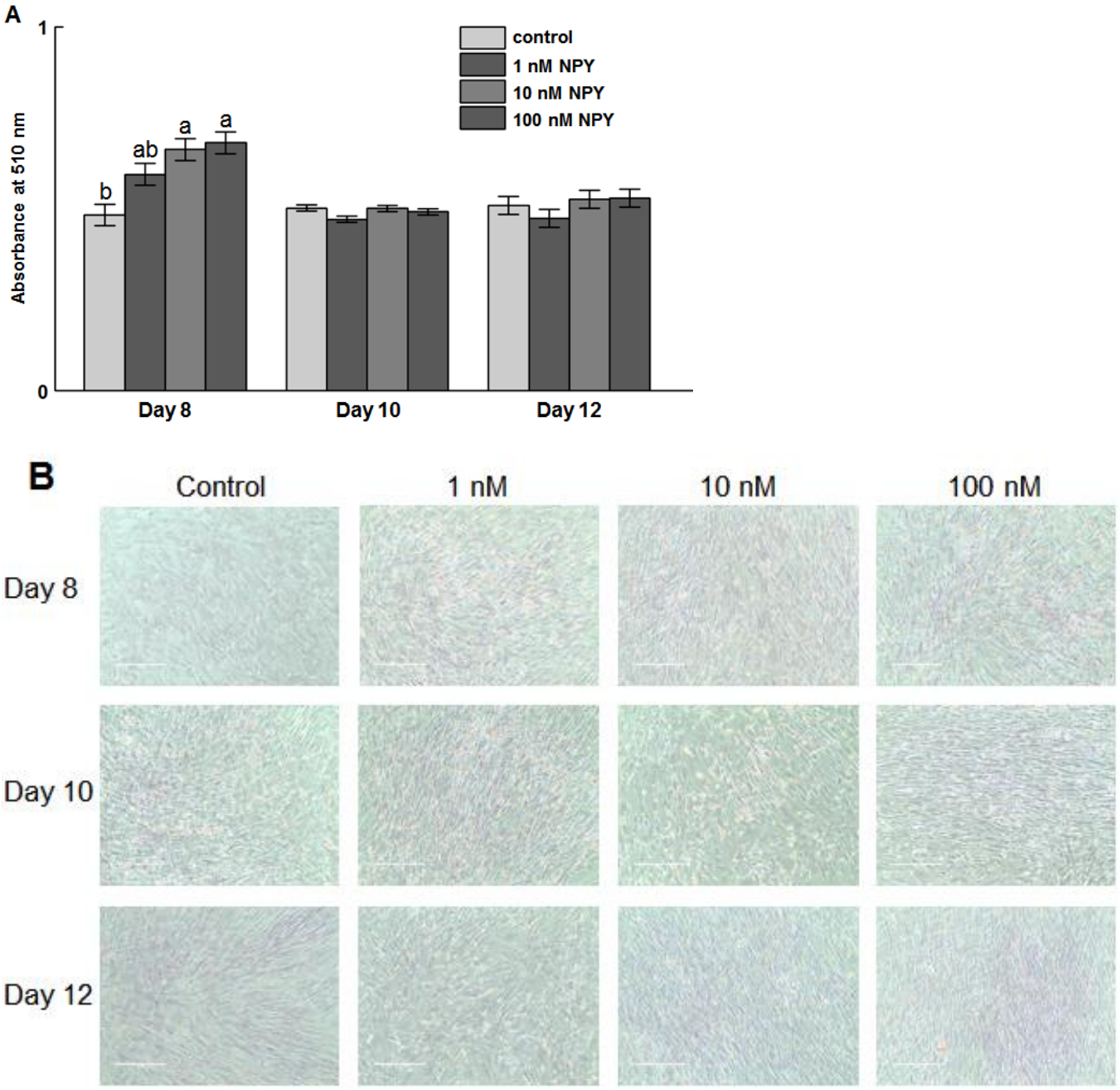
A
1
0
Absorbance at 510 nm
control
1 nM NPY
10 nM NPY
100 nM NPY
b
ab
a
a
Day 8
Day 10
Day 12
B
Control
1 nM
10 nM
100 nM
Day 8
Day 10
Day 12

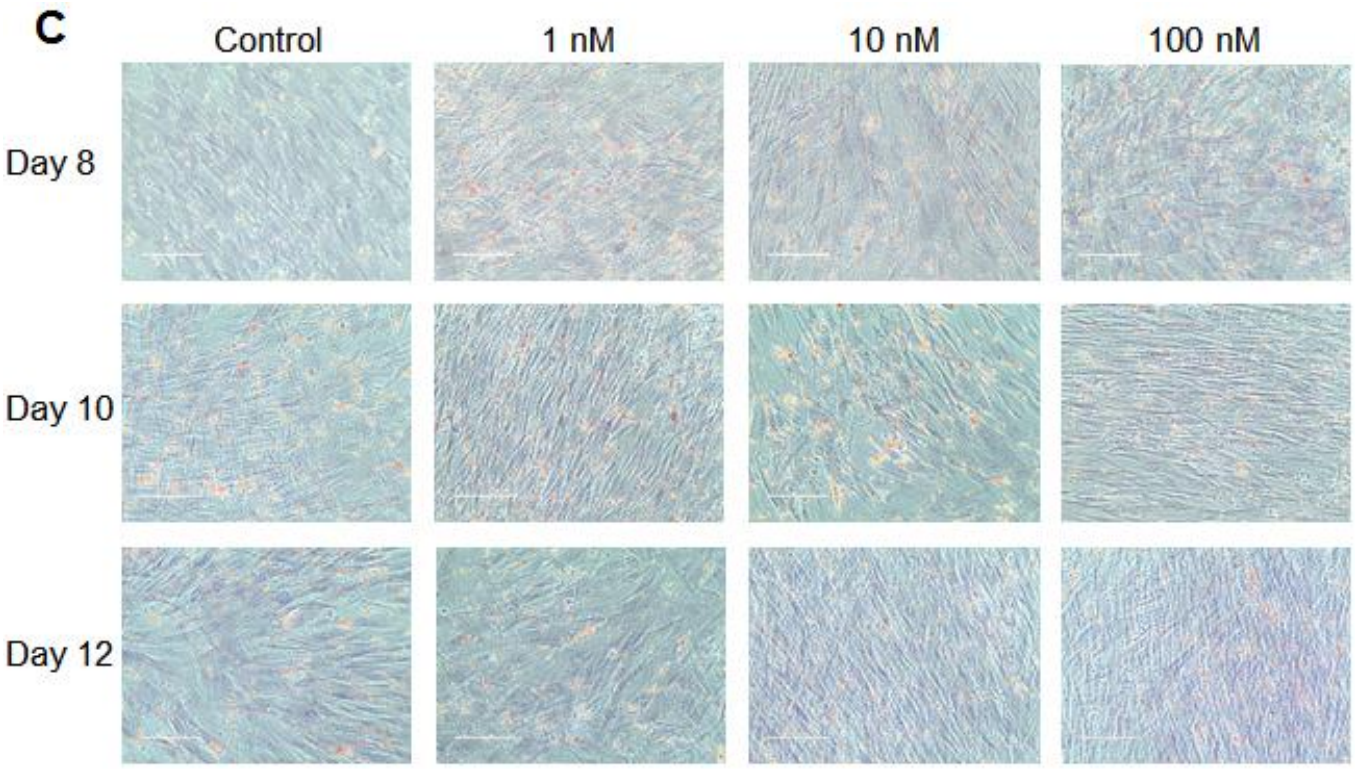

Figure 3.5. Oil Red O staining of chicken adipose cells treated with neuropeptide Y (NPY). The stromal–vascular fraction of cells was isolated from abdominal fat of 14 day-old broilers and upon confluence induced to differentiate in the presence of 0, 1, 10 or 100 nM chicken NPY. At 8, 10 and 12 days post-induction of differentiation cells were stained with Oil Red O and counter-stained with Modified Mayer's Hematoxylin and images captured. A) Absorbance at 510 nm on days 8, 10, and 12 post-induction of differentiation. B) Representative micrographs of 0, 1, 10, and 100 nM NPY treatment on days 8, 10, and 12 post-induction of differentiation under 20X magnification. C) Representative micrographs of 0, 1, 10, and 100 nM NPY treatment on days 8, 10, and 12 post-induction of differentiation under 40X magnification. The scale bar indicates 200 and 100 µm for B) and C), respectively. The red color indicates the staining of neutral lipids. Values represent absorbance least squares means ± SEM (n = 3). Different letters indicate a significant difference within day ($P < 0.05$; Tukey's test).

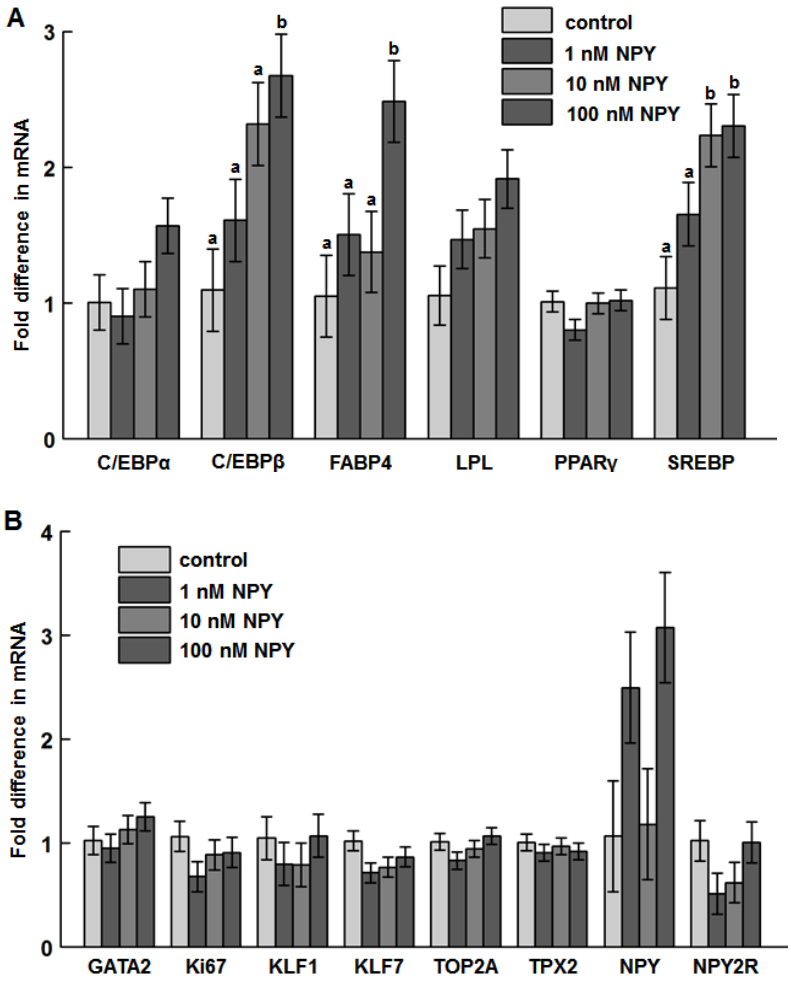

Figure 3.6. The mRNA abundance of (A) adipogenesis-associated factors, (B) preadipocyte and proliferation markers, and neuropeptide Y (NPY) and NPY receptor 2 at day 8 post-induction of differentiation in chicken adipose cells treated with 0, 1, 10 or 100 nM chicken NPY. A) C/EBPα: CCAAT/enhancer binding protein α (P = 0.18); C/EBPβ: CCAAT/enhancer binding protein β (P = 0.03*); FABP4: fatty acid binding protein 4 (P = 0.04*); LPL: lipoprotein lipase (P = 0.12); PPARγ: peroxisome proliferator activated receptor γ (P = 0.21); SREBP: sterol regulatory element-binding protein (P = 0.02*); B) GATA2: GATA-binding protein 2 (P = 0.48); Ki67: Ki67 (P = 0.37); KLF1: Krüppel-like factor 1 (P = 0.67); KLF7: Krüppel-like factor 7 (P = 0.19); TOP2A: topoisomerase II alpha (P = 0.26); TPX2: thioredoxin-dependent peroxidase 2 (P = 0.81); NPY (P = 0.07); NPY2R (P = 0.22). Values represent least squares

means ± pooled SEM (n = 3). Bars with different letters within a gene represent a significant difference, $P < 0.05$ (Tukey's test).

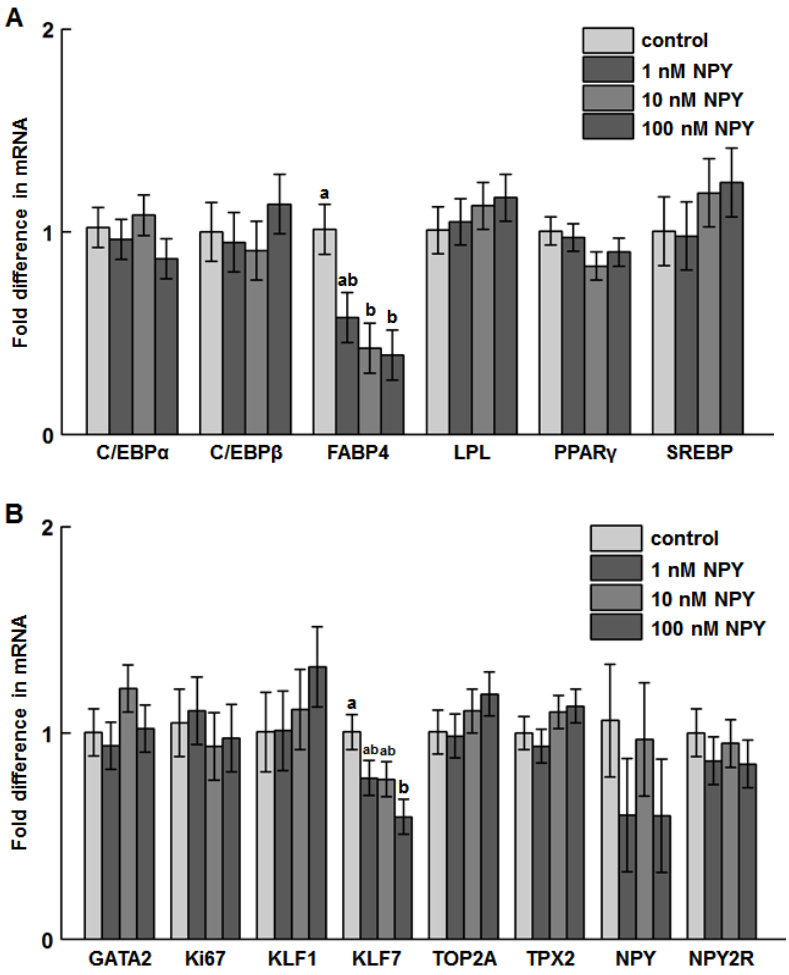

Figure 3.7. The mRNA abundance of (A) adipogenesis-associated factors, (B) preadipocyte and proliferation markers, and neuropeptide Y (NPY) and NPY receptor 2 at day 10 post-induction of differentiation in chicken adipose cells treated with 0, 1, 10 or 100 nM chicken NPY. A) C/EBPα: CCAAT/enhancer binding protein α (P = 0.51); C/EBPβ: CCAAT/enhancer binding protein β (P = 0.71); FABP4: fatty acid binding protein 4 (P = 0.03*); LPL: lipoprotein lipase (P = 0.76); PPARγ: peroxisome proliferator activated receptor γ (P = 0.35); SREBP: sterol regulatory element-binding protein (P = 0.62); B) GATA2: GATA-binding protein 2 (P = 0.40); Ki67: Ki67 (P = 0.88); KLF1: Krüppel-like factor 1 (P = 0.64); KLF7: Krüppel-like factor 7 (P = 0.05); TOP2A: topoisomerase II alpha (P = 0.53); TPX2: thioredoxin-dependent peroxidase 2 (P = 0.36); NPY (P = 0.54); NPY2R (P = 0.77).Values represent least squares means ± pooled SEM

(n = 3). Bars with different letters within a gene represent a significant difference, $P < 0.05$ (Tukey's test).

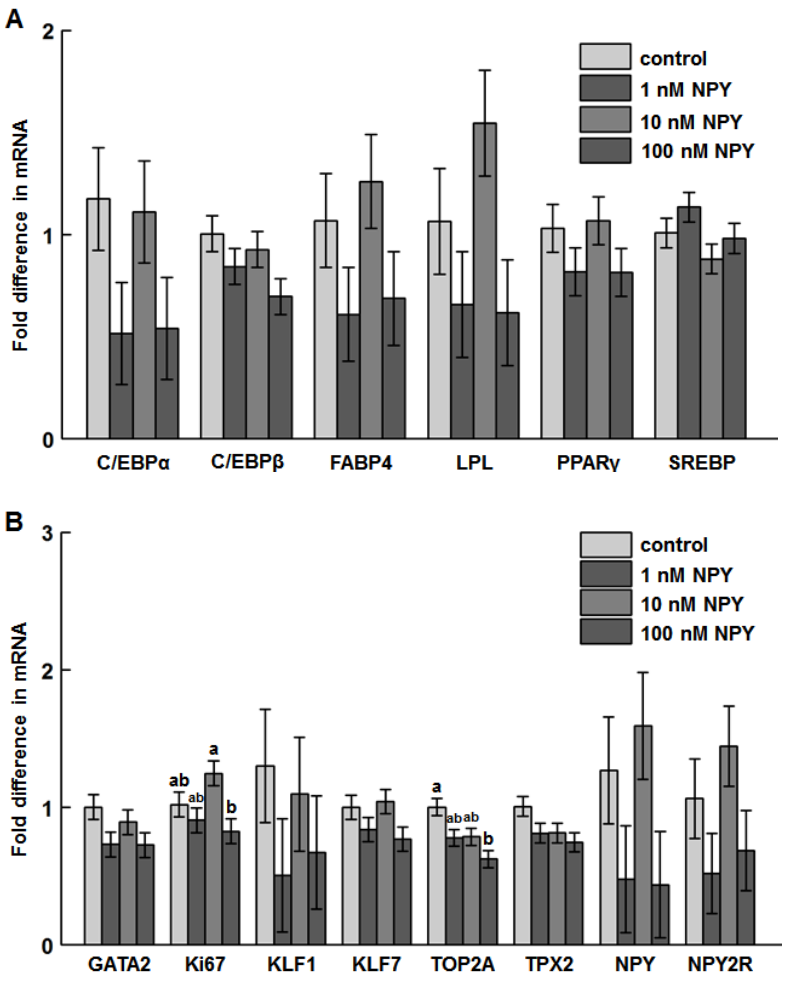

Figure 3.8. The mRNA abundance of (A) adipogenesis-associated factors, (B) preadipocyte and proliferation markers, and neuropeptide Y (NPY) and NPY receptor 2 at day 12 post-induction of differentiation in chicken adipose cells treated with 0, 1, 10 or 100 nM chicken NPY. A) C/EBPα: CCAAT/enhancer binding protein α (P = 0.19); C/EBPβ: CCAAT/enhancer binding protein β (P = 0.16); FABP4: fatty acid binding protein 4 (P = 0.22); LPL: lipoprotein lipase (P = 0.11); PPARγ: peroxisome proliferator activated receptor γ (P = 0.33); SREBP: sterol regulatory element-binding protein (P = 0.19); B) GATA2: GATA-binding protein 2 (P = 0.17); Ki67: Ki67 (P = 0.04*); KLF1: Krüppel-like factor 1 (P = 0.53); KLF7: Krüppel-like factor 7 (P = 0.16); TOP2A: topoisomerase II alpha (P = 0.02*); TPX2: thioredoxin-dependent peroxidase 2 (P = 0.13); NPY (P = 0.16); NPY2R (P = 0.19). Values represent least squares means ± pooled

SEM (n = 3). Bars with different letters within a gene represent a significant difference, $P < 0.05$ (Tukey's test).

Chapter 4: Chick subcutaneous and abdominal adipose tissue depots respond differently in lipolytic and adipogenic activity to α-melanocyte stimulating hormone (α-MSH)

Steven L Shipp, Guoqing Wang, Mark A. Cline, Elizabeth R. Gilbert

Department of Animal and Poultry Sciences, Virginia Tech, Blacksburg, VA 24061

Abstract

In birds, although α-MSH is highly anorexigenic, its effects on adipose tissue physiology have not been reported. At 4 days post-hatch, chicks were intraperitoneally injected with 0 (vehicle), 5, 10, or 50 µg of α-MSH and subcutaneous and abdominal adipose tissue collected 60 minutes later for RNA isolation. Plasma was collected at 60 and 180 minutes for measuring non-esterified fatty acids (NEFA) and α-MSH. Cells isolated from abdominal fat of male chicks were treated with 0 (control), 1, 10, or 100 nM α-MSH and RNA isolated at 4 hours. On day 9 of differentiation, cells were harvested at 4 hours post-treatment to measure glycerol-3-phosphate dehydrogenase (G3PDH) activity. Food intake was reduced in the 50 µg-treated group. Plasma NEFAs were greater in 10 µg than vehicle-treated chicks at 180 minutes. Plasma α-MSH was 3.06 ± 0.57 ng/ml. In subcutaneous adipose tissue, melanocortin receptor 5 (MC5R) mRNA was increased in 10 µg, MC2R and CCAAT-enhancer-binding protein β (C/EBPβ) mRNAs increased in 50 µg, peroxisome proliferator-activated receptor γ and C/EBPα decreased in 5, 10 and 50 µg, and Ki67 mRNA decreased in 50 µg α-MSH-injected chicks. In abdominal adipose tissue, adipose triglyceride lipase mRNA increased in chicks that received 10 µg α-MSH. Cells treated with 10 and 100 nM α-MSH expressed more MC5R and perilipin-1. Cells that received 100 nM α-MSH expressed more fatty acid binding protein 4 and comparative gene identification-58 mRNA. G3PDH activity was greater in cells that were treated with 1 and 100 nM α-MSH. Results suggest that α-MSH increases lipolysis and reduces adipogenesis in chick adipose tissue.

Keywords: chick, adipose, α-MSH, lipolysis, adipogenesis

Introduction

Alpha-melanocyte stimulating hormone (α-MSH) is a 13 amino acid pro-opiomelanocortin (POMC)-derived hormone [18] whose sequence is highly conserved among vertebrates [211]. It has been intensely studied for its involvement in pigmentation [212] and energy balance [19], and is associated with the melanocortin system [157]. The melanocortin system is comprised of POMC-derived peptides, melanocortin receptors (MCR) 1-5, and agouti and agouti-related peptide that act as endogenous MCR antagonists, as reviewed [6, 157, 158]. It is highly anorexigenic in a multitude of species, including rats [20], goldfish [21], and chicks [22], and centrally, is thought to mediate satiety via MCR 3 and 4 [213].

Additionally, α-MSH has effects on the adipose tissue, with MCR 2 and 5 both contributing to its lipolytic actions in mice [214]. In differentiated 3T3-L1 adipocytes, expression of MCR 2 and 5, but not MCR 1, 3, and 4 was detected [201, 214], and α-MSH treatment increased lipolysis and impaired fatty acid re-esterification, effects that were shown to be mediated via MC5R [23]. In mouse preadipocytes isolated from the epididymal and inguinal fat pads (1 nM) and human preadipocytes isolated from superficial subcutaneous adipose tissue lateral to the umbilicus (0.1 nM and 1 nM), α-MSH inhibited proliferation [215]. Collectively, these results indicate that α-MSH decreases adipogenic activity by inhibiting proliferation of preadipocytes, and increase the break-down of triacylglycerols in adipocyte lipid droplets by stimulating lipolysis and impairing fatty acid re-esterification.

While the anorexigenic effect of α-MSH has been demonstrated in chicks, its possible lipolytic or other adipose-metabolism-related effects have not been evaluated in any avian species.

Therefore, the purpose of the current study was to determine the effects of α-MSH on chick adipose tissue physiology.

Materials and Methods

Animals

All animal protocols were approved by the Institutional Animal Care and Use Committee at Virginia Tech and animals were cared for in accordance with the Guide for the Care and Use of Laboratory Animals. Day of hatch Cobb-500 broiler chicks were obtained from a local hatchery. Chicks were group caged on day 1 at 30 ± 1 °C and 50 ± 5% relative humidity with free access to water and a mash diet (22% crude protein and 3,000 kcal ME/kg). The composition of the diet has been described elsewhere [203]. The ambient temperature was gradually decreased from 30 °C on day 1 to 25 °C by 0.5 °C per day, and then 25 °C until 14 days post-hatch.

Primary Adipose Cell Culture and α-MSH Treatment

Reagents were purchased from Sigma Aldrich (MO, USA) unless otherwise stated. Approximately two grams of abdominal fat was collected from day 14 of age male chicks by sterile dissection and submerged in DMEM/F12 Glutamax (Gibco, NY, USA) media containing 1% penicillin/streptomycin (HyClone, MA, USA) warmed to 37 °C. Under the biological safety cabinet, adipose tissue was minced into fine sections with scalpel blades and incubated in 10 mL of 4-(2-hydroxyethyl) piperazine-1-ethanesulfonic acid (HEPES) solution (0.1 M HEPES, 5 mM d-glucose, 1.5 % bovine serum albumin; BSA) containing 500 units/mL Collagenase, Type I (Worthington Biochemical Corporation, NJ, USA) for 1 hour at 37 °C in a shaking water bath. After the incubation, the contents were filtered through 250 μm filters (Pierce, IL, USA). The filtrate was then centrifuged at 200 ×g for 10 min to separate floating adipocytes from the other

cell types. The supernatant was discarded, and cell pellets were resuspended in 10 mL of red blood cell lysis buffer (155 mM NH_4Cl, 10 mM $KHCO_3$, 0.1 mM EDTA) to remove the red blood cells. The contents were then filtered through a 20 μm mesh (Celltrics, NJ, USA) to filter out the endothelial clumps. The filtrate was then centrifuged at 200 ×g for 5 min to obtain the stromal vascular fraction (SVF) of cells. The SVF was resuspended in plating media (DMEM/F12 containing 10% defined fetal bovine serum (FBS); HyClone, and 1% penicillin/streptomycin) and seeded directly into a petri dish. After 72 hours, cells were passaged one time, and then seeded 24 hours later at a density of 3×10^4 cells per mL into 12-well plates (Falcon, MA, USA) and incubated at 37 °C in a 5 % CO^2 humidified atmosphere for at least 48 h (to minimize pro-inflammatory cytokine secretion) before beginning experiments. Cells were cultured in plating media until 80% confluence. In order to minimize the confounding effects of serum-derived α-MSH, cells were cultured in basic media (DMEM/F12 with1% penicillin/streptomycin) containing 1.5% FBS and 0, 1, 10, or 100 nM α-MSH, and total RNA was extracted from cells at 4 hours post-treatment. For all cell-culture experiments, there were at least three biological replicates, where the experimental unit represented cells from an individual chick (n = 3 chicks), with triplicate wells of each treatment within an experiment for cells collected from a single chick. The triplicate values were averaged before statistical analysis.

Adipocyte Differentiation and α-MSH Treatment

The adipocyte differentiation protocol was similar to a method that has been described [93]. Briefly, cells were cultured in plating media and allowed to reach complete confluence. Plating media (DMEM/F12 basic media with 10% FBS) was replaced with induction media (DMEM/F12 basic media containing 200 nM insulin, 1 μM dexamethasone, 10 U/mL heparin,

and 2.5% chicken serum; CS). At 48 h post-induction, media was replaced with insulin-containing media (DMEM/F12 basic media containing 2.5% CS and 200 nM insulin). After another 48 h, and until day 9 post-induction of differentiation, cells were cultured in maintenance media (DMEM/F12 basic media with 2.5% CS), and changed every 48 hours. At day 9 post-induction of differentiation, glycerol-3-phosphate dehydrogenase (G3PDH) specific activity was evaluated after a 4-hour treatment with media containing 0, 1, 10, or 100 nM α-MSH (BACHEM, Torrance, CA).

Glycerol-3-phosphate dehydrogenase (G3PDH) Activity

The method for assaying G3PDH specific activity was adapted from two other studies [205, 206]. Briefly, cells were cultured in 12-well plates and treated as described above. On the day of the experiment, cells were washed with PBS, and 200 µL of lysis buffer (50 mM Tris–Cl, 1 mM EDTA, and 1 mM β-mercaptoethanol, pH 7.5) was added to each well, and cells detached from the plate using cell scrapers. Lysates were transferred to microcentrifuge tubes and further lysed with a 21 gauge needle, then sonicated at 4 °C using a Bioruptor 300 (Diagenode) with 4 cycles of 30 sec on and 30 sec off at high frequency. Lysates were then centrifuged at 12,000 ×g at 4 °C for 30 min, and the supernatant used for measuring G3PDH activity and for determining total protein concentration. The G3PDH activity was measured for each sample in duplicate in assay buffer (100 mM triethanolamine–HCl, 2.5 mM EDTA, 0.12 mM NADH, 0.2 mM dihydroxyacetone phosphate (DHAP), 0.1 mM β-mercaptoethanol, pH 7.5) in a total reaction volume of 200 µL in UV transparent plates (Corning, MA, USA) using a µQuant plate reader and KC Junior software (Bio-Tek, VT, USA). Absorbance was measured at 340 nm for 20 cycles at 25 °C and the maximum slope calculated from the absorbance data. Protein concentration was

quantified with Bradford BCA reagent (Sigma-Aldrich, MO, USA) using an Infinite M200Pro multi-mode plate reader and Magellan software (Tecan, CA, USA). The maximum slope was normalized to the protein concentration to calculate specific activity, which is reported as μmol/min · mg.

Intraperitoneal Injection and Tissue Collection

On day 4 post-hatch, using a randomized complete block design with body weight as the blocking factor, individually caged Cobb-500 broilers with ad libitum access to food and water were assigned to receive intraperitoneal injection of 0 (vehicle), 5, 10, or 50 micrograms of α-MSH (BACHEM, Torrance, CA) (n=10/treatment) diluted in phosphate-buffered saline, injected via insulin syringes (BD Biosciences). Chicks were returned to home cages with ad libitum access to food and water, and at 60 minutes post-injection, chicks were euthanized and the abdominal fat (attached to gizzard), subcutaneous fat and pectoralis major skeletal muscle samples were excised and collected in RNA*later*® (Qiagen). Concurrently, trunk blood was collected and feed intake recorded. In a second experiment, methods were the same except that at both 1 and 3 hours post-injection, trunk blood was collected for measuring plasma NEFA concentrations as described below.

Total RNA Isolation and Real Time PCR

For the in vitro study, cells in 12-well plates were washed once with PBS and lysed with a 21-gauge needle in 350 μL RLT buffer (Qiagen, CA, USA), and total RNA was extracted with the RNeasy Mini kit (Qiagen, CA, USA) according to the manufacturer's instructions. For the in vivo study, tissues were homogenized in 1 mL Isol RNA Lysis reagent (5-Prime, Gaithersburg,

MD, USA) using 5 mm stainless steel beads (Qiagen, Valencia, CA, USA) and a Tissue Lyser II (Qiagen) for 2 × 2 min at 25 Hz. Total RNA was separated following the manufacturer's instructions (5-Prime) and following the step of addition to 70% ethanol, samples were transferred to spin columns and further purified using the RNeasy Mini Kit (Qiagen). Both types of extractions included the optional on-column RNase-Free DNase I (Qiagen, CA, USA) treatment.

The total RNA samples were quantified and assessed for purity by spectrophotometry at 260/280/230 nm using a Nanophotometer™ Pearl (IMPLEN, CA, USA), and their integrity evaluated by agarose gel electrophoresis. The first strand cDNA was synthesized from 200 ng total RNA using the High Capacity cDNA Reverse Transcription kit, according to the manufacturer's instructions (Applied Biosystems, NY, USA). Primers were designed in Primer Express 3.0 (Applied Biosystems, NY, USA; Table 1). All primers were evaluated for amplification efficiency before use. Efficiency of target genes was within 5% of the reference gene (Actin). A total volume of 10 μL in each reaction contained 5 μL fast SYBR Green Master Mix (Applied Biosystems, NY, USA), 0.25 μL each of 5 μM forward and reverse primers, and 3 μL of 10-fold diluted cDNA. Real-time PCR reactions were performed in duplicate for all samples on an Applied Biosystems 7500 FAST system, under the following conditions: enzyme activation for 20 sec at 95 °C and 40 cycles of 1) melting step for 3 seconds at 95 °C and 2) annealing/extension step for 30 seconds at 60 °C. A melting curve analysis was performed after all reactions to ensure amplification specificity.

Plasma NEFA Concentrations

At 1 and 3 hours post-injection, approximately 200 µL blood was collected from the trunk via capillary blood collection tubes (Microvette® 200 K3E) immediately following euthanasia by decapitation. After collection, blood samples were centrifuged at 2,000 ×g at room temperature for 5 minutes after which plasma was transferred to sterile microcentrifuge tubes on ice. Plasma NEFA concentrations were measured using the NEFA-HR2 kit (Wako Diagnostics) according to the manufacturer's instructions. Absorbance was measured at 550 nm using an Infinite M200 Pro multi-mode plate reader (Tecan). Sample concentration was calculated using the following formula: Sample Concentration = Standard Concentration × (Sample Absorbance) / (Standard Absorbance). Units for the concentrations are reported as mEq/L.

α-MSH ELISA

Because plasma concentrations of α-MSH are unreported in birds, the objective of this part of the experiment was to determine average concentrations in non-injected chicks. Approximately 200 µL blood was collected from the trunk of non-injected day 4 of age chicks (n = 10 chicks) via capillary blood collection tubes (Microvette® 200 K3E) immediately following euthanasia by decapitation. After collection, blood samples were centrifuged at 2,000 ×g at room temperature for 5 minutes after which the plasma was transferred to sterile microcentrifuge tubes on ice. Samples were diluted 1:5 and plasma α-MSH concentrations were measured using the human alpha MSH ELISA kit (competitive EIA) - LS-F4608 (LifeSpan Biosciences, Inc.) according to the manufacturer's instructions. Absorbance was measured at 450 nm using an Infinite M200 Pro multi-mode plate reader (Tecan). Sample concentration was calculated using the following formula: Sample concentration = $10^{((\log(\text{Standard concentration}) \times \text{Sample Absorbance}) / \text{Standard Absorbance})}$, which was then multiplied by the dilution factor. Units for the concentrations are reported as ng/ml.

Statistical Analysis

The real time PCR data were analyzed using the ΔΔCT method, where ΔCT = CT target gene − CT Actin, and ΔΔCT = ΔCT target sample − ΔCT calibrator [207]. The average of the control group (vehicle-injected for in vivo and control-treated for cell culture experiments) within a time point was used as the calibrator sample. The relative quantity ($2^{-\Delta\Delta CT}$) values were subjected to ANOVA using the Fit Model Platform of JMP (SAS Ins., Cary, NC). The statistical model included the main effect of treatment. Tukey's test was used for pairwise comparisons between treatments. A similar model was used for the NEFA concentration experiment and for G3PDH specific activity data. Tukey's test was used for pairwise comparisons between different time points. Results were considered significant at $P < 0.05$.

Results

mRNA abundance of adipose lipid metabolism-associated factors, and melanocortin receptors 1-5

The following genes were evaluated: 1-Acylglycerol-3-Phosphate O-Acyltransferase 2 (AGPAT2), CCAAT/enhancer-binding protein α (C/EBPα), CCAAT/enhancer-binding protein β (C/EBPβ), fatty acid binding protein 4 (FABP4), Peroxisome proliferator-activated receptor γ (PPARγ), sterol regulatory element binding protein 1 (SREBP), acyl-CoA dehydrogenase long chain (ACADL), adipose triglyceride lipase (ATGL), comparative gene identification - 58 (CGI-58), lipoprotein lipase (LPL), Perilipin - 1 (PLIN-1), monoacylglycerol lipase (MGLL), GATA binding protein 2 (GATA2), Ki67 (Ki67), Kruppel-Like Factor 1 (KLF1), Kruppel-Like Factor 7 (KLF7), Topoisomerase II alpha (TOP2A), thioredoxin-dependent peroxidase 2 (TPX2), melanocortin receptors (MCR) 1-5, and proopiomelanocortin (POMC).

Subcutaneous adipose tissue

In the subcutaneous adipose tissue, there was decreased mRNA abundance of PPARγ (P = 0.0004) and C/EBPα (P = 0.003; Figure 4.1A) in chicks that received 5, 10, and 50 µg of α-MSH, decreased mRNA abundance of Ki67 (P = 0.04; Figure 4.1C) in chicks that received 50 µg of α-MSH, increased mRNA abundance of MC2R (P = 0.01; Figure 4.1D) and C/EBPβ (P = 0.02; Figure 4.1A) in chicks receiving 50 micrograms α-MSH, and increased mRNA abundance of MC5R (P = 0.04; Figure 4.1D) in chicks receiving 10 micrograms α-MSH, in comparison to vehicle-injected chicks. Of the MCRs, only MCR 2 and 5 were detectable, with MCRs 1, 3, and 4 and POMC negligibly expressed, and data thus not reported. The mRNA abundance of AGPAT2 (P = 0.57), FABP4 (P = 0.94), SREBP (P = 0.37; Figure 4.1A), ACADL (P = 0.90), ATGL (P = 0.98), CGI-58 (P = 0.62), LPL (P = 0.28), MGLL (P = 0.72), PLIN-1 (P = 0.76; Figure 4.1B), GATA2 (P = 0.17), KLF1 (P = 0.30), KLF7 (P = 0.20), TOP2A (P = 0.22), and TPX2 (P = 0.06; Figure 4.1C) was not affected by treatment.

Abdominal adipose tissue

In the abdominal adipose tissue, ATGL mRNA was greater in 10 µg α-MSH-injected than vehicle-injected chicks (P = 0.04; Figure 4.2B). Of the MCRs, only MCR5 was detectable, with MCRs 1, 2, 3, and 4 and POMC negligibly expressed, and data thus not reported. Abundance of AGPAT2 (P = 0.57), C/EBPα (P = 0.92), C/EBPβ (P = 0.23), FABP4 (P = 0.53), PPARγ (P = 0.80), SREBP (P = 0.25; Figure 4.2A), ACADL (P = 0.59), CGI-58 (P = 0.57), LPL (P = 0.96), PLIN-1 (P = 0.79), MGLL (P = 0.44; Figure 4.2B), GATA2 (P = 0.74), Ki67 (P = 0.20), KLF1

(P = 0.71), KLF7 (P = 0.73), TOP2A (P = 0.15), TPX2 (P = 0.22; Figure 4.2C), and MC5R (P = 0.57; Figure 4.2D) was not affected by treatment.

Breast muscle (*Pectoralis major*)

Of the MCR's, only MCR 3 and 5 were detectable, with MCRs 1, 2, and 4 and POMC negligibly expressed. There was no effect of treatment on mRNA abundance of MCR 3 (P = 0.94) or 5 (P = 0.46). Other genes were not measured in this tissue.

In vitro (abdominal fat SVF)

There was greater FABP4 (P = 0.006; Figure 4.3A) and CGI-58 (P = 0.01; Figure 4.3B) in response to 100 nM α-MSH, and PLIN-1 (P = 0.009; Figure 4.3B) and MC5R (P = 0.0008; Figure 4.3D) in response to 10 and 100 nM α-MSH, relative to control cells at 4 hours post-treatment. Of the MCRs, only MCR5 was expressed, with MCRs 1, 2, 3, and 4 and POMC below the threshold for detection, and data thus not reported. Abundance of AGPAT2 (P = 0.30), C/EBPα (P = 0.1346), C/EBPβ (P = 0.43), PPARγ (P = 0.41), SREBP (P = 0.2993; Figure 4.3A), ACADL (P = 0.62), ATGL (P = 0.37), LPL (P = 0.42), MGLL (P = 0.18; Figure 4.3B), GATA2 (P = 0.14), Ki67 (P = 0.15), KLF1 (P = 0.03), KLF7 (P = 0.1078), TOP2A (P = 0.39), and TPX2 (P = 0.37; Figure 4.3C) mRNA was not affected. Although for KLF1 the main effect of treatment was $P < 0.05$, Tukey's test showed no significant differences between treatments.

G3PDH Activity

There was greater G3PDH activity in 1 and 100 nM α-MSH-treated cells than control cells at 4 hours post-treatment at day 9 post-induction of differentiation (P = 0.006; Figure 4.4).

Plasma NEFA and α-MSH Concentrations

At 3 hours post-injection, plasma NEFA concentrations were elevated in chicks that received 10 micrograms of α-MSH as compared to the vehicle (Figure 4.5). Plasma α-MSH concentrations in non-injected chicks were 3.06 ± 0.57 ng/ml (n = 10).

Food Intake

Chicks that received 50 μg α-MSH ate less than vehicle-injected chicks during the first hour post-injection (Figure 4.6).

Discussion

Results from current study demonstrate that α-MSH has effects on the adipose tissue of chicks, with gene expression differences in adipose tissue and isolated cells reflecting transcriptional regulation of the melanocortin system, increased lipolytic activity, and decreased adipogenic activity. Although previously reported to stimulate lipolysis, effects on other pathways associated with adipocyte physiology, including adipogenesis and hypertrophy have not been reported. Thus, we profiled expression of a multitude of genes related to numerous facets of adipose tissue physiology to comprehensively assess the role of α-MSH in chick adipose tissue physiology, although it should be noted that transcript abundance is not necessarily a reflector of protein quantity and activity.

A subset of the genes evaluated are associated with adipogenesis and fat development, as AGPAT2 is associated with *de novo* phospholipid biosynthesis [216] and is important during adipose tissue development [217], the transcription factors C/EBPα, C/EBPβ, PPARγ, and

SREBP are also involved during adipocyte differentiation, as reviewed [38, 39], with PPARγ known as the "master regulator" of adipogenesis in mammals [218] and chickens [219], and FABP4 is a fatty acid transporter in the adipose tissue [202]. The second group of genes is associated with lipolysis and fat oxidation: ACADL mediates β-oxidation [220], ATGL, MGLL, and LPL are lipases and are associated with the initial step in triglyceride hydrolysis [221], catalyzing the hydrolysis of monoacylglycerols [222], and hydrolysis of plasma lipoprotein triacylglycerols [200], respectively, and PLIN-1 and CGI-58 regulate activity of ATGL [223-225]. The third group of genes represent preadipocyte and proliferation markers, with GATA2, KLF1, and KLF7 associated with preadipocyte function and proliferation [226, 227], and Ki67, TOP2A, and TPX2 all associated with cell proliferation [198, 199, 228]. Lastly, we measured expression of the 5 melanocortin receptors, and the melanocortin preproprotein precursor, POMC [18] to understand the effect of α-MSH on the adipose tissue melanocortin system.

***In vivo* response to α-MSH**

At 60 minutes post-injection of α-MSH there was increased expression of the enzyme ATGL in the abdominal adipose tissue. In the subcutaneous adipose tissue, there was increased expression of both MCR 2 and 5, both of which are associated with mediating lipolytic actions of α-MSH, although it is unknown if α-MSH induces changes in expression of these receptors in other species [168]. Another study also showed involvement of MC5R in the response to α-MSH, which involved an increase in lipolysis and impaired fatty acid re-esterification in differentiated 3T3-L1 adipocytes [23]. That this receptor's mRNA expression is upregulated in the adipose tissue of the chick and is responsible for the lipolytic effects of α-MSH in the murine 3T3-L1 cell line suggests that the effect of α-MSH on MC5R was conserved through divergent evolution.

Expression of MC5R was not affected by α-MSH in the abdominal adipose tissue depot, suggesting that the effect on MC5R may be depot specific. That treatment did not affect MCR sub-type expression in another metabolically-important tissue, the skeletal muscle, also suggests that the effect is adipose tissue depot-specific. That ATGL, an important lipolytic enzyme was up-regulated in abdominal but not subcutaneous adipose tissue suggests that this depot might be more sensitive to the lipolytic effects of α-MSH, or α-MSH has different depot functions.

In subcutaneous fat on the other hand, mRNAs that were affected encode adipogenic transcription factors C/EBPα and PPARγ, as well as cell proliferation marker Ki67. In 3T3-L1 cells that were differentiated, a 24 hour treatment with tumor necrosis factor α (TNF- α) led to lipolytic effects and reduced protein expression of PPARγ, an effect that was partially reversed by overexpression of PPARγ, leading authors to believe that reduced PPARγ plays a role in mediating the lipolytic effects of TNF- α [229]. It is possible that decreased PPARγ in response to α-MSH treatment in the present study serves a similar function. Reduced expression of Ki67 could be associated with a reduction in cell proliferation, an effect that is observed in human and mouse preadipocytes in response to α-MSH [215].

In addition to the effects described earlier, α-MSH is also a regulator of bone metabolism; increasing cell proliferation in primary cultures of osteoblasts and chondrocytes and stimulating osteoclastogenesis in bone marrow cultures [230]. C/EBPβ is upregulated during osteoclastogenesis [231], thus increased expression of C/EBPβ in the subcutaneous adipose tissue may indicate that α-MSH communicates with MSC to induce osteoclastogenesis rather

than adipogenesis in this depot. This is also supported by the decreased expression of PPARγ, as MSC are driven towards adipogenesis by PPARγ [232].

Plasma NEFA concentrations were elevated at 3 hours post-injection of 10 μg α-MSH, but not at 1 hour. That mRNA expression of ATGL was elevated in the abdominal adipose tissue at 1 hour post-injection in response to the same dose, suggests that transcriptional up-regulation was associated with a time lag that led to the observed increase in plasma NEFAs at 3 hours post-injection. That food intake was not different at this dose suggests that this effect on metabolism was not an indirect consequence of reduced feeding but rather due to changes initiated via melanocortin receptor signaling in the adipose tissue. That the two adipose tissue depots behaved differently in terms of gene expression responses is interesting and suggests that the two are metabolically distinct and that the abdominal fat may be more responsive to hormonal stimuli.

Plasma α-MSH levels in the current study were 3.06 ± 0.57 ng/ml. Blood plasma concentrations in human patients are reported to be 23.5 ± 2.27 pg/ml [233] and 14.5 ± 1.0 pg/ml [234] in fasted patients, and slightly lower than 200 ng/ml (exact number not specified) in specific pathogen-free NC/Nga mice [235]. Thus, chicks appear to have higher circulating concentrations than humans, but lower than mice. This may suggest that α-MSH plays a greater role in the periphery of mice and chickens or that the various species display differential sensitivity to α-MSH. Although the values are reported in separate studies, that human plasma α-MSH concentrations seem to differ between the fed and fasted states supports that α-MSH may play a role in energy homeostasis.

***In vitro* response to α-MSH**

In cells isolated from the SVF of chick abdominal adipose tissue after 4 hours of incubation with α-MSH there was up-regulation in expression of MCR5 mRNA. Both MC2R and MC5R mediate α-MSH effects in 3T3-L1 adipocytes [168, 214], and increased expression of MC5R was also observed in 3T3-L1 cells treated with α-MSH [23]. That MCR5 was up-regulated in this study supports that α-MSH may affect lipolysis through the melanocortin system.

Expression of CGI-58 and PLIN-1 also increased in response to α-MSH treatment in cultured cells from the SVF of abdominal fat. These two factors contribute to regulation of ATGL; when PLIN-1 is unphosphorylated, CGI-58 is bound, but when PLIN-1 is phosphorylated CGI-58 dissociates and binds to ATGL to then increase its activity [223-225, 236]. Quantity of mRNA does not indicate where CGI-58 is localized in the cell, and without knowing if PLIN-1 is phosphorylated, it is unclear whether the increase in CGI-58 and PLIN-1 expression would be associated with greater coating of the lipid droplet [224], or if these two factors are upregulated in order to increase the lipolytic activity of ATGL. Because the cells in this experiment are cells isolated from the SVF of cells that were not induced to differentiate, adipocytes were not present. This suggests that the increase in expression of CGI-58 and PLIN-1 mRNA may be associated with increased activity of ATGL, especially since lipolytic receptor MCR5 is upregulated. Although expression of lipolytic enzymes was not affected, up-regulation of the fatty acid transporter FABP4 could be a response to fatty acid liberation.

In cells from the SVF that are induced to differentiate, and then treated with α-MSH for 4 hours on day 9 post-induction of differentiation, there was increased G3PDH activity, an indirect

marker of fat synthesis [153, 154]. This effect was unexpected as we hypothesized that α-MSH would either decrease or have no effect on G3PDH activity. The increased activity may be explained by the amount of time that the cells were exposed to α-MSH. The effect of 4 hours may reflect adipose tissue remodeling. Lipid remodeling in adipocytes is highly dynamic, and fluctuates in response to adipocyte death, adipokine secretion, fatty acid flux, adipogenesis, and lipolysis [237, 238].

The 3T3-L1 cells in a previous study were treated with 1 μM α-MSH [23], a dose ten times the highest dose, and one thousand times the lowest effective dose used in the current study. There are several explanations for the effects of α-MSH on gene expression and enzyme activity in the current study as compared to the 3T3-L1 study. First, these data may imply that chicken cells are more sensitive to α-MSH, although a dose lower than 1 μM α-MSH was not evaluated in the previous study [23]. Second, the current study utilized the first passage of primary cells isolated from the SVF, predominantly preadipocytes, which may respond differently to α-MSH than 3T3-L1 cells from a clonal cell line that have undergone terminal differentiation after multiple passages. This is less likely as cells on day 9 post-induction of differentiation also displayed increased G3PDH activity in response to 1 and 100 nM α-MSH, thus both the precursor cells and differentiated cells from the SVF are able to respond to the same doses of α-MSH, although gene expression was not evaluated in our differentiation study.

The anorexigenic effect of α-MSH is well documented although most studies evaluate the central response to α-MSH. In the current study α-MSH was administered via intraperitoneal injection; a peripheral treatment. That food intake was affected has a few explanations, the first being that

chicks at 4 days of age have not yet fully developed the blood brain barrier. Another explanation is that the highest dose of α-MSH was an overdose, and reduced food intake was due to malaise. It is also possible that the decrease in food intake observed in chicks receiving 50 μg of α-MSH could account for the changes in gene expression caused by this treatment. It is unlikely however, that changes were due to decreased food intake rather than α-MSH, because chicks receiving 5 and 10 μg of α-MSH also had significant differences in gene expression and plasma NEFA, but none in food intake when compared to the control.

In conclusion, α-MSH treatment was associated with changes in MCR expression, and expression of genes encoding factors associated with increased lipolytic activity and decreased adipogenic activity. Expression of receptors and other factors differed between adipose tissue depots, suggesting that the subcutaneous adipose tissue may respond to α-MSH with decreased adipogenic activity and the abdominal adipose tissue with increased lipolytic activity. These effects on gene expression were supported by the observed increase in circulating plasma NEFAs at 3 hours post-injection. Overall, α-MSH most likely works to decrease fat mass by increasing lipolysis and reducing adipogenesis. Additionally, this is the first report of how α-MSH affects any aspect of adipose tissue physiology in any avian species, results of which could also shed light on how α-MSH affects the adipose tissue in other species, including humans.

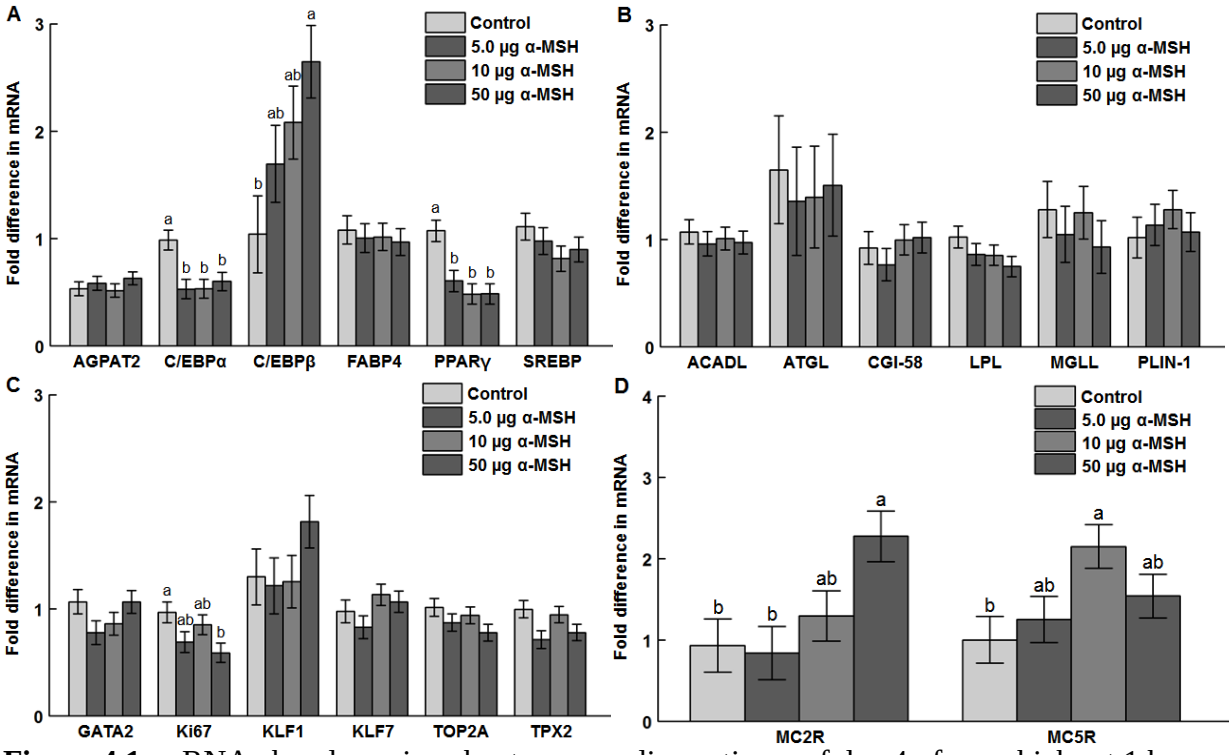

Figure 4.1. mRNA abundance in subcutaneous adipose tissue of day 4 of age chicks at 1 hour post-injection. (A) 1-Acylglycerol-3-Phosphate O-Acyltransferase 2 (AGPAT2), CCAAT/enhancer-binding protein α (C/EBPα), CCAAT/enhancer-binding protein β (C/EBPβ), fatty acid binding protein 4 (FABP4), Peroxisome proliferator-activated receptor γ (PPARγ), and sterol regulatory element binding protein (SREBP); (B) acyl-CoA dehydrogenase long chain (ACADL), adipose triglyceride lipase (ATGL), comparative gene identification - 58 (CGI-58), lipoprotein lipase (LPL), monoacylglycerol lipase (MGLL), and Perilipin-1 (PLIN-1); (C) GATA binding protein 2 (GATA2), Ki67 (Ki67), Kruppel-Like Factor 1 (KLF1), Kruppel-Like Factor 7 (KLF7), Topoisomerase II alpha (TOP2A), thioredoxin-dependent peroxidase 2 (TPX2); (D) melanocortin receptors (MCR) 2 and 5. Values represent least squares means ± SEM (n = 10 per group). Different letters within a gene indicate a significant difference ($P < 0.05$; Tukey's test).

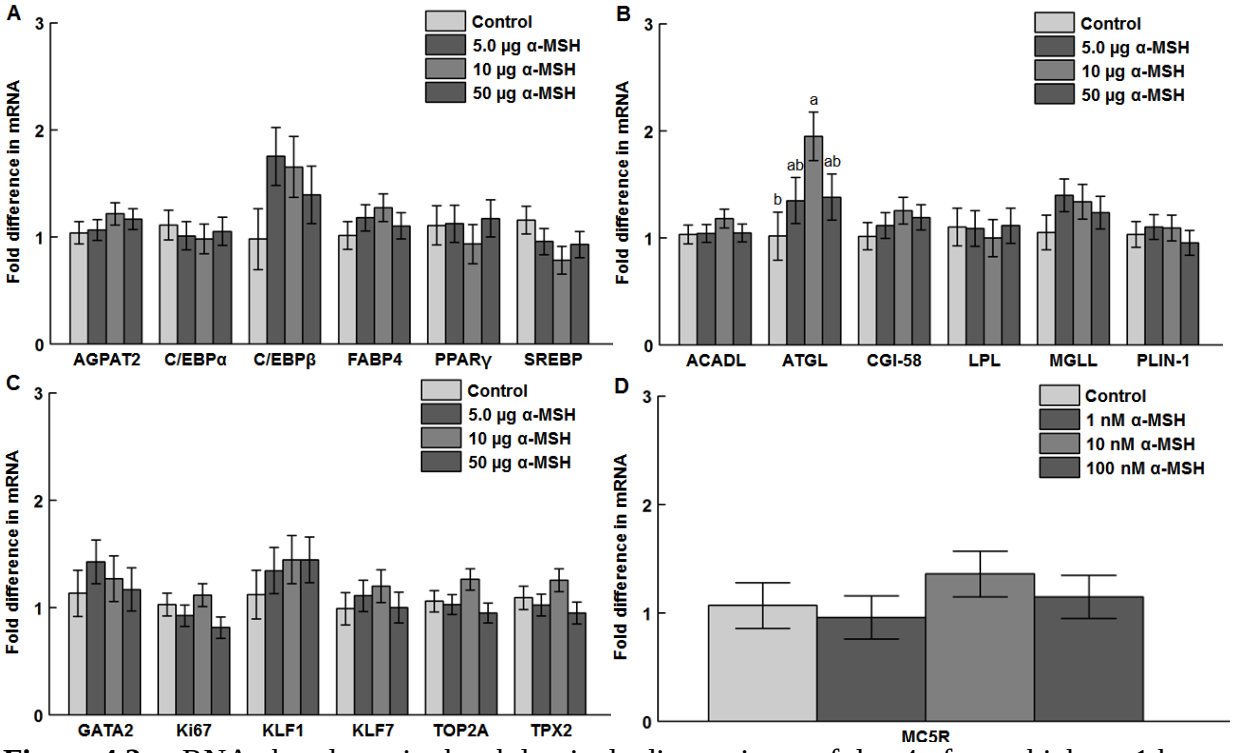

Figure 4.2. mRNA abundance in the abdominal adipose tissue of day 4 of age chicks at 1 hour post-injection. (A) 1-Acylglycerol-3-Phosphate O-Acyltransferase 2 (AGPAT2), CCAAT/enhancer-binding protein α (C/EBPα), CCAAT/enhancer-binding protein β (C/EBPβ), fatty acid binding protein 4 (FABP4), Peroxisome proliferator-activated receptor γ (PPARγ), and sterol regulatory element binding protein (SREBP), (B) acyl-CoA dehydrogenase long chain (ACADL), adipose triglyceride lipase (ATGL), comparative gene identification - 58 (CGI-58), lipoprotein lipase (LPL), monoacylglycerol lipase (MGLL), and Perilipin-1 (PLIN-1); (C) GATA binding protein 2 (GATA2), Ki67 (Ki67), Kruppel-Like Factor 1 (KLF1), Kruppel-Like Factor 7 (KLF7), Topoisomerase II alpha (TOP2A), and thioredoxin-dependent peroxidase 2 (TPX2). Values represent least squares means ± SEM (n = 10 per group). Different letters within a gene indicate a significant difference ($P < 0.05$; Tukey's test).

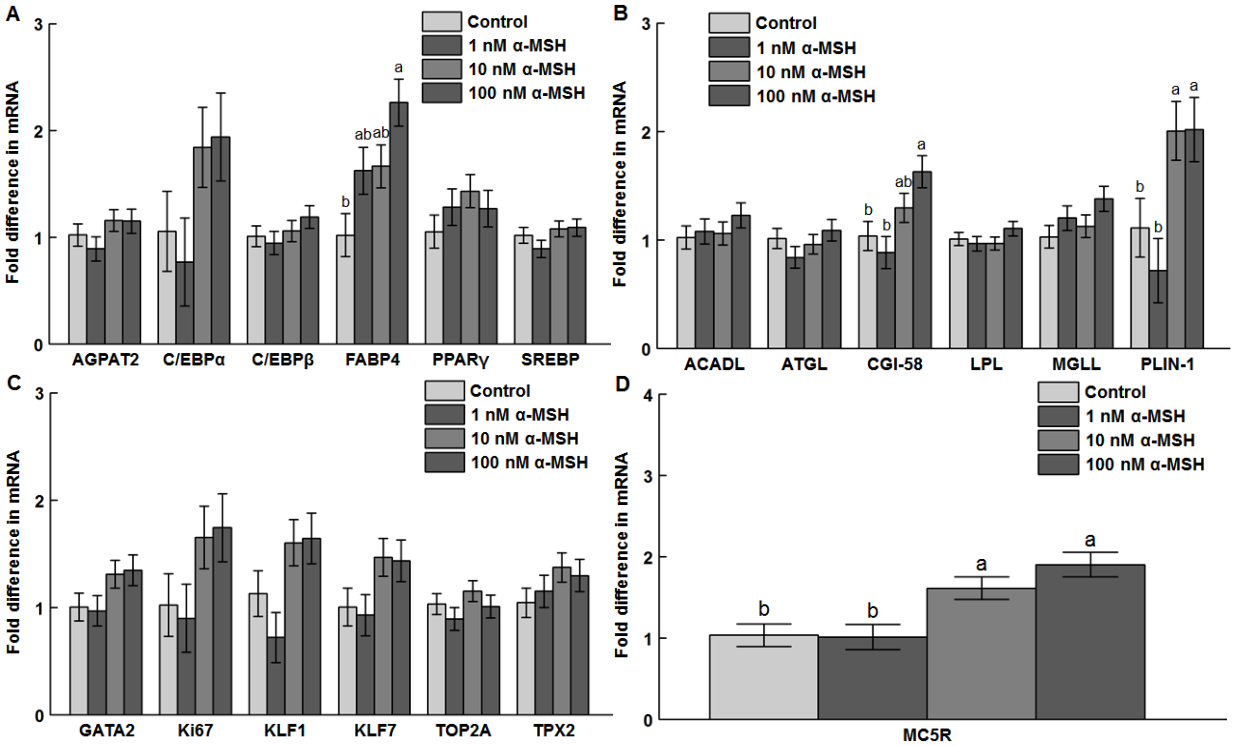

Figure 4.3. mRNA abundance in the stromal–vascular fraction of cells isolated from abdominal fat of day 14 of age broilers at 4 hours post-treatment. (A) 1-Acylglycerol-3-Phosphate O-Acyltransferase 2 (AGPAT2), CCAAT/enhancer-binding protein α (C/EBPα), CCAAT/enhancer-binding protein β (C/EBPβ), fatty acid binding protein 4 (FABP4), Peroxisome proliferator-activated receptor γ (PPARγ), sterol regulatory element binding protein (SREBP); (B) acyl-CoA dehydrogenase long chain (ACADL), adipose triglyceride lipase (ATGL), comparative gene identification - 58 (CGI-58), lipoprotein lipase (LPL), monoacylglycerol lipase (MGLL), and Perilipin-1 (PLIN-1); (C) GATA binding protein 2 (GATA2), Ki67 (Ki67), Kruppel-Like Factor 1 (KLF1), Kruppel-Like Factor 7 (KLF7), Topoisomerase II alpha (TOP2A), and thioredoxin-dependent peroxidase 2 (TPX2); (D) melanocortin receptor 5 (MCR5). Values represent least squares means ± SEM (n = 6 per group). Different letters within a gene indicate a significant difference ($P < 0.05$; Tukey's test).

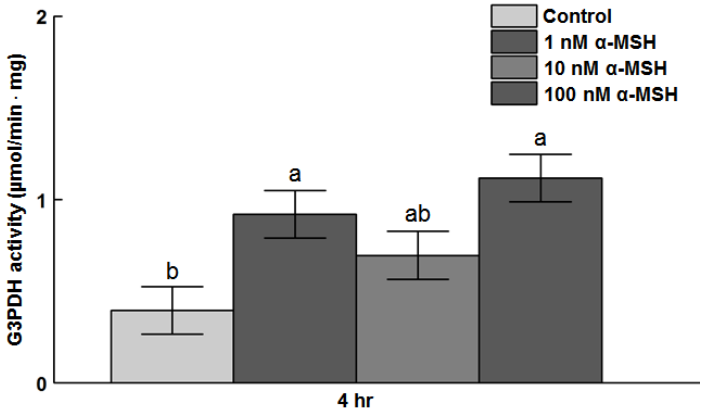

Figure 4.4. Specific activity of glycerol-3-phosphate dehydrogenase (G3PDH). Activity at day 9 post-induction of differentiation following 4 hours of incubation with 0, 1, 10 or 100 nM α-MSH. Values represent least squares means ± SEM (n = 3). Different letters indicate a significant difference ($P < 0.05$; Tukey's test).

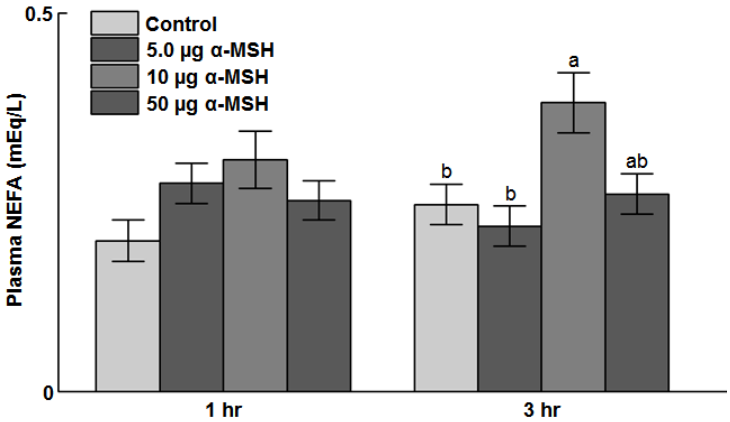

Figure 4.5. Plasma non-esterified fatty acid (NEFA) concentrations at 1 and 3 hours post-injection in day 4 of age chicks. Values represent least squares means ± SEM (n = 20 for 0, 5.0, and 50 µg α-MSH and 10 for 10 µg α-MSH). Different letters within a group indicate a significant difference ($P < 0.05$; Tukey's test).

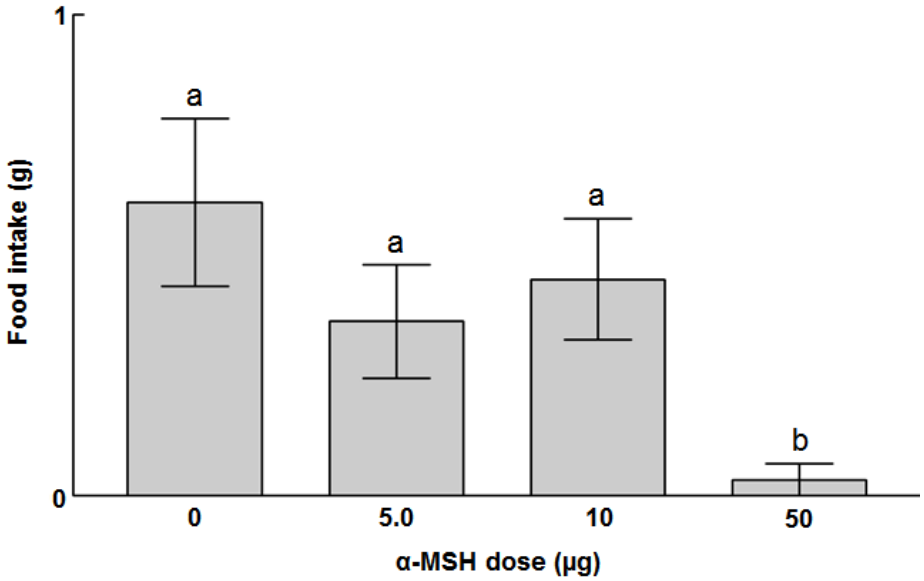

Figure 4.6. Food intake at 1 hour post-injection of 0, 5, 10, or 50 micrograms α-MSH in day 4 of age chicks. Values represent least squares means ± SEM (n = 10 per dose). Different letters indicate a significant difference ($P < 0.05$).

Table 4.1. Primers used for real time PCR

Gene[1]	Accession ID	Sequence 5' to 3' (forward/reverse)
β-Actin	NM_205518.1	GTCCACCGCAAATGCTTCTAA/ TGCGCATTTATGGGTTTTGTT
KLF1	XM_422416.4	GGCTGATTCTGGCCAAGCT/ GAGCGGAACCCAGAGTTGTG
KLF7	XM_004942644.2	GATGCTGGTTTTCCTCACAGTTT/ CCTCCTGTCCCAAAAGTGTTCA
GATA2	NM_001003797.1	CCACGAAGCAAGGCCAGAT/ GGTAGCGGTTGCTCCACAGT
Ki67	XM_004942360.2	AAAAACCTGATTCCTGAACAATCTG/ GACCTAGAGCTATCAGGCTGTGAAG
TOP2A	NM_204791.1	GCACAGCTGGCGGAAGTAAT/ TGCAGTGACCCGAGGAACA
TPX2	NM_204437.1	TGGAGGGTGGGCCAATC/ TTGGCTGTGTGAGTTCCTTCAC
PPARγ	NM_001001460.1	CACTGCAGGAACAGAACAAAGAA/ TCCACAGAGCGAAACTGACATC
C/EBPα	NM_001031459.1	CGCGGCAAATCCAAAAAG/ GGCGCACGCGGTACTC
C/EBPβ	NM_205253.2	GCCGCCCGCCTTTAAA/ CCAAACAGTCCGCCTCGTAA
SREBP	NM_204126.1	CATCCATCAACGACAAGATCGT/

		CTCAGGATCGCCGACTTGTT
FABP4	NM_204290.1	CAGAAGTGGGATGGCAAAGAG/ CCAGCAGGTTCCCATCCA
LPL	NM_205282.1	GACAGCTTGGCACAGTGCAA/ CACCCATGGATCACCACAAA
MC1R	NM_001031462.1	GCTCTGCCTCATTGGCTTCT/ TGCCAGCGCGAACATGT
MC2R	NM_001031515.1	GCTGTTGGGCCCCCTTT/ AAGGGTTGTGTGGGCAAAAC
MC3R	XM_004947236.1	GCCTCCCTTTACGTTCACATGT/ GCTGCGATGCGCTTCAC
MC4R	NM_001031514.1	CCTCGGGAGGCTGCTATGA/ GATGCCCAGAGTCACAAACACTT
MC5R	NM_001031015.1	GCCCTGCGTTACCACAACAT/ CCAAATGCATGCAATGATAAGC
POMC	NM_001031098.1	GCCAGACCCCGCTGATG/ CTTGTAGGCGCTTTTGACGAT
ATGL	NM_001113291.1	GCCTCTGCGTAGGCCATGT/ GCAGCCGGCGAAGGA
ACADL	NM_001006511.2	GACATCGGCACTCGGAAGA/ CCTGGTGCTCTCCCTGAAGA
AGPAT2	XM_015279793.1	GCCAAACACCGAAGGAACAT/ CCATGGCATCCCCAGAGTT

CGI-58	NM_001278145.1	CGCCCAGTGGTGAAAC/ GCCTTTTTGCCCATCCATAA
MGLL	XM_015293082.1	GCAGACGAGCATAGACTCA/ GGGAATAGCCTGGTTTACAA
PLIN-1	NM_001127439.1	GGAGGACGTGGCATGATGAC/ GGCCCTTCCATTCTGCAA

[1] β-Actin; KLF1: Krüppel-like factor 1; KLF7: Krüppel-like factor 7; GATA2: GATA-binding protein 2; Ki67: Ki67; TOP2A: topoisomerase II alpha; TPX2: thioredoxin-dependent peroxidase 2; PPARγ: peroxisome proliferator activated receptor γ; C/EBPα: CCAAT/enhancer binding protein α; C/EBPβ: CCAAT/enhancer binding protein β; SREBP: sterol regulatory element-binding protein; FABP4: fatty acid binding protein 4; LPL: lipoprotein lipase; MC1R: melanocortin receptor 1; MC2R: melanocortin receptor 2; MC3R: melanocortin receptor 3; MC4R: melanocortin receptor 4; MC5R: melanocortin receptor 5; POMC: proopiomelanocortin; ATGL: adipose triglyceride lipase; ACADL: acyl-CoA dehydrogenase long chain; AGPAT2: 1-acylglycerol-3-phosphate O-acyltransferase 2; CGI-58: comparative gene identification - 58; MGLL: monoacylglycerol lipase; PLIN-1: Perilipin - 1.

Chapter 5: Epilogue

The physiological mechanisms governing adipose tissue responses to NPY and α-MSH still remain poorly understood, especially in avian species. Although my research has led to advancements in our understanding, there is still much to learn.

Compared to α-MSH, there is a better understanding of how NPY affects adipose tissue physiology. Chapter 3 expands on what we have previously reported, and has helped to clarify how NPY affects the later stages of adipocyte differentiation. Where the research should be expanded is in the earlier timeframe. We measured mRNA abundance of preadipocyte and proliferation markers and NPY and NPY2R at 4, 12, 24, and 48 hours post-treatment, with transcriptional changes detectable at 4 and 12 hours. To better understand this response, the experiment should be repeated but at multiple time points before 4 hours, such as 1, 2, and 3 hours, and between 4 and 12 hours. This may reveal what genes are the first to be transcriptionally regulated in response to NPY, and also may provide a better understanding of how NPY affects transcriptional regulation over time.

NPY has a short half-life. There is ambiguity in the actual half-life reported, with considerable variability across studies. With the use of different types of assays manufactured by different companies, potential differences in gene expression and proteolytic processing that regulate differences in the amount of circulating NPY, and differential susceptibility to proteolytic degradation across tissues, it is not surprising that such variation in reported concentrations exists. Consistent across studies though is that the half-life is less than an hour. That effects of NPY in cultured cells after a 12-hour treatment were observed is striking. The effects directly

due to NPY likely happen during a short time interval, and to still have measurable effects at 12 hours is evidence that multiple pathways are being affected; possibly intracellular pathways as well as cell to cell communication as well as other routes of communication through changes in gene transcription. Measuring mRNA abundance in response to NPY at many time points may appear excessive, however to truly assess NPY's effect for up to 12 hours it is necessary to evaluate transcriptional regulation at multiple time points, otherwise we cannot accurately pinpoint when the transcriptional changes are happening in relation to induced cellular mechanisms and pathways.

If the effects of NPY are this long-lasting in the animal, there are many ways to intervene in its effects. NPY is likely to be released more often in the animal as compared to cell culture due to the many cell types expressing NPY and the multiple routes through which NPY can come into contact with the adipose tissue. This could mean that there are multiple routes for intervention other than receptor blockade. It may or may not be more fruitful to intervene in a particular intracellular pathway rather than NPY receptor antagonism, especially because of the diverse effects mediated by NPY throughout the body.

The effects of α-MSH on adipose tissue physiology are neither as well understood nor comprehensively studied as NPY. Chapter 4 is the first report of how α-MSH affects adipose tissue physiology in any avian species, and was designed based on the small amount of information reported on how α-MSH affects adipose tissue physiology in rodent cells. A major strength of this study is the report of gene expression of factors involved in multiple pathways affecting adipose tissue physiology. By measuring expression of genes encoding factors in

pathways related to preadipocyte activity and proliferation, lipolysis, and adipogenesis, we can better understand the early transcriptional effects of α-MSH, which may indicate the involvement of certain cellular pathways. As it turned out, adipose tissue depots responded differently. This finding is significant, as some studies tend to focus on a particular adipose tissue depot, usually because of convenience in extraction from the animal and because of total yield of tissue, especially in primary cell culture studies; as we did in Chapter 3. Future *in vitro* studies on α-MSH and adipose tissue in chickens should consider that the response *in vivo* is depot-dependent. Thus the response under *in vitro* conditions can at most, in terms of depot comparisons, only be attributed to the depot from which the cells were isolated.

A future study would be to isolate cells from both the subcutaneous and abdominal adipose tissue depots, and determine if the response to α-MSH *in vitro* differs between depots. This could indicate whether an *in vitro* response to α-MSH is cell type specific, meaning that the same cell type responds similarly as long as it is isolated, or if the cells isolated from a particular depot are different prior to isolation, and the difference in development accounts for the difference in response to α-MSH. If the *in vitro* response is the same between depots, this could indicate that the differences between depots *in vivo* are due to a difference in the distribution and/or number of different cell types. Different depots could also be innervated by the nervous system differently as in mammals, thus outflow from the nervous system may be depot dependent based on environmental stimuli, current energy/growth status, and other factors.

While plasma NEFA concentrations were elevated in response to α-MSH, we were unable to attribute this liberation of fatty acids to a particular adipose tissue depot. There are commercially

available lipolysis kits for measuring glycerol release in adipocytes that are freshly isolated from collagenase-digested adipose tissue. Assays performed with adipocytes from different adipose tissue depots might provide insight on which depot(s) contribute to the release of NEFA into the blood in response to a particular stimulus.

It is understood that MCRs 2 and 5 initiate signaling that leads to lipolytic effects in rodent adipocytes, and we have reported that there is increased mRNA of both of those receptors in response to α-MSH treatment in chick adipose tissue. The shortcoming of the data reported herein is that we report mRNA quantities, which may not reflect protein abundance of these receptors, whether or not the receptor is bound by α-MSH, or the affinity with which it binds. What can be conducted is immunostaining to detect the presence and amount of each receptor in the adipose tissue to determine receptor location, binding affinity assays for each receptor in culture, and western blot analyses on membrane extracts from cultured cells that were treated with α-MSH, to determine if protein expression also increases in response to α-MSH.

Limited availability of antibodies that cross-react with chicken proteins is a major shortcoming for molecular biologists using chicken as a model. In terms of intracellular pathways, second messengers and effectors tend to be more highly conserved among species, thus conducting assays such as western blots should be more straightforward because of the greater availability of reagents and antibodies that have been validated for use in other species. Because of the high degree of sequence conservation, we were able to use a human ELISA for measuring α-MSH in chick protein abundance. However, multiple attempts to measure NPY using a custom-made ELISA kit (based on the chicken sequence) and other kits and antibodies designed to target a

particular species such as human or mouse were unsuccessful (data not reported in this thesis). Thus, antibody availability and cross-reactivity is a challenge in protein research.

A shortcoming of both Chapter 3 and 4 was that they lacked data on protein expression. In molecular biology, each aspect of the central dogma from DNA being transcribed into RNA to RNA being translated into protein is important. By studying mRNA abundance in response to treatment, we attempted to better understand the transcriptional regulation. These changes however may not reflect rates of translation and level of protein function. These concerns are relevant whether the protein is a preprohormone, neuropeptide, receptor, or enzyme. Future studies should focus on measuring protein abundance, receptor activation, and enzyme activity.

Nonetheless, the data reported herein represent a major development in the understanding of how appetite-regulatory peptides affect adipose tissue physiology. By studying gene expression, enzyme activity, lipid and nuclear staining, circulating plasma levels, and food intake, both in vitro and in vivo, we have gained a better understanding of adipose tissue physiology in chicks, with effects that are unique to avians. Future research in this vein will focus on suppressing expression of NPY (and α-MSH precursor POMC) and its receptors in chick preadipocytes and adipocytes and evaluating effects on different facets of adipogenesis and lipid metabolism.

Appendix

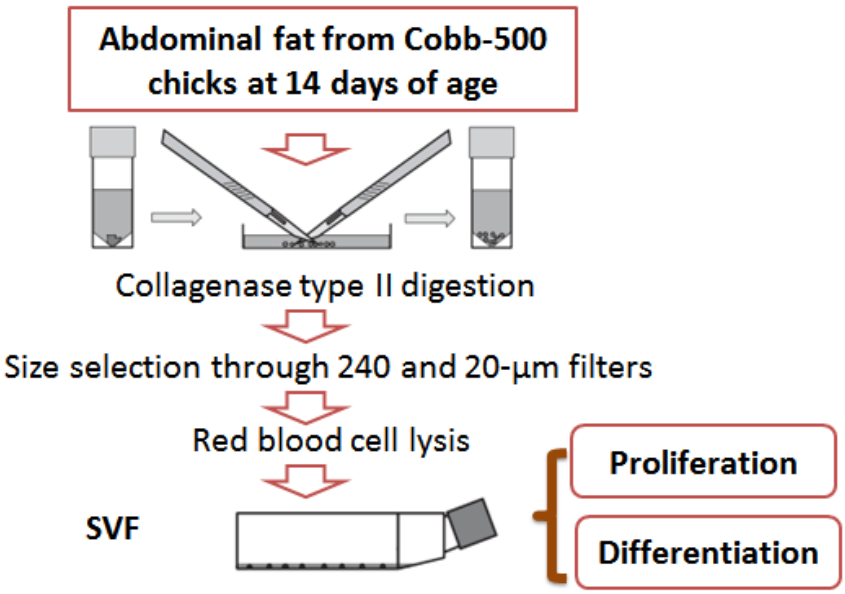

Methods for isolating the stromal vascular fraction of cells (SVF). Cobb-500 chicks are grown to day 14 of age, and 2 grams of abdominal adipose tissue are excised. The tissue is then finely minced, collagenase type II digested, and size selected through 240 and 20-µm filters, and a red blood cell lysis buffer is added. This results in the isolation of cells from the SVF. While the SVF contains preadipocytes, mesenchymal stem cells, endothelial progenitor cells and immune cells, this protocol enriches for preadipocytes and mesenchymal stem cells.

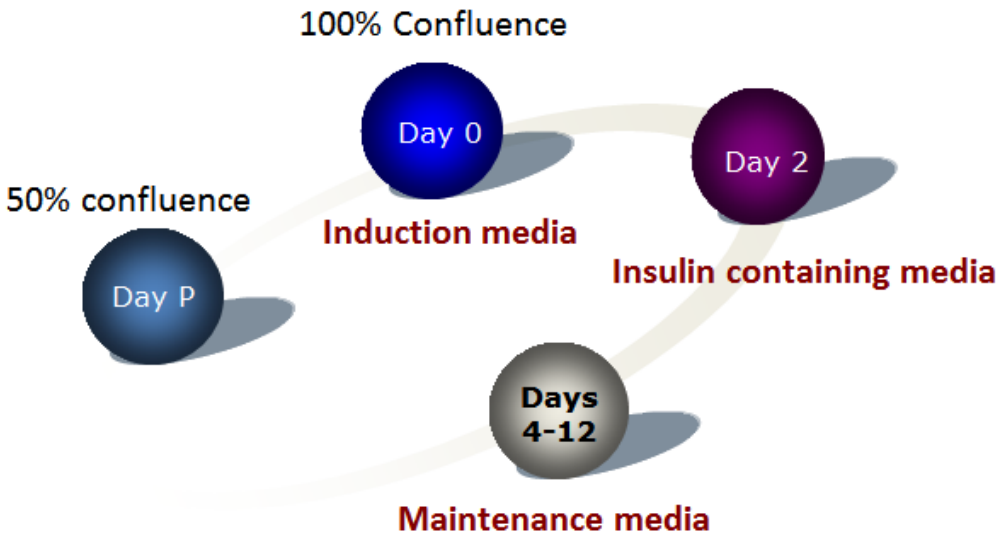

Experimental time points for preadipocyte differentiation studies. Once cells have reached 50% confluence, day P is the day for preadipocyte experiments. When cells reach confluence, this is day 0, where the cells are induced to differentiate by adding induction media. Forty-eight hours later, the induction media is changed to insulin containing media. Beginning at day 4, maintenance media is added to the cells, and changed every forty-eight hours. NPY was supplemented daily in the differentiation experiment reported in Chapter 3, and no other supplementation was included during differentiation in Chapter 4.

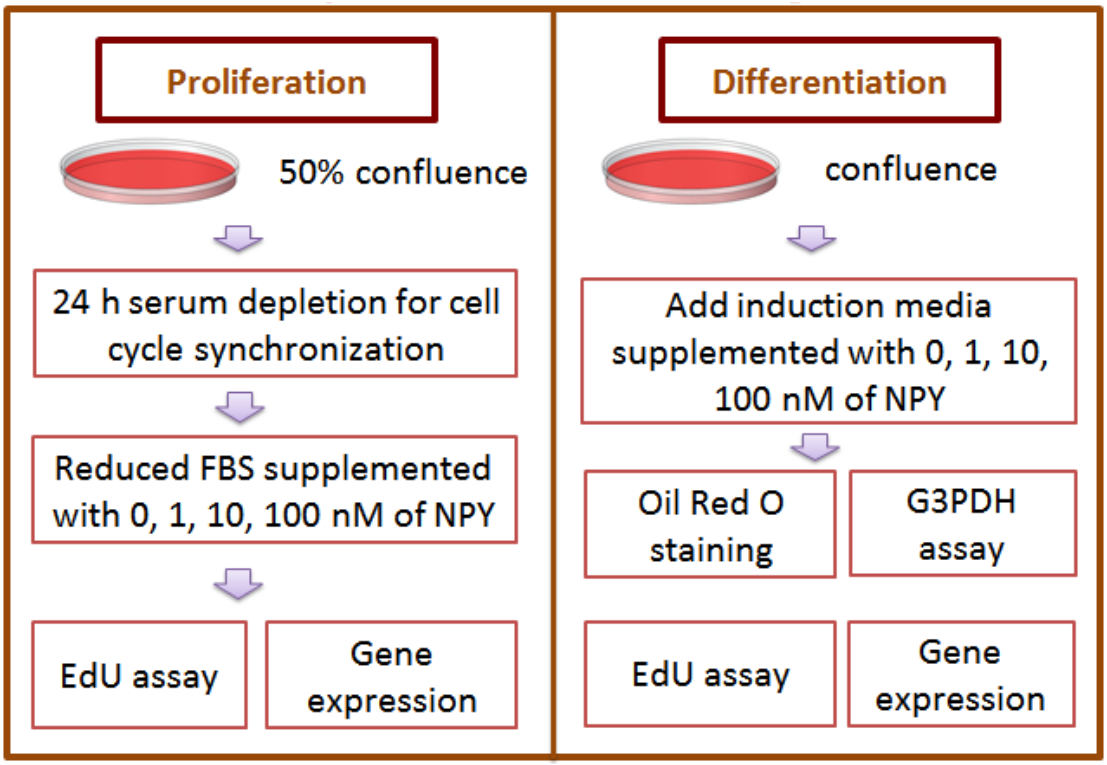

Experimental design for proliferation and differentiation experiments. Proliferation: After cells reach 50% confluence, they are serum deprived for 24 hours for cell cycle synchronization. A reduced fetal bovine serum (FBS) media supplemented with different concentrations of NPY is then added, and after the experimental treatment time, the 5-Ethynyl-2´-deoxyuridine (Edu) assay and gene expression assays are performed. Differentiation: After reaching confluence, cells are induced to differentiate in the presence of different concentrations of NPY. After the experimental time point, oil red O staining, glycerol – 3 – phosphate dehydrogenase (G3PDH) assay, Edu assay, and gene expression assays are performed.

References

1. Sullivan, P.W., et al., *Obesity, inactivity, and the prevalence of diabetes and diabetes-related cardiovascular comorbidities in the U.S., 2000-2002.* Diabetes Care, 2005. **28**(7): p. 1599-603.
2. Byrd, J.B. and R.D. Brook, *A critical review of the evidence supporting aldosterone in the etiology and its blockade in the treatment of obesity-associated hypertension.* J Hum Hypertens, 2014. **28**(1): p. 3-9.
3. Oguma, Y., et al., *Weight change and risk of developing type 2 diabetes.* Obes Res, 2005. **13**(5): p. 945-51.
4. Basen-Engquist, K. and M. Chang, *Obesity and cancer risk: recent review and evidence.* Curr Oncol Rep, 2011. **13**(1): p. 71-6.
5. Urdaneta-Rincon, M. and S. Leeson, *Quantitative and qualitative feed restriction on growth characteristics of male broiler chickens.* Poult Sci, 2002. **81**(5): p. 679-88.
6. Shipp, S.L., M.A. Cline, and E.R. Gilbert, *Recent advances in the understanding of how neuropeptide Y and α-melanocyte stimulating hormone function in adipose physiology.* Adipocyte, 2016: p. 1-18.
7. Brothers, S.P. and C. Wahlestedt, *Therapeutic potential of neuropeptide Y (NPY) receptor ligands.* EMBO Mol Med, 2010. **2**(11): p. 429-39.
8. Cyr, N.E., et al., *Mechanisms by which the orexigen NPY regulates anorexigenic alpha-MSH and TRH.* Am J Physiol Endocrinol Metab, 2013. **304**(6): p. E640-50.
9. Tatemoto, K., M. Carlquist, and V. Mutt, *Neuropeptide Y--a novel brain peptide with structural similarities to peptide YY and pancreatic polypeptide.* Nature, 1982. **296**(5858): p. 659-60.
10. Clark, J.T., et al., *Neuropeptide Y and human pancreatic polypeptide stimulate feeding behavior in rats.* Endocrinology, 1984. **115**(1): p. 427-9.
11. Pau, M.Y., K.Y. Pau, and H.G. Spies, *Characterization of central actions of neuropeptide Y on food and water intake in rabbits.* Physiol Behav, 1988. **44**(6): p. 797-802.
12. Matsuda, K., et al., *Neuroendocrine control of feeding behavior and psychomotor activity by neuropeptideY in fish.* Neuropeptides, 2012. **46**(6): p. 275-83.
13. Richardson, R.D., et al., *NPY increases food intake in white-crowned sparrows: effect in short and long photoperiods.* Am J Physiol, 1995. **268**(6 Pt 2): p. R1418-22.
14. Kuenzel, W.J., L.W. Douglass, and B.A. Davison, *Robust feeding following central administration of neuropeptide Y or peptide YY in chicks, Gallus domesticus.* Peptides, 1987. **8**(5): p. 823-8.
15. Newmyer, B.A., et al., *Neuropeptide Y is associated with changes in appetite-associated hypothalamic nuclei but not food intake in a hypophagic avian model.* Behav Brain Res, 2013. **236**(1): p. 327-31.
16. Kuo, L.E., et al., *Neuropeptide Y acts directly in the periphery on fat tissue and mediates stress-induced obesity and metabolic syndrome.* Nat Med, 2007. **13**(7): p. 803-11.
17. Zhang, W., et al., *Neuropeptide Y promotes adipogenesis in chicken adipose cells in vitro.* Comp Biochem Physiol A Mol Integr Physiol, 2015. **181**: p. 62-70.

18. Wardlaw, S.L., *Hypothalamic proopiomelanocortin processing and the regulation of energy balance.* Eur J Pharmacol, 2011. **660**(1): p. 213-9.
19. Zimanyi, I.A. and M.A. Pelleymounter, *The role of melanocortin peptides and receptors in regulation of energy balance.* Curr Pharm Des, 2003. **9**(8): p. 627-41.
20. Al-Barazanji, K.A., et al., *C-terminal fragments of ACTH stimulate feeding in fasted rats.* Horm Metab Res, 2001. **33**(8): p. 480-5.
21. Cerda-Reverter, J.M., H.B. Schioth, and R.E. Peter, *The central melanocortin system regulates food intake in goldfish.* Regul Pept, 2003. **115**(2): p. 101-13.
22. Saneyasu, T., et al., *Alpha-melanocyte stimulating hormone plays an important role in the regulation of food intake by the central melanocortin system in chicks.* Peptides, 2011. **32**(5): p. 996-1000.
23. Rodrigues, A.R., H. Almeida, and A.M. Gouveia, *Alpha-MSH signalling via melanocortin 5 receptor promotes lipolysis and impairs re-esterification in adipocytes.* Biochim Biophys Acta, 2013. **1831**(7): p. 1267-75.
24. Zhang, W., M.A. Cline, and E.R. Gilbert, *Hypothalamus-adipose tissue crosstalk: neuropeptide Y and the regulation of energy metabolism.* Nutr Metab (Lond), 2014. **11**: p. 27.
25. Zuk, P.A., et al., *Human adipose tissue is a source of multipotent stem cells.* Mol Biol Cell, 2002. **13**(12): p. 4279-95.
26. Billon, N., et al., *The generation of adipocytes by the neural crest.* Development, 2007. **134**(12): p. 2283-92.
27. Le Lievre, C.S. and N.M. Le Douarin, *Mesenchymal derivatives of the neural crest: analysis of chimaeric quail and chick embryos.* J Embryol Exp Morphol, 1975. **34**(1): p. 125-54.
28. Hauner, H., P. Schmid, and E.F. Pfeiffer, *Glucocorticoids and insulin promote the differentiation of human adipocyte precursor cells into fat cells.* J Clin Endocrinol Metab, 1987. **64**(4): p. 832-5.
29. Grigoriadis, A.E., J.N. Heersche, and J.E. Aubin, *Differentiation of muscle, fat, cartilage, and bone from progenitor cells present in a bone-derived clonal cell population: effect of dexamethasone.* J Cell Biol, 1988. **106**(6): p. 2139-51.
30. Wakitani, S., T. Saito, and A.I. Caplan, *Myogenic cells derived from rat bone marrow mesenchymal stem cells exposed to 5-azacytidine.* Muscle Nerve, 1995. **18**(12): p. 1417-26.
31. Ferrari, G., et al., *Muscle regeneration by bone marrow-derived myogenic progenitors.* Science, 1998. **279**(5356): p. 1528-30.
32. Johnstone, B., et al., *In vitro chondrogenesis of bone marrow-derived mesenchymal progenitor cells.* Exp Cell Res, 1998. **238**(1): p. 265-72.
33. Pittenger, M.F., et al., *Multilineage potential of adult human mesenchymal stem cells.* Science, 1999. **284**(5411): p. 143-7.
34. Wang, W.G., et al., *In vitro chondrogenesis of human bone marrow-derived mesenchymal progenitor cells in monolayer culture: activation by transfection with TGF-beta2.* Tissue Cell, 2003. **35**(1): p. 69-77.
35. Gao, S., et al., *Differentiation of human adipose-derived stem cells into neuron-like cells which are compatible with photocurable three-dimensional scaffolds.* Tissue Eng Part A, 2014. **20**(7-8): p. 1271-84.

36. Zhu, T., et al., *GDNF and NT-3 induce progenitor bone mesenchymal stem cell differentiation into neurons in fetal gut culture medium.* Cell Mol Neurobiol, 2015. **35**(2): p. 255-64.
37. Huang, T., et al., *Neuron-like differentiation of adipose-derived stem cells from infant piglets in vitro.* J Spinal Cord Med, 2007. **30 Suppl 1**: p. S35-40.
38. Rosen, E.D. and O.A. MacDougald, *Adipocyte differentiation from the inside out.* Nat Rev Mol Cell Biol, 2006. **7**(12): p. 885-96.
39. Rosen, E.D., et al., *Transcriptional regulation of adipogenesis.* Genes Dev, 2000. **14**(11): p. 1293-307.
40. Barak, Y., et al., *PPAR gamma is required for placental, cardiac, and adipose tissue development.* Mol Cell, 1999. **4**(4): p. 585-95.
41. Tontonoz, P., et al., *mPPAR gamma 2: tissue-specific regulator of an adipocyte enhancer.* Genes Dev, 1994. **8**(10): p. 1224-34.
42. Tontonoz, P., E. Hu, and B.M. Spiegelman, *Stimulation of adipogenesis in fibroblasts by PPAR gamma 2, a lipid-activated transcription factor.* Cell, 1994. **79**(7): p. 1147-56.
43. Hu, E., P. Tontonoz, and B.M. Spiegelman, *Transdifferentiation of myoblasts by the adipogenic transcription factors PPAR gamma and C/EBP alpha.* Proc Natl Acad Sci U S A, 1995. **92**(21): p. 9856-60.
44. Tamori, Y., et al., *Role of peroxisome proliferator-activated receptor-gamma in maintenance of the characteristics of mature 3T3-L1 adipocytes.* Diabetes, 2002. **51**(7): p. 2045-55.
45. Imai, T., et al., *Peroxisome proliferator-activated receptor gamma is required in mature white and brown adipocytes for their survival in the mouse.* Proc Natl Acad Sci U S A, 2004. **101**(13): p. 4543-7.
46. Kawaguchi, N., et al., *De novo adipogenesis in mice at the site of injection of basement membrane and basic fibroblast growth factor.* Proc Natl Acad Sci U S A, 1998. **95**(3): p. 1062-6.
47. Eberle, D., et al., *SREBP transcription factors: master regulators of lipid homeostasis.* Biochimie, 2004. **86**(11): p. 839-48.
48. Horton, J.D., *Sterol regulatory element-binding proteins: transcriptional activators of lipid synthesis.* Biochem Soc Trans, 2002. **30**(Pt 6): p. 1091-5.
49. Georgiadi, A. and S. Kersten, *Mechanisms of gene regulation by fatty acids.* Adv Nutr, 2012. **3**(2): p. 127-34.
50. Kim, J.B., et al., *ADD1/SREBP1 activates PPARgamma through the production of endogenous ligand.* Proc Natl Acad Sci U S A, 1998. **95**(8): p. 4333-7.
51. Forman, B.M., et al., *15-Deoxy-delta 12, 14-prostaglandin J2 is a ligand for the adipocyte determination factor PPAR gamma.* Cell, 1995. **83**(5): p. 803-12.
52. Kliewer, S.A., et al., *A prostaglandin J2 metabolite binds peroxisome proliferator-activated receptor gamma and promotes adipocyte differentiation.* Cell, 1995. **83**(5): p. 813-9.
53. Krey, G., et al., *Fatty acids, eicosanoids, and hypolipidemic agents identified as ligands of peroxisome proliferator-activated receptors by coactivator-dependent receptor ligand assay.* Mol Endocrinol, 1997. **11**(6): p. 779-91.

54. Kim, J.B., et al., *Nutritional and insulin regulation of fatty acid synthetase and leptin gene expression through ADD1/SREBP1.* J Clin Invest, 1998. **101**(1): p. 1-9.
55. Cao, Z., R.M. Umek, and S.L. McKnight, *Regulated expression of three C/EBP isoforms during adipose conversion of 3T3-L1 cells.* Genes Dev, 1991. **5**(9): p. 1538-52.
56. Yeh, W.C., et al., *Cascade regulation of terminal adipocyte differentiation by three members of the C/EBP family of leucine zipper proteins.* Genes Dev, 1995. **9**(2): p. 168-81.
57. Linhart, H.G., et al., *C/EBPalpha is required for differentiation of white, but not brown, adipose tissue.* Proc Natl Acad Sci U S A, 2001. **98**(22): p. 12532-7.
58. Chen, S.S., et al., *C/EBPbeta, when expressed from the C/ebpalpha gene locus, can functionally replace C/EBPalpha in liver but not in adipose tissue.* Mol Cell Biol, 2000. **20**(19): p. 7292-9.
59. Wu, Z., et al., *Cross-regulation of C/EBP alpha and PPAR gamma controls the transcriptional pathway of adipogenesis and insulin sensitivity.* Mol Cell, 1999. **3**(2): p. 151-8.
60. Zuo, Y., L. Qiang, and S.R. Farmer, *Activation of CCAAT/enhancer-binding protein (C/EBP) alpha expression by C/EBP beta during adipogenesis requires a peroxisome proliferator-activated receptor-gamma-associated repression of HDAC1 at the C/ebp alpha gene promoter.* J Biol Chem, 2006. **281**(12): p. 7960-7.
61. Henry, S.L., et al., *White adipocytes: more than just fat depots.* Int J Biochem Cell Biol, 2012. **44**(3): p. 435-40.
62. Saely, C.H., K. Geiger, and H. Drexel, *Brown versus white adipose tissue: a mini-review.* Gerontology, 2012. **58**(1): p. 15-23.
63. Cannon, B. and J. Nedergaard, *Brown adipose tissue: function and physiological significance.* Physiol Rev, 2004. **84**(1): p. 277-359.
64. Saarela, S., et al., *Is the "mammalian" brown fat-specific mitochondrial uncoupling protein present in adipose tissues of birds?* Comp Biochem Physiol B, 1991. **100**(1): p. 45-9.
65. Mezentseva, N.V., J.S. Kumaratilake, and S.A. Newman, *The brown adipocyte differentiation pathway in birds: an evolutionary road not taken.* BMC Biol, 2008. **6**: p. 17.
66. Johnston, D.W., *The absence of brown adipose tissue in birds.* Comp Biochem Physiol A Comp Physiol, 1971. **40**(4): p. 1107-8.
67. Mozo, J., et al., *Thermoregulation: what role for UCPs in mammals and birds?* Biosci Rep, 2005. **25**(3-4): p. 227-49.
68. Bjorndal, B., et al., *Different adipose depots: their role in the development of metabolic syndrome and mitochondrial response to hypolipidemic agents.* J Obes, 2011. **2011**: p. 490650.
69. Dodson, M.V., et al., *Adipose depots differ in cellularity, adipokines produced, gene expression, and cell systems.* Adipocyte, 2014. **3**(4): p. 236-41.
70. Speake, B.K., et al., *Adipose tissue development in the chick embryo.* Biochem Soc Trans, 1996. **24**(2): p. 161S.

71. Chen, P., et al., *Developmental regulation of adipose tissue growth through hyperplasia and hypertrophy in the embryonic Leghorn and broiler.* Poult Sci, 2014. **93**(7): p. 1809-17.
72. Bai, S., et al., *Broiler chicken adipose tissue dynamics during the first two weeks post-hatch.* Comp Biochem Physiol A Mol Integr Physiol, 2015. **189**: p. 115-23.
73. Zhang, W., et al., *Quantity of glucose transporter and appetite-associated factor mRNA in various tissues after insulin injection in chickens selected for low or high body weight.* Physiol Genomics, 2013. **45**(22): p. 1084-94.
74. Zhang, S., et al., *Chickens from lines selected for high and low body weight show differences in fatty acid oxidation efficiency and metabolic flexibility in skeletal muscle and white adipose tissue.* Int J Obes (Lond), 2014. **38**(10): p. 1374-82.
75. Dunnington, E.A. and P.B. Siegel, *Long-term divergent selection for eight-week body weight in white Plymouth rock chickens.* Poult Sci, 1996. **75**(10): p. 1168-79.
76. Zelenka, D.J., et al., *Anorexia and sexual maturity in female white rock chickens. I. Increasing the feed intake.* Behav Genet, 1988. **18**(3): p. 383-7.
77. Dunnington, E.A., et al., *Physiological Traits in Adult Female Chickens after Selection and Relaxation of Selection for 8-Week Body-Weight.* Journal of Animal Breeding and Genetics-Zeitschrift Fur Tierzuchtung Und Zuchtungsbiologie, 1986. **103**(1): p. 51-58.
78. Dunnington, E.A., et al., *Phenotypic responses of chickens to long-term, bidirectional selection for juvenile body weight-Historical perspective.* Poultry Science, 2013. **92**(7): p. 1724-1734.
79. Kwon, H.S. and R.A. Harris, *Mechanisms responsible for regulation of pyruvate dehydrogenase kinase 4 gene expression.* Advances in Enzyme Regulation, Vol 44, 2004. **44**: p. 109-121.
80. Constantin-Teodosiu, D., et al., *The Role of FOXO and PPAR Transcription Factors in Diet-Mediated Inhibition of PDC Activation and Carbohydrate Oxidation During Exercise in Humans and the Role of Pharmacological Activation of PDC in Overriding These Changes.* Diabetes, 2012. **61**(5): p. 1017-1024.
81. Sugden, M.C., *PDK4: A factor in fatness?* Obesity Research, 2003. **11**(2): p. 167-169.
82. Guarente, L. and C. Kenyon, *Genetic pathways that regulate ageing in model organisms.* Nature, 2000. **408**(6809): p. 255-262.
83. Gross, D.N., A.P.J. van den Heuvel, and M.J. Birnbaum, *The role of FoxO in the regulation of metabolism.* Oncogene, 2008. **27**(16): p. 2320-2336.
84. Poulos, S.P., M.V. Dodson, and G.J. Hausman, *Cell line models for differentiation: preadipocytes and adipocytes.* Exp Biol Med (Maywood), 2010. **235**(10): p. 1185-93.
85. Hollenberg, C.H. and A. Vost, *Regulation of DNA synthesis in fat cells and stromal elements from rat adipose tissue.* J Clin Invest, 1969. **47**(11): p. 2485-98.
86. Riordan, N.H., et al., *Non-expanded adipose stromal vascular fraction cell therapy for multiple sclerosis.* J Transl Med, 2009. **7**: p. 29.
87. Schipper, H.S., et al., *Adipose tissue-resident immune cells: key players in immunometabolism.* Trends Endocrinol Metab, 2012. **23**(8): p. 407-15.

88. Frisbie, D.D., et al., *Evaluation of adipose-derived stromal vascular fraction or bone marrow-derived mesenchymal stem cells for treatment of osteoarthritis.* J Orthop Res, 2009. **27**(12): p. 1675-80.
89. Zamperone, A., et al., *Isolation and characterization of a spontaneously immortalized multipotent mesenchymal cell line derived from mouse subcutaneous adipose tissue.* Stem Cells Dev, 2013. **22**(21): p. 2873-84.
90. Chen, S.Y., et al., *Isolation and characterization of mesenchymal progenitor cells from human orbital adipose tissue.* Invest Ophthalmol Vis Sci, 2014. **55**(8): p. 4842-52.
91. Thalmann, S., C.E. Juge-Aubry, and C.A. Meier, *Explant cultures of white adipose tissue.* Methods Mol Biol, 2008. **456**: p. 195-9.
92. Priya, N., et al., *Explant culture: a simple, reproducible, efficient and economic technique for isolation of mesenchymal stromal cells from human adipose tissue and lipoaspirate.* J Tissue Eng Regen Med, 2014. **8**(9): p. 706-16.
93. Ramsay, T.G. and R.W. Rosebrough, *Hormonal regulation of postnatal chicken preadipocyte differentiation in vitro.* Comp Biochem Physiol B Biochem Mol Biol, 2003. **136**(2): p. 245-53.
94. Braun, E.J. and K.L. Sweazea, *Glucose regulation in birds.* Comp Biochem Physiol B Biochem Mol Biol, 2008. **151**(1): p. 1-9.
95. Simon, J., et al., *Insulin immuno-neutralization in fed chickens: effects on liver and muscle transcriptome.* Physiol Genomics, 2012. **44**(5): p. 283-92.
96. Choudhery, M.S., et al., *Donor age negatively impacts adipose tissue-derived mesenchymal stem cell expansion and differentiation.* J Transl Med, 2014. **12**: p. 8.
97. Kershaw, E.E. and J.S. Flier, *Adipose tissue as an endocrine organ.* J Clin Endocrinol Metab, 2004. **89**(6): p. 2548-56.
98. Bamshad, M., et al., *Central nervous system origins of the sympathetic nervous system outflow to white adipose tissue.* Am J Physiol, 1998. **275**(1 Pt 2): p. R291-9.
99. Bamshad, M., C.K. Song, and T.J. Bartness, *CNS origins of the sympathetic nervous system outflow to brown adipose tissue.* Am J Physiol, 1999. **276**(6 Pt 2): p. R1569-78.
100. Jansen, A.S., D.G. Farwell, and A.D. Loewy, *Specificity of pseudorabies virus as a retrograde marker of sympathetic preganglionic neurons: implications for transneuronal labeling studies.* Brain Res, 1993. **617**(1): p. 103-12.
101. Strack, A.M. and A.D. Loewy, *Pseudorabies virus: a highly specific transneuronal cell body marker in the sympathetic nervous system.* J Neurosci, 1990. **10**(7): p. 2139-47.
102. Giordano, A., et al., *White adipose tissue lacks significant vagal innervation and immunohistochemical evidence of parasympathetic innervation.* Am J Physiol Regul Integr Comp Physiol, 2006. **291**(5): p. R1243-55.
103. Oh, C.M., et al., *Regulation of systemic energy homeostasis by serotonin in adipose tissues.* Nat Commun, 2015. **6**: p. 6794.
104. Nicolaysen, A., et al., *The components required for amino acid neurotransmitter signaling are present in adipose tissues.* J Lipid Res, 2007. **48**(10): p. 2123-32.

105. Dodd, G.T., et al., *Leptin and insulin act on POMC neurons to promote the browning of white fat.* Cell, 2015. **160**(1-2): p. 88-104.
106. Zhang, Y., et al., *Simultaneous POMC gene transfer to hypothalamus and brainstem increases physical activity, lipolysis and reduces adult-onset obesity.* Eur J Neurosci, 2011. **33**(8): p. 1541-50.
107. Bowers, R.R., et al., *Sympathetic innervation of white adipose tissue and its regulation of fat cell number.* Am J Physiol Regul Integr Comp Physiol, 2004. **286**(6): p. R1167-75.
108. Gotzsche, C.R. and D.P. Woldbye, *The role of NPY in learning and memory.* Neuropeptides, 2015.
109. Tilan, J. and J. Kitlinska, *Neuropeptide Y (NPY) in tumor growth and progression: Lessons learned from pediatric oncology.* Neuropeptides, 2015.
110. Lundberg, J.M., et al., *Pharmacology of noradrenaline and neuropeptide tyrosine (NPY)-mediated sympathetic cotransmission.* Fundam Clin Pharmacol, 1990. **4**(4): p. 373-91.
111. Cortes, V., et al., *Synergism between neuropeptide Y and norepinephrine highlights sympathetic cotransmission: studies in rat arterial mesenteric bed with neuropeptide Y, analogs, and BIBP 3226.* J Pharmacol Exp Ther, 1999. **289**(3): p. 1313-22.
112. Ruohonen, S.T., et al., *Stress-induced hypertension and increased sympathetic activity in mice overexpressing neuropeptide Y in noradrenergic neurons.* Neuroendocrinology, 2009. **89**(3): p. 351-60.
113. al-Arabi, A. and J.F. Andrews, *Synergistic action by neuropeptide Y (NPY) and norepinephrine (NE) on food intake, metabolic rate, and brown adipose tissue (BAT) causes remarkable weight loss in the obese (fa/fa) Zucker rat.* Biomed Sci Instrum, 1997. **33**: p. 216-25.
114. Li, R., H. Guan, and K. Yang, *Neuropeptide Y potentiates beta-adrenergic stimulation of lipolysis in 3T3-L1 adipocytes.* Regul Pept, 2012. **178**(1-3): p. 16-20.
115. Vahatalo, L.H., et al., *Neuropeptide Y in the noradrenergic neurones induces obesity and inhibits sympathetic tone in mice.* Acta Physiol (Oxf), 2015. **213**(4): p. 902-19.
116. Ravelli, G.P., Z.A. Stein, and M.W. Susser, *Obesity in young men after famine exposure in utero and early infancy.* N Engl J Med, 1976. **295**(7): p. 349-53.
117. Tang, W., et al., *White fat progenitor cells reside in the adipose vasculature.* Science, 2008. **322**(5901): p. 583-6.
118. Han, R., et al., *Stress hormone epinephrine enhances adipogenesis in murine embryonic stem cells by up-regulating the neuropeptide Y system.* PLoS One, 2012. **7**(5): p. e36609.
119. Tang, H.N., et al., *Dose-dependent effects of neuropeptide Y on the regulation of preadipocyte proliferation and adipocyte lipid synthesis via the PPARgamma pathways.* Endocr J, 2015. **62**(9): p. 835-46.
120. Wan, Y., et al., *The effect of neuropeptide Y on brown-like adipocyte's differentiation and activation.* Peptides, 2015. **63**: p. 126-33.
121. Rodriguez-Carballo, E., et al., *p38alpha function in osteoblasts influences adipose tissue homeostasis.* FASEB J, 2015. **29**(4): p. 1414-25.

122. Shi, Y.C. and P.A. Baldock, *Central and peripheral mechanisms of the NPY system in the regulation of bone and adipose tissue.* Bone, 2012. **50**(2): p. 430-6.
123. Baldock, P.A., et al., *Hypothalamic control of bone formation: distinct actions of leptin and y2 receptor pathways.* J Bone Miner Res, 2005. **20**(10): p. 1851-7.
124. Ducy, P., et al., *Leptin inhibits bone formation through a hypothalamic relay: a central control of bone mass.* Cell, 2000. **100**(2): p. 197-207.
125. Baldock, P.A., et al., *Neuropeptide Y knockout mice reveal a central role of NPY in the coordination of bone mass to body weight.* PLoS One, 2009. **4**(12): p. e8415.
126. Sato, N., et al., *Modulation of neuropeptide Y receptors for the treatment of obesity.* Expert Opin Ther Pat, 2009. **19**(10): p. 1401-15.
127. Parker, R.M. and H. Herzog, *Regional distribution of Y-receptor subtype mRNAs in rat brain.* Eur J Neurosci, 1999. **11**(4): p. 1431-48.
128. Gehlert, D.R., *Role of hypothalamic neuropeptide Y in feeding and obesity.* Neuropeptides, 1999. **33**(5): p. 329-38.
129. Blomqvist, A.G. and H. Herzog, *Y-receptor subtypes--how many more?* Trends Neurosci, 1997. **20**(7): p. 294-8.
130. Naveilhan, P., et al., *Complementary and overlapping expression of Y1, Y2 and Y5 receptors in the developing and adult mouse nervous system.* Neuroscience, 1998. **87**(1): p. 289-302.
131. Gong, H.X., et al., *Lipolysis and apoptosis of adipocytes induced by neuropeptide Y-Y5 receptor antisense oligodeoxynucleotides in obese rats.* Acta Pharmacol Sin, 2003. **24**(6): p. 569-75.
132. Rosmaninho-Salgado, J., et al., *Intracellular mechanisms coupled to NPY Y2 and Y5 receptor activation and lipid accumulation in murine adipocytes.* Neuropeptides, 2012. **46**(6): p. 359-66.
133. Singer, K., et al., *Neuropeptide Y is produced by adipose tissue macrophages and regulates obesity-induced inflammation.* PLoS One, 2013. **8**(3): p. e57929.
134. Yang, K., et al., *Neuropeptide Y is produced in visceral adipose tissue and promotes proliferation of adipocyte precursor cells via the Y1 receptor.* FASEB J, 2008. **22**(7): p. 2452-64.
135. Picard, F., et al., *Sirt1 promotes fat mobilization in white adipocytes by repressing PPAR-gamma.* Nature, 2004. **429**(6993): p. 771-6.
136. Xu, F., et al., *GLP-1 receptor agonist promotes brown remodelling in mouse white adipose tissue through SIRT1.* Diabetologia, 2016. **59**(5): p. 1059-69.
137. Wu, J., P. Cohen, and B.M. Spiegelman, *Adaptive thermogenesis in adipocytes: is beige the new brown?* Genes Dev, 2013. **27**(3): p. 234-50.
138. Xue, B., et al., *Transcriptional synergy and the regulation of Ucp1 during brown adipocyte induction in white fat depots.* Mol Cell Biol, 2005. **25**(18): p. 8311-22.
139. Fedorenko, A., P.V. Lishko, and Y. Kirichok, *Mechanism of fatty-acid-dependent UCP1 uncoupling in brown fat mitochondria.* Cell, 2012. **151**(2): p. 400-13.
140. Park, S., et al., *NPY antagonism reduces adiposity and attenuates age-related imbalance of adipose tissue metabolism.* FASEB J, 2014. **28**(12): p. 5337-48.
141. Bi, S., Y.J. Kim, and F. Zheng, *Dorsomedial hypothalamic NPY and energy balance control.* Neuropeptides, 2012. **46**(6): p. 309-14.

142. Chao, P.T., et al., *Knockdown of NPY expression in the dorsomedial hypothalamus promotes development of brown adipocytes and prevents diet-induced obesity.* Cell Metab, 2011. **13**(5): p. 573-83.
143. Margareto, J., et al., *A new NPY-antagonist strongly stimulates apoptosis and lipolysis on white adipocytes in an obesity model.* Life Sci, 2000. **68**(1): p. 99-107.
144. Alasvand, M., et al., *Effect of blockade of neuropeptide Y receptor on aortic intima-media thickness and adipose tissue characteristics in normal and obese mice.* Iran J Basic Med Sci, 2015. **18**(5): p. 443-8.
145. Samuel, V.T. and G.I. Shulman, *Mechanisms for insulin resistance: common threads and missing links.* Cell, 2012. **148**(5): p. 852-71.
146. Nway, N.C., et al., *Correlations between the expression of the insulin sensitizing hormones, adiponectin, visfatin, and omentin, and the appetite regulatory hormone, neuropeptide Y and its receptors in subcutaneous and visceral adipose tissues.* Obes Res Clin Pract, 2015.
147. Long, M., et al., *Long-Term Over-Expression of Neuropeptide Y in Hypothalamic Paraventricular Nucleus Contributes to Adipose Tissue Insulin Resistance Partly via the Y5 Receptor.* PLoS One, 2015. **10**(5): p. e0126714.
148. Rao, J.R., et al., *Adiponectin increases insulin content and cell proliferation in MIN6 cells via PPARgamma-dependent and PPARgamma-independent mechanisms.* Diabetes Obes Metab, 2012. **14**(11): p. 983-9.
149. Golubovic, M.V., et al., *Relationship of adipokine to insulin sensitivity and glycemic regulation in obese women--the effect of body weight reduction by caloric restriction.* Vojnosanit Pregl, 2013. **70**(3): p. 284-91.
150. Fukuhara, A., et al., *Visfatin: a protein secreted by visceral fat that mimics the effects of insulin.* Science, 2005. **307**(5708): p. 426-30.
151. Yang, R.Z., et al., *Identification of omentin as a novel depot-specific adipokine in human adipose tissue: possible role in modulating insulin action.* Am J Physiol Endocrinol Metab, 2006. **290**(6): p. E1253-61.
152. Yulyaningsih, E., et al., *NPY receptors as potential targets for anti-obesity drug development.* Br J Pharmacol, 2011. **163**(6): p. 1170-202.
153. Swierczynski, J., et al., *Enhanced glycerol 3-phosphate dehydrogenase activity in adipose tissue of obese humans.* Mol Cell Biochem, 2003. **254**(1-2): p. 55-9.
154. Sledzinski, T., et al., *Association between cytosolic glycerol 3-phosphate dehydrogenase gene expression in human subcutaneous adipose tissue and BMI.* Cell Physiol Biochem, 2013. **32**(2): p. 300-9.
155. Rice, B.B., et al., *Insulin-induced hypoglycemia associations with gene expression changes in liver and hypothalamus of chickens from lines selected for low or high body weight.* Gen Comp Endocrinol, 2014. **208C**: p. 1-4.
156. Yi, J., et al., *Fed and fasted chicks from lines divergently selected for low or high body weight have differential hypothalamic appetite-associated factor mRNA expression profiles.* Behav Brain Res, 2015. **286**: p. 58-63.
157. Yang, Y., *Structure, function and regulation of the melanocortin receptors.* Eur J Pharmacol, 2011. **660**(1): p. 125-30.

158. Rodrigues, A.R., H. Almeida, and A.M. Gouveia, *Intracellular signaling mechanisms of the melanocortin receptors: current state of the art.* Cell Mol Life Sci, 2015. **72**(7): p. 1331-45.
159. Shipp, S.L., et al., *The central anorexigenic mechanism of adrenocorticotropic hormone involves the caudal hypothalamus in chicks.* Neuropeptides, 2015. **53**: p. 29-35.
160. Shipp, S.L., et al., *Beta-cell-tropin is associated with short-term stimulation of food intake in chicks.* Gen Comp Endocrinol, 2015. **224**: p. 278-82.
161. Tung, Y.C., et al., *A comparative study of the central effects of specific proopiomelancortin (POMC)-derived melanocortin peptides on food intake and body weight in pomc null mice.* Endocrinology, 2006. **147**(12): p. 5940-7.
162. Rees, J.L., *Genetics of hair and skin color.* Annu Rev Genet, 2003. **37**: p. 67-90.
163. Catania, A., et al., *Targeting melanocortin receptors as a novel strategy to control inflammation.* Pharmacol Rev, 2004. **56**(1): p. 1-29.
164. Catania, A., et al., *The melanocortin system in control of inflammation.* ScientificWorldJournal, 2010. **10**: p. 1840-53.
165. Mountjoy, K.G., *The human melanocyte stimulating hormone receptor has evolved to become "super-sensitive" to melanocortin peptides.* Mol Cell Endocrinol, 1994. **102**(1-2): p. R7-11.
166. Hadley, M.E. and C. Haskell-Luevano, *The proopiomelanocortin system.* Ann N Y Acad Sci, 1999. **885**: p. 1-21.
167. Vale, W., et al., *Characterization of a 41-residue ovine hypothalamic peptide that stimulates secretion of corticotropin and beta-endorphin.* Science, 1981. **213**(4514): p. 1394-7.
168. Boston, B.A., *The role of melanocortins in adipocyte function.* Ann N Y Acad Sci, 1999. **885**: p. 75-84.
169. Mountjoy, K.G., *Distribution and function of melanocortin receptors within the brain.* Adv Exp Med Biol, 2010. **681**: p. 29-48.
170. Mountjoy, K.G., et al., *Localization of the melanocortin-4 receptor (MC4-R) in neuroendocrine and autonomic control circuits in the brain.* Mol Endocrinol, 1994. **8**(10): p. 1298-308.
171. Schwartz, M.W., et al., *Central nervous system control of food intake.* Nature, 2000. **404**(6778): p. 661-71.
172. Chen, A.S., et al., *Inactivation of the mouse melanocortin-3 receptor results in increased fat mass and reduced lean body mass.* Nat Genet, 2000. **26**(1): p. 97-102.
173. Fathi, Z., L.G. Iben, and E.M. Parker, *Cloning, expression, and tissue distribution of a fifth melanocortin receptor subtype.* Neurochem Res, 1995. **20**(1): p. 107-13.
174. An, J.J., et al., *Peripheral effect of alpha-melanocyte-stimulating hormone on fatty acid oxidation in skeletal muscle.* J Biol Chem, 2007. **282**(5): p. 2862-70.
175. Eerola, K., et al., *alpha-MSH overexpression in the nucleus tractus solitarius decreases fat mass and elevates heart rate.* J Endocrinol, 2014. **222**(1): p. 123-36.
176. Perino, A., et al., *Combined inhibition of PI3Kbeta and PI3Kgamma reduces fat mass by enhancing alpha-MSH-dependent sympathetic drive.* Sci Signal, 2014. **7**(352): p. ra110.

177. Gerozissis, K., *Brain insulin, energy and glucose homeostasis; genes, environment and metabolic pathologies.* Eur J Pharmacol, 2008. **585**(1): p. 38-49.
178. Becattini, B., et al., *PI3Kgamma within a nonhematopoietic cell type negatively regulates diet-induced thermogenesis and promotes obesity and insulin resistance.* Proc Natl Acad Sci U S A, 2011. **108**(42): p. E854-63.
179. Rossi, J., et al., *Melanocortin-4 receptors expressed by cholinergic neurons regulate energy balance and glucose homeostasis.* Cell Metab, 2011. **13**(2): p. 195-204.
180. Mottillo, E.P. and J.G. Granneman, *Intracellular fatty acids suppress beta-adrenergic induction of PKA-targeted gene expression in white adipocytes.* Am J Physiol Endocrinol Metab, 2011. **301**(1): p. E122-31.
181. Stralfors, P. and P. Belfrage, *Phosphorylation of hormone-sensitive lipase by cyclic AMP-dependent protein kinase.* J Biol Chem, 1983. **258**(24): p. 15146-52.
182. Moller, C.L., et al., *Melanocortin agonists stimulate lipolysis in human adipose tissue explants but not in adipocytes.* BMC Res Notes, 2015. **8**: p. 559.
183. Martinez-Gonzalez, J. and L. Badimon, *The NR4A subfamily of nuclear receptors: new early genes regulated by growth factors in vascular cells.* Cardiovasc Res, 2005. **65**(3): p. 609-18.
184. Maxwell, M.A. and G.E. Muscat, *The NR4A subgroup: immediate early response genes with pleiotropic physiological roles.* Nucl Recept Signal, 2006. **4**: p. e002.
185. Wang, S.C., et al., *Nr4a1 siRNA expression attenuates alpha-MSH regulated gene expression in 3T3-L1 adipocytes.* Mol Endocrinol, 2011. **25**(2): p. 291-306.
186. Cline, M.A. and M.L. Smith, *Central alpha-melanocyte stimulating hormone attenuates behavioral effects of neuropeptide Y in chicks.* Physiol Behav, 2007. **91**(5): p. 588-92.
187. Raposinho, P.D., R.B. White, and M.L. Aubert, *The melanocortin agonist Melanotan-II reduces the orexigenic and adipogenic effects of neuropeptide Y (NPY) but does not affect the NPY-driven suppressive effects on the gonadotropic and somatotropic axes in the male rat.* J Neuroendocrinol, 2003. **15**(2): p. 173-81.
188. Baltazi, M., et al., *Plasma neuropeptide Y (NPY) and alpha-melanocyte stimulating hormone (a-MSH) levels in patients with or without hypertension and/or obesity: a pilot study.* Am J Cardiovasc Dis, 2011. **1**(1): p. 48-59.
189. Nam, S.Y., et al., *Cerebrospinal fluid and plasma concentrations of leptin, NPY, and alpha-MSH in obese women and their relationship to negative energy balance.* J Clin Endocrinol Metab, 2001. **86**(10): p. 4849-53.
190. Rosmaninho-Salgado, J., et al., *Dipeptidyl-peptidase-IV by cleaving neuropeptide Y induces lipid accumulation and PPAR-gamma expression.* Peptides, 2012. **37**(1): p. 49-54.
191. Labelle, M., et al., *Tissue-specific regulation of fat cell lipolysis by NPY in 6-OHDA-treated rats.* Peptides, 1997. **18**(6): p. 801-8.
192. Della-Zuana, O., et al., *A potent and selective NPY Y5 antagonist reduces food intake but not through blockade of the NPY Y5 receptor.* Int J Obes Relat Metab Disord, 2004. **28**(4): p. 628-39.

193. Hahn, T.M., et al., *Coexpression of Agrp and NPY in fasting-activated hypothalamic neurons.* Nat Neurosci, 1998. **1**(4): p. 271-2.
194. Ishihara, A., et al., *A neuropeptide Y Y5 antagonist selectively ameliorates body weight gain and associated parameters in diet-induced obese mice.* Proc Natl Acad Sci U S A, 2006. **103**(18): p. 7154-8.
195. Billington, C.J., et al., *Effects of intracerebroventricular injection of neuropeptide Y on energy metabolism.* Am J Physiol, 1991. **260**(2 Pt 2): p. R321-7.
196. Shimada, K., et al., *Neuropeptide Y activates phosphorylation of ERK and STAT3 in stromal vascular cells from brown adipose tissue, but fails to affect thermogenic function of brown adipocytes.* Peptides, 2012. **34**(2): p. 336-42.
197. Shipp, S.L., M.A. Cline, and E.R. Gilbert, *Promotion of adipogenesis by neuropeptide Y during the later stages of chicken preadipocyte differentiation.* Physiol Rep, 2016. **4**(21).
198. Brizova, H., et al., *A novel quantitative PCR of proliferation markers (Ki-67, topoisomerase IIalpha, and TPX2): an immunohistochemical correlation, testing, and optimizing for mantle cell lymphoma.* Virchows Arch, 2010. **456**(6): p. 671-9.
199. Milde-Langosch, K., et al., *Validity of the proliferation markers Ki67, TOP2A, and RacGAP1 in molecular subgroups of breast cancer.* Breast Cancer Res Treat, 2013. **137**(1): p. 57-67.
200. Cryer, A., *Tissue lipoprotein lipase activity and its action in lipoprotein metabolism.* Int J Biochem, 1981. **13**(5): p. 525-41.
201. Cornelius, P., O.A. MacDougald, and M.D. Lane, *Regulation of adipocyte development.* Annu Rev Nutr, 1994. **14**: p. 99-129.
202. Amri, E.Z., et al., *Regulation of adipose cell differentiation. I. Fatty acids are inducers of the aP2 gene expression.* J Lipid Res, 1991. **32**(9): p. 1449-56.
203. Wang, G., et al., *Dietary Macronutrient Composition Affects the Influence of Exogenous Prolactin-Releasing Peptide on Appetite Responses and Hypothalamic Gene Expression in Chickens.* J Nutr, 2015. **145**(10): p. 2406-11.
204. Yang, Q.Y., et al., *Maternal obesity induces epigenetic modifications to facilitate Zfp423 expression and enhance adipogenic differentiation in fetal mice.* Diabetes, 2013. **62**(11): p. 3727-35.
205. Wise, L.S. and H. Green, *Participation of one isozyme of cytosolic glycerophosphate dehydrogenase in the adipose conversion of 3T3 cells.* J Biol Chem, 1979. **254**(2): p. 273-5.
206. Lengi, A.J. and B.A. Corl, *Factors influencing the differentiation of bovine preadipocytes in vitro.* J Anim Sci, 2010. **88**(6): p. 1999-2008.
207. Schmittgen, T.D. and K.J. Livak, *Analyzing real-time PCR data by the comparative CT method.* Nat. Protocols, 2008. **3**(6): p. 1101-1108.
208. Liu, S., et al., *Transdifferentiation of fibroblasts into adipocyte-like cells by chicken adipogenic transcription factors.* Comp Biochem Physiol A Mol Integr Physiol, 2010. **156**(4): p. 502-8.
209. Patel, Y.M. and M.D. Lane, *Mitotic clonal expansion during preadipocyte differentiation: calpain-mediated turnover of p27.* J Biol Chem, 2000. **275**(23): p. 17653-60.
210. Hausman, D.B., et al., *The biology of white adipocyte proliferation.* Obes Rev, 2001. **2**(4): p. 239-54.

211. Costa, J.L., et al., *Mutational analysis of evolutionarily conserved ACTH residues.* Gen Comp Endocrinol, 2004. **136**(1): p. 12-6.
212. Thody, A.J. and A. Graham, *Does alpha-MSH have a role in regulating skin pigmentation in humans?* Pigment Cell Res, 1998. **11**(5): p. 265-74.
213. Williams, D.L. and M.W. Schwartz, *The melanocortin system as a central integrator of direct and indirect controls of food intake.* Am J Physiol Regul Integr Comp Physiol, 2005. **289**(1): p. R2-3.
214. Boston, B.A. and R.D. Cone, *Characterization of melanocortin receptor subtype expression in murine adipose tissues and in the 3T3-L1 cell line.* Endocrinology, 1996. **137**(5): p. 2043-50.
215. Smith, S.R., et al., *Agouti expression in human adipose tissue: functional consequences and increased expression in type 2 diabetes.* Diabetes, 2003. **52**(12): p. 2914-22.
216. Agarwal, A.K. and A. Garg, *Congenital generalized lipodystrophy: significance of triglyceride biosynthetic pathways.* Trends Endocrinol Metab, 2003. **14**(5): p. 214-21.
217. Cautivo, K.M., et al., *AGPAT2 is essential for postnatal development and maintenance of white and brown adipose tissue.* Mol Metab, 2016. **5**(7): p. 491-505.
218. Tontonoz, P. and B.M. Spiegelman, *Fat and beyond: the diverse biology of PPARgamma.* Annu Rev Biochem, 2008. **77**: p. 289-312.
219. Wang, Y., et al., *Peroxisome proliferator-activated receptor-gamma gene: a key regulator of adipocyte differentiation in chickens.* Poult Sci, 2008. **87**(2): p. 226-32.
220. Lea, W., et al., *Long-chain acyl-CoA dehydrogenase is a key enzyme in the mitochondrial beta-oxidation of unsaturated fatty acids.* Biochim Biophys Acta, 2000. **1485**(2-3): p. 121-8.
221. Zimmermann, R., et al., *Fat mobilization in adipose tissue is promoted by adipose triglyceride lipase.* Science, 2004. **306**(5700): p. 1383-6.
222. Karlsson, M., et al., *cDNA cloning, tissue distribution, and identification of the catalytic triad of monoglyceride lipase. Evolutionary relationship to esterases, lysophospholipases, and haloperoxidases.* J Biol Chem, 1997. **272**(43): p. 27218-23.
223. Lass, A., et al., *Adipose triglyceride lipase-mediated lipolysis of cellular fat stores is activated by CGI-58 and defective in Chanarin-Dorfman Syndrome.* Cell Metab, 2006. **3**(5): p. 309-19.
224. Greenberg, A.S., et al., *Perilipin, a major hormonally regulated adipocyte-specific phosphoprotein associated with the periphery of lipid storage droplets.* J Biol Chem, 1991. **266**(17): p. 11341-6.
225. Granneman, J.G., et al., *Analysis of lipolytic protein trafficking and interactions in adipocytes.* J Biol Chem, 2007. **282**(8): p. 5726-35.
226. Shang, Z., et al., *Oleate promotes differentiation of chicken primary preadipocytes in vitro.* Biosci Rep, 2014.
227. Zhang, Z., et al., *Klf7 modulates the differentiation and proliferation of chicken preadipocyte.* Acta Biochim Biophys Sin (Shanghai), 2013. **45**(4): p. 280-8.

228. Struikmans, H., et al., *Prognostic significance of cell proliferation markers and DNA-ploidy in head and neck tumors.* Int J Radiat Oncol Biol Phys, 1998. **40**(1): p. 27-34.
229. Jin, D., et al., *TNF-alpha reduces g0s2 expression and stimulates lipolysis through PPAR-gamma inhibition in 3T3-L1 adipocytes.* Cytokine, 2014. **69**(2): p. 196-205.
230. Cornish, J., et al., *alpha -melanocyte-stimulating hormone is a novel regulator of bone.* Am J Physiol Endocrinol Metab, 2003. **284**(6): p. E1181-90.
231. Smink, J.J., et al., *Transcription factor C/EBPbeta isoform ratio regulates osteoclastogenesis through MafB.* EMBO J, 2009. **28**(12): p. 1769-81.
232. Hong, J.H., et al., *TAZ, a transcriptional modulator of mesenchymal stem cell differentiation.* Science, 2005. **309**(5737): p. 1074-8.
233. Airaghi, L., et al., *Plasma concentrations of alpha-melanocyte-stimulating hormone are elevated in patients on chronic haemodialysis.* Nephrol Dial Transplant, 2000. **15**(8): p. 1212-6.
234. Shishioh-Ikejima, N., et al., *The increase of alpha-melanocyte-stimulating hormone in the plasma of chronic fatigue syndrome patients.* BMC Neurol, 2010. **10**: p. 73.
235. Hiramoto, K., et al., *Increased alpha-melanocyte-stimulating hormone (alpha-MSH) levels and melanocortin receptors expression associated with pigmentation in an NC/Nga mouse model of atopic dermatitis.* Exp Dermatol, 2010. **19**(2): p. 132-6.
236. Greenberg, A.S., et al., *Lipid droplet meets a mitochondrial protein to regulate adipocyte lipolysis.* EMBO J, 2011. **30**(21): p. 4337-9.
237. Choe, S.S., et al., *Adipose Tissue Remodeling: Its Role in Energy Metabolism and Metabolic Disorders.* Front Endocrinol (Lausanne), 2016. **7**: p. 30.
238. Sun, K., C.M. Kusminski, and P.E. Scherer, *Adipose tissue remodeling and obesity.* J Clin Invest, 2011. **121**(6): p. 2094-101.